THE SYNERGETIC EFFECT OF THE 3-BROMOPUYRUVIC ACID AND EX-527 COMBINATION ON PANCREATIC DUCTAL ADENOCARCINOMA, MIAPACA-2

by
İrem Baygutalp

Submitted to Graduate School of Natural and Applied Sciences
in Partial Fulfillment of the Requirements
for the Degree of Master of Science in
Biotechnology

Yeditepe University
2019

THE SYNERGETIC EFFECT OF THE 3-BROMOPUYRUVIC ACID AND EX-527 COMBINATION ON PANCREATIC DUCTAL ADENOCARCINOMA, MIAPACA-2

APPROVED BY:

Assist. Prof. Dr. Hüseyin Çimen .....
(Thesis Supervisor)
(Yeditepe University)

Prof. Dr. Murat Kasap .....
(Kocaeli University)

Assoc. Prof. Dr. Ali Özhan Öztekin .....
(Yeditepe University)

DATE OF APPROVAL: ..../..../2019

ACKNOWLEDGEMENTS

I would like to thank the founder of the YediPROT team Hüseyin Çimen for accepting me as one of his colleagues.
I would like to thank my lab mates and graduate students who support me during my thesis preparation and thank you very much for their courage.

I would like to thank my dear friend, Öykü Boraka, who never left me alone and who supported me in every way and my dear chick Benan Ün who helped me in all matters and thanks for her special support during the preparation of my thesis.

ABSTRACT

THE SYNERGETIC EFFECT OF THE 3-BROMOPUYRUVIC ACID AND EX-527 COMBINATION ON PANCREATIC DUCTAL ADENOCARCINOMA, MIAPACA-2

Since the mortality rate of pancreatic cancer in the world has been increasing and the chances of patient survival are 5 percent after diagnosis, it is almost impossible to treat after diagnosis, particularly in advanced stages. Because of its rapid progression to metastasis, it is difficult to determine the pathways of metabolic signals and determine which treatment strategy to perform. The aim of this study is to find the suitable treatment strategies to irreversibly kill pancreatic cancer cells as soon as they are diagnosed. In recent years, one of the strategies that have been developed for more effective and fast therapeutic nature of various anti-cancer drugs is to determine their suitable doses to be applied together in order to increase the overall efficiency. In the next years, co-treatment strategy will be increased to enhance the response of patients by restricting the metastatic progression through the inhibition of multi-direction signaling pathways, and so patients may survive longer and even ending their suffer from the disease.

However, it is rather difficult to study metabolic metabolism because of the rapid progression of pancreatic cancer. One of the commonly used antiglycolytic agent, 3-bromopyruvic acid (3BP) has been demonstrated to be partly effective in interfering the cancer metabolism. Recent studies have also shown that sirtuins are implied in the modulation of cellular metabolism under stress conditions through their activities, NAD^+-dependent deacetylase or ADP-ribosyltransferase, which are related to cancer interference. The co-treatment of 3BP and the sirtuin-1 inhibitor, EX527, on pancreatic cancer cells was investigated. The application of these drugs together on pancreatic cells was found to be synergetic and their appropriate doses were optimized to investigate metabolic changes in pancreatic cancer cells. In addition, we have demonstrated affected metabolic pathways, which provided information for mitochondria-related death mechanisms.

ÖZET

3-BROMOPYRUVİK ASİT VE EX527 'NİN KOMBİNASONUNUN PANKREATİK DUKTAL ADENOKARSİNOM,MİAPACA2 HÜCRELERİ ÜZERİNDEKİ SİNERCETİSTİK ETKİSİ

Dünyadaki pankreas kanserinin mortalite oranı arttığından ve hastanın sağkalım şansı tanıdan sonra yüzde 5 olduğundan, tanıdan sonra, özellikle ileri aşamalarda tedavi etmek neredeyse imkansızdır. Metastaza hızlı ilerlemesi nedeniyle, metabolik sinyallerin yollarını belirlemek ve hangi tedavi stratejisinin gerçekleştirileceğini belirlemek zordur. Bu çalışmanın amacı, pankreas kanseri hücrelerini teşhis edildikleri anda geri dönüşsüz bir şekilde öldürmek için uygun tedavi stratejilerini bulmaktır. Son yıllarda, çeşitli anti-kanser ilaçlarının daha etkili ve hızlı terapötik doğası için geliştirilen stratejilerden biri, toplam verimi arttırmak için birlikte uygulanacak uygun dozları belirlemektir. Gelecek yıllarda, çok yönlü sinyal yollarının inhibisyonu yoluyla metastatik ilerlemeyi kısıtlayarak hastaların cevabını arttırmak için ortak tedavi stratejisi artırılacak ve böylece hastalar daha uzun süre hayatta kalabilecek ve hatta hastalıklarından dolayı acı çekebileceklerdir.

Bununla birlikte, pankreas kanserinin hızlı ilerlemesi nedeniyle metabolik metabolizmayı incelemek oldukça zordur. Yaygın olarak kullanılan antiglikolitik ajanlardan biri olan 3-bromopiruvik asidin (3BP) kanser metabolizmasına müdahale etmede kısmen etkili olduğu gösterilmiştir. Son çalışmalar, sirtuinlerin, stres koşullarında hücresel metabolizmanın modülasyonunda, kanser müdahalesiyle ilgili olan NAD + bağımlı deasetilaz veya ADP-ribosiltransferaz yoluyla gerçekleştirildiğini göstermiştir. 3BP ve sirtuin-1 inhibitörü olan EX527'nin pankreas kanseri hücrelerinde birlikte işlenmesi araştırılmıştır. Bu ilaçların pankreas hücrelerinde birlikte uygulanmasının sinerjik olduğu bulundu ve pankreas kanseri hücrelerinde metabolik değişiklikleri araştırmak için uygun dozları optimize edildi. Ek olarak, mitokondriye bağlı ölüm mekanizmaları için bilgi sağlayan etkilenen metabolik yolakları gösterdik.

TABLE OF CONTENTS

ACKNOWLEDGEMENTS iii

ABSTRACT iv

ÖZET v

LIST OF FIGURES ix

LIST OF SYMBOLS/ABBREVIATIONS xi

1. INTRODUCTION 1

1.1. PANCREAS AND ITS MORPHOLOGY 1

1.2. PANCREATIC DISORDERS 2

1.3. CANCER 4

1.3.1. The Hallmarks of Cancer 5

1.4. PANCREATIC CANCER 15

1.4.1. Pathophysiology and Molecular Pathology 16

1.4.2. Diagnosis of Pancreatic Cancer 19

1.4.3. Treatment Strategies for Pancreatic Cancer 20

1.5. STRATEGIES FOR CANCER TREATMENT 21

1.5.1. Biochemical Targets 22

1.5.2. Antiglycolytic Targets 24

1.6. MITOCONDRIA AND CANCER 28

1.6.1. Mitochondrial Cell Death Mechanisms 29

1.7. GLYCOLYSIS AND CANCER 30

1.7.1. Hexokinase and 3-Bromopyruvic Acid 31

1.8. SIRTUIN PROTEINS AND THEIR ROLES IN CANCER TREATMENT 33

1.8.1. The Glycolytic Regulation by Sirtuins 33

1.8.2. The Regulation of Reactive Oxygen Species by Sirtuins 34

1.8.3. Mitochondrial Sirtuins 34

1.9. AIM OF THE STUDY 37

2. MATERIALS AND METHODS 38

2.1. CELL CULTURE 38

2.2. CELL SUBCULTURING 38
2.3. DETERMINATION OF CONCENTRATION FOR PROTEIN SAMPLES FROM CELLS 39
2.4. IMMUNOBLOTTING 40
2.5. QUANTIFICATION OF IMMUNOBLOTTING RESULTS 42
2.6. CONFOCAL IMAGING 43
2.7. QUANTIFICATION OF CONFOCAL IMAGING RESULTS 44
2.8. DETERMINATION OF ROS LEVEL 45
2.9. QUANTIFICATION OF ROS LEVEL BY FLOW CYTOMETRY 46
2.10. DETERMINATION OF MITOCHONDRIAL MEMBRANE POTENTIAL WITH FLOW CYTOMETRY 46
2.11. QUANTIFICATION OF MITOCHONDRIAL MEMBRANE POTENTIAL WITH FLOW CYTOMETRY 47
2.12. CELL DEATH ANALYSIS WITH ANNEXIN-PI STAINING 48
2.13. THE ISOBOLOGRAM ANALYSIS FOR THE SYNERGETIC EFFECT OF 3BP AND EX527 48
2.14. STATISTICAL ANALYSIS 50

3. RESULTS 51

3.1. THE OPTIMIZATION OF MIAPACA-2 CELL TREATMENT 51
3.2. THE CELL VIABILITY ASSAY WITH MIAPACA-2 CELLS 53
3.3. ANALYSIS OF DEATH MECHANISM BY USING ANNEXIN-PI 55
3.4. ANALYSIS OF SYNERGETIC EFFECT IN MIAPACA-2 CELLS TREATED 3BP,EX527 AND CO-TREATMENT 57
3.5. SIRTUIN-1 EXPRESSION PROFILE IN MIAPACA-2 CELLS TREATED WITH 3BP, EX527, AND BOTH 57
3.6. SIRTUIN-3 EXPRESSION PROFILE IN MIAPACA-2 CELLS TREATED WITH 3-BP, EX-527, AND BOTH 58
3.7. ANALYSIS OF CELLULAR ACETYLOME IN MIAPACA-2 CELLS 60
3.8. DETERMINATION DIFFERENCES BETWEEN REACTIVE OXYGEN SPECIES IN TREATED AND NON-TREATED CELL SAMPLES 60
3.9. DETERMINATION OF DIFFERENCES OXPHOS COMPLEXES BETWEEN TREATED AND NON-TREATED SAMPLES 62

3.10. ANALYSIS MITOCHONDRIAL INNER MEMBRANE POTENTIAL AND MASS.....62
3.11. QUANTIFICATION OF MITOCHONDRIAL INNER MEMBRANE POTENTIAL BY USING FLOW CYTOMETRY.....66
4. DISCUSSION.....68
5. CONCLUSIONS AND FUTURE PERSPECTIVE.....75
REFERENCES.....76

LIST OF FIGURES

Figure 1.1. Anatomy of pancreas 3

Figure 1.2. Schematic illustration of hallmarks of cancer 13

Figure 1.3. Progression of pancreatic ductal adenocarcinoma 18

Figure 1.4. Schematic representation differences of treatment strategies between metastatic and local pancreatic cancer 20

Figure 1.5. Chemical structure of 3-bromopyruvic acid 32

Figure 1.6. Metabolic reprogramming by sirtuins through different signaling pathways ... 35

Figure 1.7. The targets of SIRT1 37

Figure 3.1. The images of cells treated with 3BP under the light microscope 52

Figure 3.2. The images of cells treated with EX527 under the light microscope 52

Figure 3.3. The images of cells co treated with EX527/3BP under the light microscope .. 53

Figure 3.4. Cell proliferation assay with Miapaca-2 cell lines treated with 3BP 54

Figure 3.5. The cell viability of Miapaca-2 cells treated with EX527 54

Figure 3.6. The cell viability of Miapaca-2 cells cotreated with EX5527 and 3BP 55

Figure 3.7. Isobologram analysis in the Miapaca-2 cell lines 56

Figure 3.8. Cell death mechanism analysis in the Miapaca-2 cell lines 58

Figure 3.9. Immunoblotting analysis of Sirtuin-1 expression profile 59

Figure 3.10. Immunoblotting analysis of Sirtuin-3 expression profile 59

Figure 3.11. Acetylation pattern changes among non-treated and treated Miapaca-2 cells 60

Figure 3.12. Acetylation pattern changes among non-treated and treated Miapaca-2 cells 61

Figure 3.13. Differences in reactive oxygen species among control and treated Miapaca-2 cells 61

Figure 3.14. Immunoblotting analysis of respiratory chain complexes among Miapaca-2 cells 62

Figure 3.15. Relative quantification of changes in OXPHOS complexes in Miapaca-2 cells 63

Figure 3.16. The images represent mitochondrial membrane potential differences between 3-BP treated cells and non-treated cells.....64

Figure 3.17. Analysis of mitochondrial membrane potential differences between 3-BP treated cells and control cells.....64

Figure 3.18. The images represent mitochondrial membrane potential changes compared to cotreated cells 65

Figure 3.19. Analysis of mitochondrial membrane potential differences compared to cotreated cells 65

Figure 3.20. Differences of mitochondrial membrane potential from flow cytometry analysis.....67

LIST OF SYMBOLS/ABBREVIATIONS

AMPK	Adenosine monophosphate-activated protein kinase
ATP	Adenosine triphosphate
ALT	Alternative lengthening of telomere
Ach	Acetylcholine
ATRA	All-trans retinoic acid
ATM	Ataxia telangiectasia mutated
BAX	BCL-2 associated X protein
BAK	BCL-2 antogonist killer 1
BCL-XL	BCL-2 related protein, long isoform
BCL-2	B-cell lymphoma protein 2
BCA	Bicinchoninic assay
BSA	Bovine serum albumin
BRAF	Serine/threonine-protein kinase B-Raf
BRCA	Breast cancer gene 1
CDKN2	Cyclin-dependent kinase Inhibitor 2
Cl	Clor
CIN	Chromosomal Instability
CTS	Computed tomography imaging
Cyt C	cytochrome C
DAPI	4′,6-diamidino-2-phenylindole
DCFDA	2’,7’ –dichlorofluorescin diacetate
DMSO	Deoxymethyl sulfoxide
DNA	Deoxyribonucleic acid
EGF	Epidermal growth factor
ER	Endoplasmic reticulum
ERK	Extracellular signal-regulated kinases
EGCG	Epigallocatechingallate
ENO1	Alpha-enolase isoform
ENO1	Alpha-enolase isoform-1
ENO2	Alpha-enolase isoform-2

ECL	Enhanced chemiluminescence
EMT	Epithelial mesenchymal transition
FAD	Flavin adenine dinucleotide
FBS	Fetal bovine serum
FCCP	Trifluoromethoxy carbonylcyanide
FGF-2	Fibroblast growth factor-2
G6P	Glucose 6 phosphate
GTP	Guanosine triphosphate
GTPase	Guanosine Triphosphatase
GLUT1	Glucose transporter-1
GLUT4	Glucose transporter-4
HD	Huntington's disease
HGF	Hepotocyte growth factor
HIF1	Hypoxia inducible factor-1
HK2	Hexokinase-2
IMM	Inner mitochondrial membrane
IMS	Inter membrane space
IPMNs	Intraductal papillary mucinous neoplasms
K	Lysine
KCN	Potassium cyanide
KO	Knock-out
LKB1	Liver kinase B1
MCNs	Mucinous cystic neoplasms
MMP	Mitochondrial membrane potential
MMPs	Matrix metalloproteinases
mTOR	Mammalian target of rapamycin
MLC-1	Megalencephalic leukoencephalopathy protein-1
NaCl	Sodium Chloride
NAD	Nicotinamide adenine dinucleotide
NF2	Neurofibromatosis Type 2
NF-κB	Nuclear factor kappa B
OMM	Outer mitochondrial membrane
OCR	Oxygen consumption rate

OXPHOS	Oxidative phosphorylation
PBS	Phosphate buffer saline
PGC	Peroxisome proliferator-activated receptor gamma coactivator
PI3K/AKT	Phosphoinositide-3-kinase–protein kinase B/Akt
PDAC	Pancreatic ductal adenocarcinoma
PMSF	Phenylmethylsulfonyl fluoride
PUMA	p53 upregulated modulator of apoptosis
PSCs	Pancreatic stellate cells
PCCs	Pancreatic cancer cells
PD	Pancreastoduodenectomy
PDGF	Platelet derived growth factor
PDH	Pyruvate dehydrogenase
PFK	Phosphofruktokinase
PI	Propodium Iodide
PGC-1alpha	Peroxisome proliferator-activated receptor γ coactivator 1α
PFK-2/FBPase	6-phosphofructo-2-kinase / fructose-2.6-biphosphatase
PGM	Phosphoglycerate mutase
PGM1	Phosphoglycerate mutase-1
POLG	Mitochondrial- DNA polymerase
PPP	Pentose Phosphate Pathway
ROS	Reactive Oxygen Species
Ras	Rat Sarcoma
Rb	Retinoblastoma protein
RIPA	Radioimmunoprecipitation assay
ROS	Reactive oxygen species
RIP1	Receptor-interacting serine/threonine-protein kinase 1
RIP3	Receptor-interacting serine/threonine-protein kinase 3
SMAD4	Mothers against decapentaplegic homolog 4
SIRT3	Sirtuin 1
SIRT1	Sirtuin3
SIRT	Sirtuin
TCA	Tricarboxylic acid
TBS	Tris buffer saline

TBS-T	Tris buffer saline tween
TP53	Tumor protein 53
TMRE	Tetramethylrhodamine ethyl ester perchlorate
TERT	Telomease reverse transcriptase
TGF-β	Transforming growth factor Beta
TPE	Telomere position effect
TMM	Telomere maintenance mechanisms
VEGF	Vascular endothelial growth factor
VDAC	Voltage-dependent anion channel

1. INTRODUCTION

1.1. PANCREAS AND ITS MORPHOLOGY

Pancreas, which belongs to the digestive and endocrine systems, is located posterior to the stomach. It has head, neck, tail, and body parts, and the head part is around “C” part of the duedonum [1]. Also, it consists of right and left lobes and the body. These lobes are surrounded by connective tissue that holds blood vessels, nerves, and lymph cells. The main pancreatic duct called Wirsung extends along the gland and its jointures the common bile duct to enter the second part of the duodenum. The accessory duct known as Santorini enters to duedonum proximal in the main duct [2]. The pancreas is called as exocrine pancreas and almost the whole pancreas is composed of these exocrine parts [3] The lobulated gland produces digestive hormones by exocrine secretion from secreting cells. Langerhan islets are arranged between these cells and are composed of A cells, B cells and D cells [2]. The islets produce and secrete somastastatin, insulin, glucagon, and pancreatic polypeptide that are released into the bloodstream [3]. The pancreas has both exocrine and endocrine functions. The pancreas emerges from the dorsal diverticulum of the duodenum and a small portion of the common bile duct via budding, embryologically (Figure 1.1). The exocrine pancreas forms a tubular network of acinar and ductal cells, and enters into the intestine. These cells of the tubular network transport, secrete, and produce digestive enzymes [2]. An acinus is an acinic cell cluster comprising zymogen granules with a storage compartment for pancreatic digestive enzymes. An acinus can be from an intermediate structure made by ducts on either side and also as a culde sac at the end of the tubular network. This model allows us to understand the changes related to pancreatic diseases and cancer [5]. The acinar cell structure indicates the cell function, which provide synthesis and secretion of some digestive enzymes [2]. The main pancreatic duct system is composed of intralobular ducts that form its major branches. Acinar and ductal cells release enzymes into a highly bicarbonate-containing solution [2]. Endocrine pancreas is comprised of islets of Langerhans that synthesizes and secretes hormones including insulin, glucagon and polypeptides. Small islets are scattered over the acinar lobules and ample islets extend across the grand and interlobular of the pancreatic ducts. It has been

reported that great consistency of islets is in the tail part of the pancreas, as compared to the head and body parts [4]. There are numerous mitochondria and small secretory granules in the islet cells.

Pancreas is mainly composed of acinar cells while blood vessels, endocrine cells and extracellular matrix comprise the rest of the tissue [6]. Acinar cells are not functional in exocrine pancreatic tissues alone but are found in acini consisting of hundreds of acinar cells. These cells are attached to each other through gap junctions that enable them to communicate electrically and chemically [7].

The main function of acinar cells in the pancreas is to secrete digestive enzymes that provide digestion of ingested food. This response is interceded by the release of acetylcholine from the nerve cells that are placed near the acinar cells, which allows the circulation of hormone cholecystokinin [3]. These digestive enzymes are carried in secretory sacs called zymogen granules released by exocytosis, but these zymogens need a circulation to transport the digestive enzymes into the duct system. Therefore, acinar cells secrete a neutral highly Cl-containing liquid and this process is stimulated by acetylcholine (ACh). This Cl-rich fluid contains precursor enzymes related to digestion, namely trypsinogen, chymotrypsin, and pro carboxypeptidases, which are then activated by small intestine. Additionally, the fluid has active enzymes such as α-amylase, lipases, colipase, collagenase, elastase and phospholipase [8]. The neutral high NaCl-containing liquid retains the enzymes, thus they are transported to small ducts where they mix with the HCO3-rich liquids that are produced by the duct cells in response to secretion [3]. This secretion is mediated by Ca^{2+} channels and in this sense calcium balance is important. This secretion is mediated by Calcium-activated Cl channels and calcium acts as an important signaling molecule [9]. Ductal fluid and HCO3 secretion not only break down digestive enzymes in the gut but also protect the parenchyma from stress-related damage in the pancreas [10].

1.2. PANCREATIC DISORDERS

Damage to ductal secretion leads to various diseases related to pancreas, including pancreatitis and cystic fibrosis [3]. Acute pancreatitis is a pancreatitis- inflammation disorder that may cause a risk of death [11]. A special treatment method for acute

pancreatitis has not been developed yet. Several *in vitro* studies applied on animal models tested the pathogenicity of the disease in recent years [3].

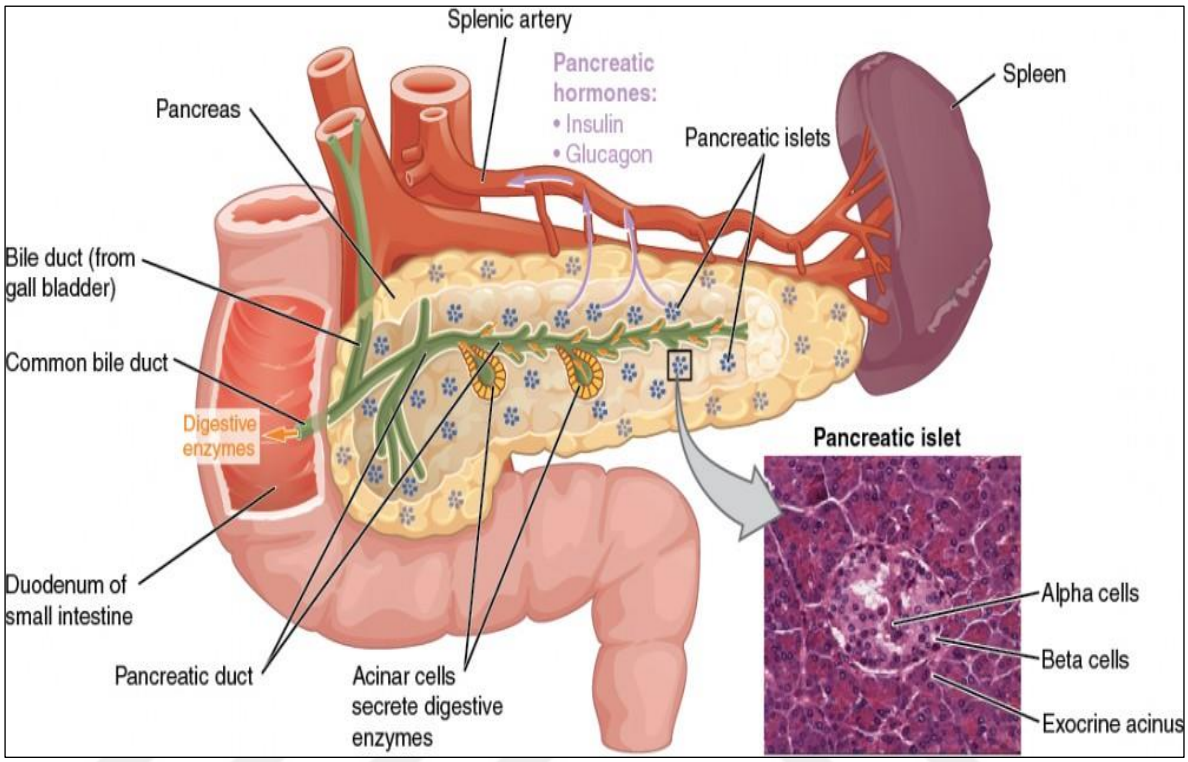

Figure 1.1. Anatomy of pancreas [12]

Chronic pancreatitis initiates a pathological process involving immunological responses that result in damage and destruction of the endocrine and exocrine pancreas [3]. Acute and chronic pancreatitis have also been associated with cancer risk, due to their relevance to the immune system. The most commonly known pancreatic diseases are pancreatic cancer, acute pancreatitis, and chronic pancreatitis. Acute pancreatitis is one of the gastrointestinal disorders and it has a frequency of about 13-45/100,000 per year. [13] In a cohort study, patients with chronic pancreatitis were observed during 5 years and their risk of cancer incidence was 14.4 [14]. In 2014, Tong and colleagues published a review of detailed epidemiological studies showing the link between pancreatitis and pancreatic cancer [15]. Acute pancreatitis is the best-known of the metabolic diseases caused by hyperlipidemia and hypercalcemia [16]. The mechanism of death associated with acute pancreatitis is the occurrence of necrosis in the parenchyma.

Chronic pancreatitis is a pathological process involving fibrotic and immunological responses to damage. This results in the displacement and loss-of-function of the exocrine

and endocrine pancreas of the glandular function. Chronic pancreatitis is described as a complex disorder. It is characterized by cellular stress, fibrosis, pancreatic injury, chronic pain syndrome and duct distortion [3]. To treat chronic pancreatitis, digestive enzymes such as lipases and proteases, nutritional supportive therapies and some antioxidant applications have been used.

Autoimmune pancreatitis is another disease related to the pancreas. Patients with autoimmune pancreatitis may be under the risk to development of pancreatic cancer; however some studies have presented contradictory results. The risk of cancer in these patients may be high during the first year after diagnosis [17]. Importantly, individuals with hereditary pancreatitis are under a high risk of pancreatic cancer, with a 40 percent [18]. Understanding and evaluating the linkage between pancreatitis and pancreatic cancer is quite difficult due to differences between chronic and acute pancreatitis [19].

There are many causes of pancreatic cancer, including smoking, diabetes and pancreatitis. There is a possibility of pancreas cancer in case of inflammation and prolonged pancreatitis[3]. In improved countries, the incidence of pancreatic cancer is predicted to expand with the aging of the general population [21]. It is estimated that the number of people who died of pancreatic cancer in the United States until 2030 will be second in comparison with other types of cancer [20].

1.3. CANCER

Cancer is a complex disease that occurs due to an uncontrolled division of cells in our body. The diagnosis of this disease is difficult in some cases and it is extremely fatal. A single gene change in one or more cells causes rapid progression of cancer and very rapid release of the body. Tumors are formed by progression of this growth. Since cancer cells are invasive, their uncontrolled proliferation is rapidly spreading from other cells to tissues and even across all parts of the body. Unlike normal cells, cancer cells do not recognize cell division signals in a regular manner, so they cannot initiate programmed cell death or apoptosis as required. Normally, apoptosis is necessary to get rid of the old and damaged cells; however, cancer cells overcome the pathophysiologic conditions. It has been elucidated in many studies that cancer cells can overcome all extreme conditions by

altering many metabolic and energetic molecular mechanisms, including cell death pathways.

Hanahan and Weinberg have published Hallmarks of Cancer and Hallmarks of Cancer: The Next Generation in 2000 and 2011. This unprecedented paper in which the main principles of cancer cells, their differences from the normal cells, and the findings of how cancer cells adapt to extreme conditions are explained, have enlightened us about the disease.

1.3.1. The Hallmarks of Cancer

One of the hallmarks of cancer is that cancer cells sustain their cell life cycles and the cells show aggressive proliferation ability (Figure 1.2). However, normal cells have growth-stimulating signals to drive cell cycle process and are controlled by these signals at each cycle stage, thereby ensure persistence of homoeostasis in the cell and maintain integrity and number of the cells in tissues [22]. Cancer cells reorganize these signals that trigger limitless cell division and to maintain cellular functions. The signals are initiated by growth factors which especially bind tyrosine kinase domains of cell surface receptors [23]. In order to promote growth in tumor cells, the number of growth factors are increased through autocrine or paracrine signaling pathways, which inhibits cell growth while promoting the proliferation of cancer cells. This strategy is thought to permit the escape of cancer cells from death pathways [22]. The number and capacity of the ligands found in the cell surface are important in promoting growth of cancer cells.

The receptors that bind the ligands on cancer cell surface can be altered in different manners; some of these receptors can be overexpressed via gene amplification, somatic mutations in patients can be triggering constituent signals by growth factor receptors, or chromosomal translocations can cause the production of fusion proteins and abnormal signaling [24]. For instance, the catalytic subunit of phosphoinositide 3-kinase causes the hyperactive PI3-kinase activation by mutations [25]. Some activating signaling pathways are complex and difficult to understand. For example, oncogenic mutations in Ras gene deface Ras GTPase activity so it carries on a feedback mechanism that is involved in proliferative signaling [28]. This signaling network is activated by inactivated mutations that occur in the regulators of Ras protein or by missense mutations in the Ras gene

[26,27]. This signaling is functional in 30 percent of cancers and more than 90 percent of pancreatic cancers [26,27].

The proliferation of cancer cells can also be controlled by feedback mechanisms such as in the case of mTOR and PI3K signaling. mTOR activation can inhibit PI3K signaling by negative feedback, thus, inhibition of mTOR kinase through pharmaceutical drugs may affect the negative feedback mechanism, resulting in increased PI3K activation. The impaired feedback mechanism can provide proliferative independence of the cancer cells and distributed signaling can enhance drug resistance among cancer cells [28,29]. PTEN, a negative regulator of the PI3K signaling, affects the PI3K/AKT pathway in the upstream of mTOR and its expression is diminished in several cancers, including pancreatic cancers, and it can be downregulated by mechanisms such as mutations, methylation and deletions [30]. For these reasons, mTOR inhibitors or dual PI3K / mTOR inhibitors have been applied to the patients with pancreatic ductal adenocarcinoma [33,34]. Inhibitors of mTORC1 may cause the activation of PI3K-, AKT- or ERK- pathways and a dual inhibitor of mTORC1/TORC2, AZD2014, enables survival of PDAC mouse model [31,32,34].

In cancer research, another remarkable issue is the increased expression of some genes and proteins that trigger some signaling pathways that ensure the proliferation of cancer cells. This elevated signaling is provided by various oncoproteins such as RAS, MYC, Raf [24]. Although growth signaling is included cancer hallmarks that triggers cancer cells, it is tightly controlled with regulatory proteins. The deterioration of the cell cycle checkpoints and the inability to regulate cell cycle are very critical for the progression of cancer [24,35]. One of the of regulator proteins is retinoblastoma protein (Rb) involved in the checkpoints in G1 phase during cell division. In some tumors this Rb gene may be mutated. This protein has been shown to play a role in the protection of cells against apoptosis, genomic stability, in the regulation and repair of DNA and the maintenance of cell cycle, thus acting as a tumor suppressor [36,37]. Another cell cycle regulator is p53 that was put down by methylation in different cancer cells. The transcription factor p53 regulates the expression of more than 500 genes, which takes part in the signaling of glucose, lipid and amino acid metabolism, oxidative phosphorylation, production of reactive oxygen species, and signaling of the growth factors. The studies have also shown opposite effects in the expression of mutant p53 and wild -type metabolic genes. The

changes in p53 expression may lead to drug resistance, while it can also regulate cellular events such as apoptosis, autophagy, senescence [38].

For pancreatic adenocarcinoma the known precursor genes are KRAS, TP53, CDKN2A and SMAD4 [39]. Mutations in the genes encoding KRAS, TP53, SMAD4 and CDKN2 were previously presented at the stages of metastasis and primary tumors [40]. There are mutations occurring in the p53 gene through molecular mechanisms such as nonsense mutations and frameshifts, which make up to 85 percent in pancreatic cancer. Furthermore, mutations occurring in other genes in non-mutant pancreatic cancer may make TP53 function ineffective [39].

By identifying the contact inhibition mechanism within the context of the hallmarks of cancer, it has been clarified how cancer cells can perform limitless cell proliferation. One of the known factors in limitless cell proliferation is the product of NF2 gene [28-41]. Merlin (Moesin-ezrin-radixin-like protein, also known as schwannomin) is encoded by the neurofibromatosis type 2 (NF2) gene. The loss-function mutations or deletions in this gene, which are determined firstly related to the nervous system, cause tumorigenesis in several types of cancer. NF2 mutations and the loss of Merlin function modulate cancer progression and may affect pharmacological resistance [41]. Merlin supports cell to cell contact by regulating cadherins in the cell membrane and is a requisite for obstructing the mitogenic signaling pathways [42-43].

Another contact inhibition mechanism involves LKB1 epithelial polarity protein, which ensures tissue aggregations and arrange epithelial structure. Another known function of LKB1 is tumor suppression, lost in many cases of tumorigenesis. When LKB1 is suppressed, it can induce Myc-oncogene transformation, thus mitogenic signal activation can be triggered [44,45]. TGF-beta is a barrier in the development of cancer hallmarks,being a potential pleiotropic cytokine in healthy tissues and cells, which stimulates metastasis and invasion in cancer cells [46].

Another characteristic of cancer cells is to escape from cell death mechanisms like autophagy and apoptosis. Apoptosis does not only depend on mitogenic signaling but also on extensive stress factors. These factors inducing apoptosis cause imbalance due to an increase in oncogenic signaling. Normally, in response to internal apoptotic stimuli, intrinsic apoptosis pathway is activated. However, cancer cells can nip off this response.

The evasion of apoptosis might occur due to alterations in transcriptional, translational, and post-translational levels. Additionally, increasing and decreasing expression of anti and pro-apoptotic genes enable this escape. These anti or pro-apoptotic proteins can be stabilized [28,47].

Apoptosis pathway in cancer cells, is modulated by both upstream and down-stream effects on the signaling. Apoptosis regulatory proteins are members of BCL-2 family. Bcl-2, Bcl-XL,MLC-1,BCL-related gene A1 and BAX, BAK are related with apoptotic activities. Pro-apoptotic BAX and BAK initiate programmed cell death, followed by permeabilization of the outer mitochondrial membrane (OMM) and the activation of caspase cascade. BAK and BAX pro-apoptotic proteins can translocate and retrotranslocate to the outer mitochondrial membrane and then back into the cytosol. If and BAK are activated in the cell, they can oligomerize and cause pore formation in the outer mitochondrial membrane, which leads to the release of cytochrome c due to impairment of the integrity of OMM [47-48]. Cell death is regulated by two mechanisms. One is to upregulate pro-death signals and the other is to down-regulate anti-death factors [48]. For instance, BIM-EL, which is one of the pro-apoptotic proteins, is kept at low phosphorylation level by ERK (extracellular signal-regulated kinase) signaling, but stabilized if the ERK pathway is inhibited [48-49]. When FOXO3A is translocated to the nucleus it can stimulate BIM, after inhibition of the PI3K / AKT pathway [51-52]. AKT, which phosphorylates BAD and BAX, regulates their pro-apoptotic functions [49,51,52]. BID, PUMA, NOXA and BAX are induced by the p53 transcription factor, which induces a response to DNA damage and ensures that cell death and cell cycle are maintained in equilibrium [48-54]. In addition, another transcriptional factor is FOXO3A, mediating the regulation of PUMA (p53 upregulated modulator of apoptosis). BCL-2, BCL-xL and BFL-1 are anti-apoptotic proteins targeting the NF-κB signal pathway [49].

Autophagy, one of the mechanisms of cellular death, is a physiological process that enables the removal of protein aggregates, misfolded proteins, and damaged organelles. It has a double role in both tumor formation and in encouraging the branch out of tumors [57]. Autophagy acts as the regulatory system within the cell that is affected by various physiological events, such as stress conditions including caloric restriction, reactive oxygen species, infection, hypoxia. For example, the energy sensor AMPK pathway arbitrate to commence autophagy process under stress conditions such as oxidative or

nutrient stress [56]. On other hand, the relationship between expression of BCL-2 and protein-3 (BNIP3) is response to deprivation of oxygen during hypoxia and it causes autophagy by dissociating Bcl-2/Beclin-1 complex [58]. This complex allows BH3 binding to Bcl-2\ Bcl-xL proteins, which can substitute with each other and /or Beclin-1 and trigger autophagy by the releasing of Beclin-1 [58]. In contrast to apoptosis, which is regulated in a strict manner, necrosis is defined by an increasingly transparent cytoplasm, organelle swelling and mitochondrial dysfunction resulting in interruption of plasma membrane potential. Hypoxia-induced necrosis, which causes acidosis, inhibits OXPHOS and decreases ATP level in the cell, essentially leading to the destruction of the cytoskeleton and membrane. This has been well elaborated as the main road leading to necrosis in recent years [59]. Necrosis, which is a known defense against cancer cells, is under the control of RIP1, RIP3 and various kinase domains. Genetic and epigenetic alterations of necrotic regulators cause cancer cells to survive [60]. The necrotic components which in involve necrosome has been expressed extremely in pancreatic dual adenocarcinoma (PDAC) [61-64].

Cancer cells have unlimited capacity in terms of the cell division [65]. The upregulation of oncogenes or oncoproteins in the immortality process increases the cell division rate. The cell immortalization and cell senescence mechanisms can be defined depending on some cellular controlling process; one of them is two-stages mechanism defined by Wright and Shay: up-regulation of telomere and telomerase activity, telomerase reverse transcriptase (TERT), onco-genes or onco-proteins such as p53, p16, pRb, Protein kinase-Cı and telomere position effect (TPE) [66]. The limitless growth and proliferation, which has remained a mystery of cancer cells, has enabled the understanding of some molecular pathways through the discovery of cell immortality. Normal cells are exposed to telomerase shortening so that the cells are subjected to replicative proliferation along with aging and the senescence mechanism can conduct apoptosis. Telomeres are conserved nucleoprotein constructs which are located at the ends of chromosomes and contain TTAGGG repeat sequences in humans. Telomerase shortening occurs in each replication of the somatic cells because DNA polymerases cannot replicate the chromosome terminate in each division [68]. Cancer cells have telomere maintenance mechanisms (TMMs) to prevent telomere shortness, in contrast to normal cells. This mechanism leads to protection

of telomeres from DNA damage-repair manner and resultantly, cells evade from senescence and apoptosis induced by telomerase [67].

There are two known mechanisms for TMM : telomerase-mediated telomere maintenance and alternative lengthening of telomere (ALT). Telomerase is a reverse transcriptase heterodimer that may be produced by using de-novo synthesis with the telomeric DNA sequence and TERT (telomerase reverse transcriptase) enzyme thanks to the non-coding RNA in a template (telomerase RNA component, TERC). This is achieved by adding on the repeats into the chromosome tip [69]. Telomerase activity is not observed in most somatic cells due to the suppression of TERT gene expression, except for endothelial and lymphocytes [70,71,72]. This telomerase activity is persistent in stem cells and germ line cells or in cancer cells [73,74]. It was remarkable that TMMs exist in some types of tumors like breast, stomach, small intestine, colon and rectum, exocrine pancreas, lung, and prostate, but not all subtypes of these cancers display this activity. It was found that breast and colorectal tumors have a raised frequency of TERT amplifications [75]. ATRX and DAXX genes that are related to ALT gene activation have not represented any changes and evidence of TERT expression was not found by the study of Barthel et al. Furthermore, Barthel et al hypothesized that no defined TMM mechanism may be present for immortalization in all cells. An undefined or unknown TMM may include changes of RB1 or TP53 that may overpass the DNA repair mechanisms owing to telomere induced genomic instability [75,76]. In a case study by Skinnis et al, it was reported that shortened telomeres in pancreatic tissues play a role in the pathogenesis of cancer. In addition, it was stated in the same publication that the occurrence of glucose metabolism events related to the development of pancreatic cancer may be explained by telomerase shortening in patients [77].

Another hallmark of tumor progression is angiogenesis induced via the tumor microenvironment. Tumor microenvironment includes many signaling and pathways involved in the formation of angiogenesis response. Blood vessels and stromal constituents respond to pro and antiangiogenic regulators that provide vascular remodeling during development, pregnancy and wound healing [79]. Oncogenic events increase the survival of cancer cells, but also require blood support for this prolonged and sustained growth [78]. Providing this blood supply; the activation of the tumors from their microenvironment is triggered to induce angiogenic factors leading to vascular growth [79]. The tumor

microenvironment keep together different types of cells that can induce the angiogenic respond to tumors [80]. When tumor lesions reach a specific size, stress conditions such as hypoxia and nutrient deprivation allow tumor progression by stimulating angiogenic switch [82]. The cytokines and growth factors in the tumor microenvironment initiate a number of cascade events that are dysregulated around the tumor. One of them is endothelial growth factor VEGF that activate the proliferation of endothelial cells by release from the tumor cells [81]. The vascular leakage that occurs in a local site of the basal lamina improves and activates the platelets, allowing the release of angiogenic and permeable factors into the environment to increase response [83]. The platelets increase the platelet-derived growth factor (PDGF) and endothelial cells renew and activate perivascular cells [80]. The remodeling response generated by the treatment of tumor-associated fibroblasts accumulates extracellular matrix proteins in a perverse manner and releases stimulating factors [84,85]. Matrix metalloproteinases (MMPs) are broken down to expose pre-hidden epitopes that act as endogenous inhibitors of angiogenesis, such as tumstatin or endostatin [86].

The relationship of VEGF-A that provides tumor micro vascularity to pancreatic ductal adenocarcinoma progression has been reported in different studies [87]. Moreover, both PSCs (pancreatic stellate cells) and PCCs (pancreatic cancer cells) produce matrix metalloproteinase-12 (MMP-12) to partition the endostatin from collagen XVIII [87]. Endostatin, while inhibiting angiogenesis, accelerates the hypoxic conditions while stimulating the secretion of matrix metalloproteinases by PSCs [88]. For example, the hypoxic microenvironment not only contributes to the pro-fibrogenic activity of the PSCs, but also prompt the production of the molecules of PSCs such as VEGF, fibroblast growth factor-2 (FGF-2), platelet derived growth factor (PDGF), interleukin-8 (IL-8) and vasohibin-1 [88,89].

Another one of the hallmarks associated with cancer is to promote invasion and metastasis, Although there are many in studies in this area, the factors that trigger progression of cancer metastasis, the translocation of cancer cells to a secondary position, are still not fully understood [90]. Intercellular structures and cell adhesion are important factors in the maintenance of primary tumors.

Abnormalities that may occur through mutations or dysfunction in these structures may cause cancer cells to settle and metastasize to another location [91,92,93]. The cancer cells

change their shape to settle elsewhere and to attach to the extracellular matrix, indicating changes in their adherent properties. One of these changes occurs in tight junctions (TJ) and gap junctions, which are also found in normal cells. It is the E-cadherin (cadherin-1 or CDH1) protein which is either dysfunctional or lost in cancer cells [90]. E-cadherin is the key element of epithelial mesenchymal transition (EMT). For this reason, increased expression profile of cadherin may be important in controlling metastatic spreading [91].

Cellular migration is an important characteristic in cancer metastasis. Growth factor receptors including epidermal growth factor (EGF), hepatocyte growth factor (HGF) and insulin like growth factor (IGF) and Claudine are important for cell proliferation and survival. The expression of migration-related factors are regulated by Snail / Slug family [94-95]. By the loss of epithelial cell junctions, proteins such as E-cadherin, claudins and ZO-1, cell-cell adhesion in EMT disappears and a polarized epithelial morphology occurs and there is observed increase in N-cadherin, vimentin and fibronectin and cytoskeletal regulation [95-96]. In the EMT process, EGF and transforming growth factor β (TGF-β) are thought to be initiators, which result in the upregulation of transcriptional factors like Snail, Slug and Twist. These transcription factors are also associated with metastasis because they affect EMT protein expression [90].

The most important properties of pancreatic cancer are the rapid progression and differences among localization of tumors [97-98]. A good understanding of these features may contribute to the diagnosis of most patients and to determine the high mortality rate among patients with pancreatic cancer [99-100].

Another hallmark is genomic instability in cancer cells. Genomic changes during cell divisions are an increasing trend [100]. It leads to cancer progression due to damage to multiple genes that govern cell division and tumor suppressor genes [98]. In most cancer cells there is a state called chromosomal instability, which means changes in the number and structure of chromosomes [101]. The presence of both of CIN (Chromosomal Instability) and non-CIN forms in hereditary cancers are associated with mutations that occurred the DNA repair genes. For example; hereditary non-polyposis colon cancer leads to this MSI of mutations in DNA miss-match genes [101-102-103]. The mutations in DNA repair genes in hereditary cancers allows genomic instability in precancerous lesions [104,105].

Mutations in care-taker genes are thought to support genomic instability in precancerous lesions, and the genes primarily function to maintain genomic instability [104,105,106]. These classic care-takers are DNA repair genes and mitotic checkpoints. The tumor suppressor gene TP53 and ATM (The ataxia telangiectasia mutated) are some examples, both of which refer to caretaker genes as they play a role in DNA damage [101].

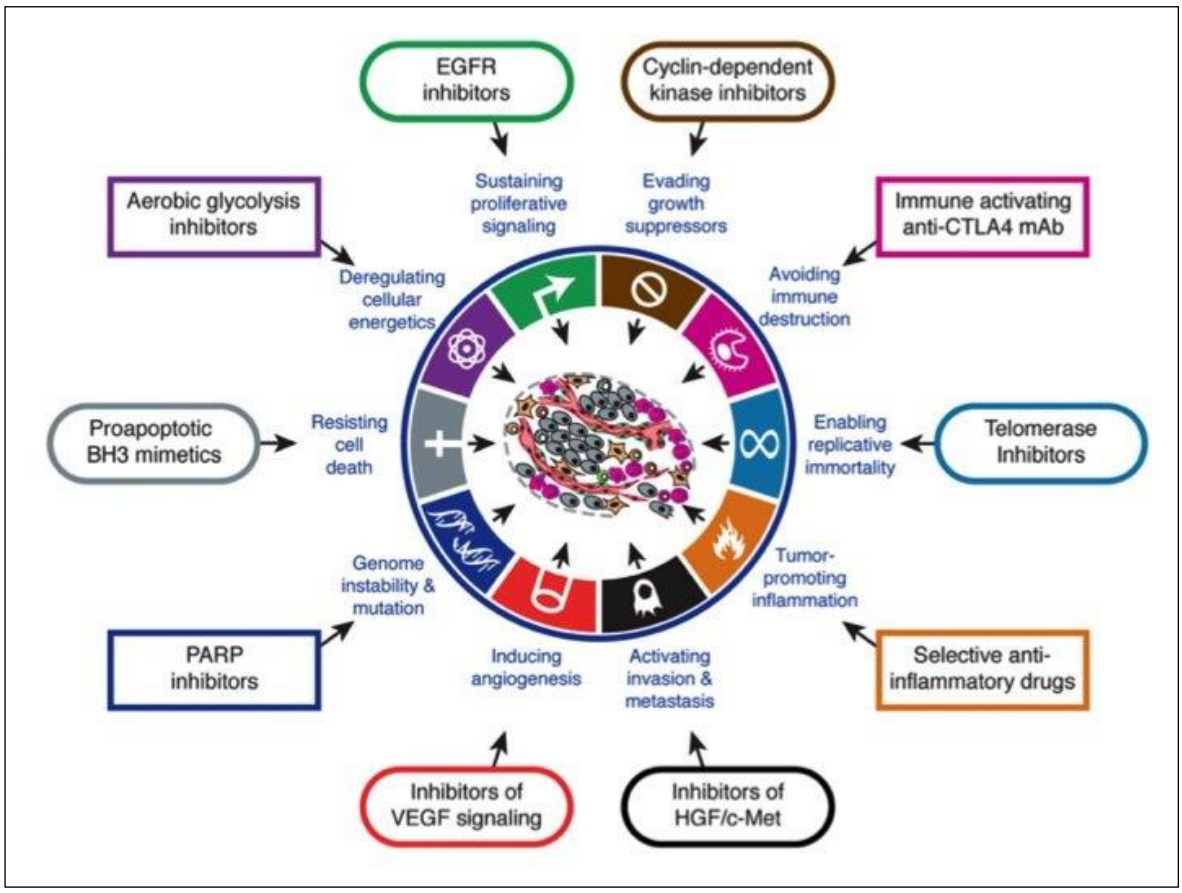

Figure 1.2. Schematic illustration of hallmarks of cancer [102]

Recent large-scale studies have revealed various signaling pathways that have been activated or silenced in multi-staging pancreatic carcinogenesis. Although the expansion of pancreatic cancer with complexity of the genomic changes have emerged as a potential, the genomic footprint of pancreatic cancer has been understood, and it has also been possible to target the pathways that affect clinical outcomes [108-109]. Genomic sequencing of 13 pancreatic cancer patients was performed in a study, explaining the relationship between genomic instability and disease [110]. A study by Campbell et al., genomic instability has

been shown to rely on genetic modifications leading to the progression and development of pancreatic cancer [109-111]. One important hallmarks of cancer is the reprogramming of energy metabolism in proliferative cancer cells. After discovering that Otto Warburg's acidic tumor cells transformed most of the glucose into lactate under oxygen conditions, he argued that this metabolism has been specific for cancer cells and that glucose carbon was effectively inhibited by the ability of carbon to oxidize to carbon dioxide [112]. Glucose uptake has been increased by multiple mechanisms and signaling pathways in cancer cells [112-114-115]. In addition, the expression of hexokinase and GLUT is increased by HIF, and when PI3K / Akt signaling pathway operates abnormally, it increases the expression of GLUT1 and proteins that will translocate to cellular membranes and additionally on oncogenes such as KRAS and BRAF [125]. The first explanation of the Warburg theorem is that it has two defective oxidative phosphorylation in cancer cells, while it also has normal functioning mitochondria. In fact, targeting both mitochondrial DNA of cells *in vitro* and *in vivo* reduces the tumorigenic potential [116-117-118]. Although this metabolic reprogramming is regulated in cancer cells, the extreme saturation of the TCA cycle increases the quantity of reactive oxygen species [119-125]. The moderate production of ROS is, in fact, useful for cancer cells, stimulating stress signaling, increasing the rate of mutation and promoting the progression of cancer. However, it is critical that the increased level of ROSin be harmed because the cells will be damaged [120 -125].

Inflammatory processes play a role in the development of the tumor at different stages, which is one of the hallmarks of cancer. Inflammation also affects the response to therapy, in which the immune cells provide large-scale infiltrate to tumor cells and are in a dynamic relationship with cancer cells and are mediated by certain molecular mechanisms [121]. In addition to various immune modulators and modifiers, the presence and activation of different types of cells in the tumor microenvironment determine whether anti-tumor immunity or tumor-promoting infusion is achieved [121-123].

Consequently, different forms of inflammation occurring in tumorigenesis, innate immune cells, macrophages, neutrophils, , myeloid-derived suppressor cells (dendritic cells and natural killer cells), mast cells, macrophages and adaptive immune cells (T and B lymphocytes) and cancer cells and stroma. The stroma also includes fibroblasts, mesenchymal cells, pericytes and endothelial cells. Cells of this different nature act in an autocrine and paracrine manner to promote and direct cancer growth, and communicate

directly through contact or cytokine and chemokine delivery [121-123]. In advanced tumor cells have presented inflammatory infiltrates, the direct effect of the immune system (both adaptive and innate) is to stimulate tumor spreading [121].

Cancer cells express antigens that do not represent their own changes against the backdrop of stress and dangerous signals that provide antigen presentation. Thereupon, by the activated T and natural cells, they may be subject to immune surveillance and killing [121-123]. It is accepted that there is a relationship between the tumor-related inflammation and infiltration, another hallmark of cancer, however, a direct relationship has not yet been shown [121-125].

In pancreatic cancers, inflammation occurs both as a result of cancer and as a risk factor [126]. The risk of life expectancy for pancreatic adenocarcinoma development in patients with inherited autoimmune pancreatitis is 40 percent, whereas in patients with chronic pancreatitis risk, there is a 13-fold greater risk of developing PDAC [125-127-128]. The duration of pancreatitis is positively correlated with the recurrence of KRAS mutation which is thought to have a mutagenic role with recurrent inflammation seizures [126-129].

1.4. PANCREATIC CANCER

Pancreatic cancer is a highly lethal disease, with a 5-year survival rate of 8 percent. After surgery, most of the patients can relapse from this cancer and the progress in chemotherapy has doubled survival over the last 10 years [130]. Pancreatic cancer is comprehended to be difficult to diagnose, being among types of cancer that have a parallel relationship between mortality and the occurrence of the disease [131]. Most patients with pancreatic cancer abide asymptomatic conditions until the disease reaches an advanced level. There is no useful screening program for patients with a high risk of disease, such as if the family has suffered from pancreatic cancer or chronic pancreatitis in the past. Most pancreatic cancer arises from microscopic noninvasive epithelial proliferations located in the pancreas ducts, termed pancreatic intraplayated neoplasias [131]. Tumor biological properties of pancreatic cancer help to the metastasis and early recurrence of the disease, as well as resistance to radiotherapy and chemotherapy. Autopsy results have shown that up to 90 percent of pancreatic cancer cases are complicated by distant metastases [132]. Improved screening programs for early diagnosis of pancreatic cancers are required. The risk factors for

pancreatic cancer such as the familial history of pancreatic cancer, diabetes mellitus, smoking, chronic pancreatitis have been described, but there is no standard program recently available for patients at high risk [133-137]. The incidence of pancreatic cancer may vary between sexes, with a 50 percent greater frequency for men than women. It typically transpires in adults between 60 and 80 years of age [138].

1.4.1. Pathophysiology and Molecular Pathology

Pancreatic ductal adenocarcinomas evolve among noninvasive precursor lesions, most typically acquiring intraepithelial neoplasia and clonally selective genetic and epigenetic changes [139]. This invasive mucin-producing neoplasm produces diaper stromal intense desmoplastic reactions [130].

For the diagnosis of pancreatic adenocarcinomas, several histological features may be utilized; for example, random re-organization of the glands, nuclear pleomorphism, incomplete glandular lamina, luminal necrosis, adhesion of neoplastic glands to muscular vesicles, perineural invasion and lymph vascular invasion [131].

Pancreatic ductal adenocarcinomas are determinate as three classes temper to their degree of differentiation; well, moderately and weakly differentiating. In addition to the changing morphology of the pancreatic ductal adenocarcinomas, several morphological variants have unique features [140]. As is the case in most other types of tumors, pancreatic ductal adenocarcinomas are also staged by exploitation of the tumor, node, and metastasis staging system. Tumor amount and invasion of structures such as duodenum and bile duct should be evaluated in order to exactly determine T stage. Although it is still a contradictory issue, it is urged that at least 15 nodes are required to determine N stage [141].

Pancreatic ductal adenocarcinomas consisting of some macROScopic cystic precursors are called intraductal papillary mucinous neoplasms (IPMNs) and mucinous cystic neoplasms (MCNs). IPMNs are mucinous cysts found in the pancreatic duct system and are known to be more than 1 cm in volume. IPMNs are classified in 3 categories as low-grade, intermediate-grade and high-grade dysplasias according to the degree of dysplasias in the epithelium[142]. According to IPMNs, MCNs are less common and almost solely seen in

women and are mostly in the tail and body region of the pancreas [142]. MCNs that do not resemble IPMNs are not within the pancreatic duct system.

Cancer is a genetic malady caused by somatic mutations in oncogenes and tumor suppressor genes [143]. Pancreatic ductal adenocarcinoma is also known to be maintained by four main functional genes, one oncogene gene and three different tumor suppressor genes [131].

PanIN shows the progression of multiple lesions with disease development. KRAS mutations start to increase early with the progression of precursor lesions called PanIN (Figure 3.1).

Most of the genetic abnormalities in invasive pancreatic adenocarcinoma are the activation of mutations in KRAS oncogenes, inactivation of tumor suppressor genes such as CDKN2A, TP53, SMAD4 and BRCA2 , large-scale chromosomal losses and gene amplifications [144], and telomere shortening [145-146]. The oldest known genetic anomalies in low-grade pancreatic intraepithelial neoplasia are KRAS mutations and telomere shortening [145-146]. The KRAS gene encodes GTPases that mediate signals from growth factor receptors, and KRAS is often among the mutated oncogenes. Most of the somatic mutations in tumors occur continually in codon 12 hotspots [131]. CDKN2A, which is an important cell cycle regulator, is one of the most frequently changed tumor suppressor genes and the loss of function mutation ratio is very high in ductal adenocarcinomas. Mutations in the TP53 tumor suppressor gene are quite high and the protein encoded by this gene plays an important role in the response to cellular stress and is mutated in many types of tumors. The SMAD4 gene, one of these tumor suppressor genes, mediates the signaling pathway which involves transforming growth factor-beta (TGFβ), but this gene is also inactivated; although it varies between tumors [148].

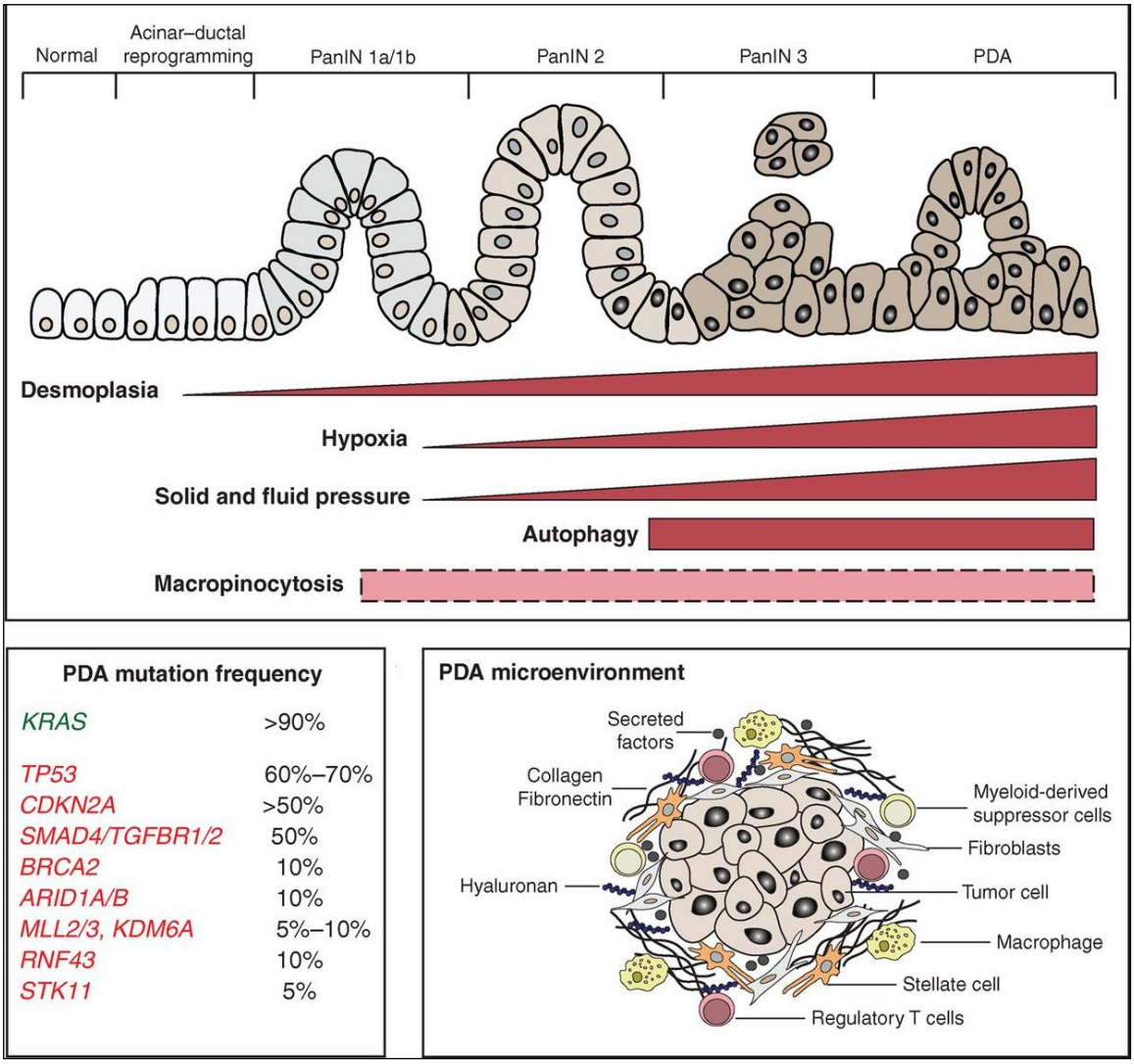

Figure 1.3. Progression of pancreatic ductal adenocarcinoma [145]

Studies on pancreatic cancer with precursor lesions have been aimed to determine the timing of genetic changes. Most of the somatic cramp mutations are caused by low-grade pancreatic intraepithelial neoplasia, suggesting that it is one of the earliest mutation changes in pancreatic tumors [147].Whole exome sequencing performed in pancreatic intraepithelial neoplasia showed that most mutations seen are common in ductal adenocarcinomas. It is suggested that pancreatic intraepithelial neoplasia increases ductal adenocarcinomas [149]. All exome sequencing of premalignant pancreatic cysts exhibited that common genes were shared with ductal adenocarcinomas, such as SMAD, KRAS and TP53 [150].

1.4.2. Diagnosis of Pancreatic Cancer

There are no early detection strategies for patients with a high risk of pancreatic cancer. Although there are options to determine this, imaging centers have whole-body scanning computed tomography imaging (CTS) for healthy patients, but there is still lacking data to increase their usefulness [151]. In the assessment of patients with pancreatic cancer, physical examination, patient family history, laboratory tests, and applicable imaging are needed. The first presentation of the patient is related to the localization of the tumor in the body [151]. In patients with a mass on the right side of the pancreas (especially in the head, neck and uncinate process of the pancreas), the rate of jaundice is usually high and the bile duct is obstructed. Other symptoms are weight loss (50 percent), abdominal pain (40 percent), nausea (10 percent) and new-onset diabetes (10 percent). Pancreatic duct obstruction and acute pancreatitis are exocrine insufficiencies. In patients with a lesion on the left side, abdominal pain, diabetes, and nausea occur frequently. Laboratory tests applied to patients require complete blood count and evaluation of metabolic panel, which is necessary to assess abnormal liver transaminases and their function [151]. The evaluation of cROSs-sectional imaging is required for the pancreatic or periampullary mass as well as for determining which cancer stage the patient is at. In addition, evaluations and recommendations for treatment are based on stages for which cancer is considered to be prescribed (stage 1 and 2 remained at the border, stage 3 is locally advanced and stage 4 is metastatic, the TNM Staging scheme published by the American Joint Committee on table for exocrine pancreatic cancer) (Figure 3.3). In patients suspected of pancreatic cancer, the imaging modality is triphasic computed tomography in the late arterial phase, in the early arterial phase, and in the portal venous phase [149]. Chest imaging with radiography or computed tomography is applied to investigate pulmonary metastases. Also, PET-CT imaging provides additional contribution to other screening methods to invitigate the hink cases. Endoscopic ultrasound is preferred for tissue-based direct diagnosis, especially in irreversible diseases before chemotherapy. This test is not required when a high degree of PDA is suspected in the patient since these individuals are resected. This test is critical for selective cases, for example in cases where diagnoses such as pancreatitis are likely to occur.

1.4.3. Treatment Strategies for Pancreatic Cancer

In the therapy of pancreatic cancer, surgery, chemotherapy, immunotherapy, radiotherapy and temporary treatment methods, as well as the combination of some of these approaches have been applied.

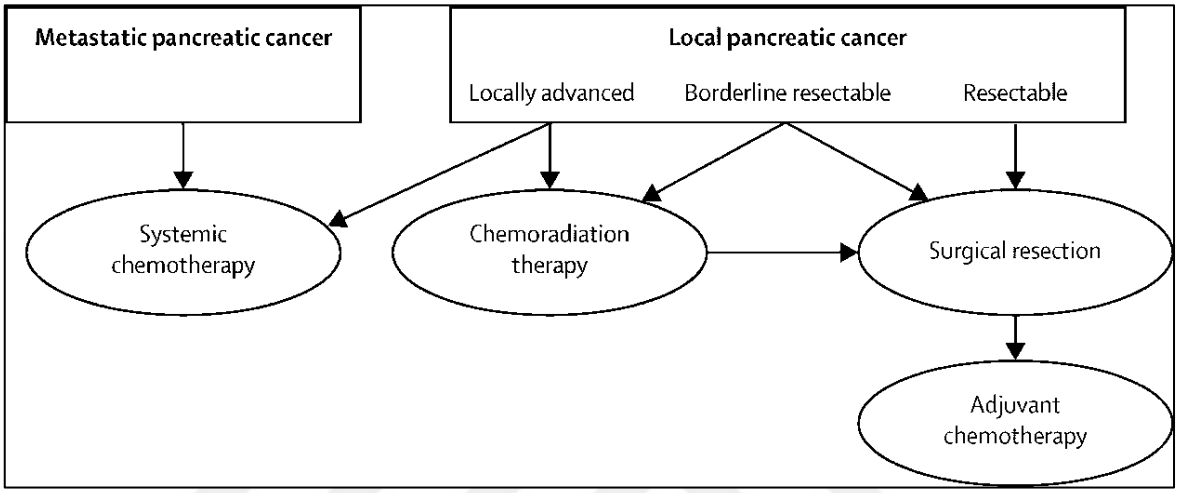

Figure 1.4. Schematic representation differences of treatment strategies between metastatic and local pancreatic cancer [131]

1.4.3.1. Surgery

The pancreas offers a single solution for the treatment of cancer and provides a significant survival rate. The distal regions are divided into 3 categories for non-metastatic pancreatic cancer. However, these 3 categorical distinctions are not a definite rule. The surgical removal of the tumor depends on the surgical technique, limited-irreversible and localization in which the tumor resides [131].

Resection in tumor patients with a localized tumor is generally preferred [152]. Pancreastoduodenectomy (PD) is performed in right-sided pancreatic cancers, bile duct, pancreatic head region, duodenum, proximal jejunum and distal common bile duct. Mortality rate was significantly decreased after PD application. However, the morbidity rate remained high at 40 percent. Complications after administration are gastric emptying, wound infection and pancreatic lesion formation [153].

1.4.3.2. Chemotherapy

In a previous study, fifty percent of patients diagnosed with PDA were identified as metastatic levels [154] (Figure 1.4). At this stage, chemotherapy is mitigating and the disease is calming and it is the main approach that aims to improve the quality of life of the patient and to control the disease. The patients who underwent chemotherapy drugs are subjected to weekly toxicity tests. The responses of the drug therapies are monitored by CT. CA-125 carcinoembryonic antigen monitoring can be performed if the percentage of patients cannot express the CA19-9 antigen due to its detectable Lewis antigen polymorphism [155].

Food and Drug Administration (FDA) propose some drugs for pancreatic cancer that are applied and recommended. The treatments using these drugs vary according to the patient's condition and the response to the drug. It usually involves a resting period. The preferred drugs for pancreatic cancer chemotherapy are Capecitabine (Xeloda), Erlotinib (Tarceva), Fluorouracil (5-FU), Gemcitabine (Gemzar), Irinotecan (Camptosar), Leucovorin (Wellcovorin), Nab-paclitaxel (Abraxane), Nanoliposomal irinotecan (Onivyde Oxaliplatin (Eloxatin) [158].

1.4.3.3. Radiation therapy

The benefits of chemoradiation treatments for locally advanced pancreatic cancer have been controversial, but have remained in conflict with patients' survival rates [156]. In the ECOG 4201 trial, chemotherapy and radiochemotherapy were compared in patients with aggressive level of local pancreatic cancer and mean survival was 9.2 months for gemcitabine and 11.1 months for chemoradiotherapy [131]. Patients require sedative treatment for the course of the disease and obstructive jaundice and bowel obstruction may require surgery, endoscopy or radiological intervention in patients with pancreatic cancer.

1.5. STRATEGIES FOR CANCER TREATMENT

Two main characteristics of cancer are its genetic constructability and its tendency to metastasize. These two main features were first described in 2000 by Hanahan and

Weinberg and in 2011, new features were added to these characteristics. Considering all of these features, no drug has been developed which can stabilize gene mutations leading to cancer. As a result of intense cancer research, alternative treatments such as genomic stabilizers, diversified molecular methods, virotherapy, cytotoxic therapy, immunotherapy, biochemical strategies, anti-angiogenesis strategies, immunotherapy, oxidative therapy, stem cell suppressor therapies, anti-inflammatory therapy, detox and nutrient therapies have currently been used against cancer [157]. For example, vitamin D has been used as a therapeutic agent against cancer. In addition to its contribution to DNA repair, it also stops cancer growth and directs them to apoptosis. Another therapeutic agent is indole-3-carbinol which reduces ER stress, induces caspase activation, regulates Akt-NFKβ signaling pathway, cell cycle, estrogen balance, and cyclin-dependent kinase activities, and also controls BRCA gene expression. Curcumin is also one of the natural compounds which has been used as an anti-cancer agent. Curcumin stimulates the expression of carcinogenic detoxifying enzymes such as glutathione S-transferases. Curcumin is found in foods such as broccoli and colloquial cabbage. Curcumin has been tested in cell culture and animal models. Differentiation therapies against cancer date up to the late 1980s. These therapies promote morphological changes of the cells, thereby prevent abnormal growth of the cells. Many substances have been found to show this effect, including phenyl butyrate, dimethyl sulfoxide (DMSO), all-trans retinoic acid (ATRA), vitamin D, and epigallocatechingallate (EGCG).

1.5.1. Biochemical Targets

Biochemical treatments date back many years, and vitamin C is one of the most well-known. Historically, in 1954, cancer patients were getting better when the treatment was supported with vitamin C which induced the synthesis of collagen in healthy tissues. In the following years; vitamin C was suggested to inhibit hyaluronidase which is involved in the prevention of cancer, and it was found that patients consuming vitamin C had a longer life span. In the pathological studies, cancer cell death mechanisms have been defined and vitamin C has been found to be involved in mechanisms such as hydrogen peroxide formation, redox cycle, oxidative metabolism.

In later 1920, by Otto Warburg, the metabolic differences of normal and cancerous cells were revealed which was a groundbreaking study. Warburg argued that the metabolism of cancer cells is highly damaged, and this is related to the upregulation of anaerobic fermentation metabolism caused by disorders in mitochondria. After this explanation, the development of biochemical therapies was increased against cancer. One anti-cancer treatment strategy is the use of α-lipoic acid and hydroxycitrate. In cancerous cells, PDH is downregulated and ATP citrate lyase shows excessive expression. Alpha-lipoic acid is a cofactor of PDH, while hydroxycitrate is a known inhibitor of ATP citrate lyase. When hydroxycitrate and α-lipoic acid were used together, no significant toxic effect was observed in cancer cell culture models. The efficacy of these two agents combined with chemotherapy treatment was established to be highly effective, especially in melanoma, bladder and lung cancers without any toxicity. The main factor limiting the use of these agents in combination therapies is that they are only effective when mitochondria are functional which may not be the case in aggressive tumors.

Cancer treatments can be indirect or direct, depending on the effect of the agents used. Direct treatment drugs are usually targeted at enzymes, genes, or proteins, to change signal responses. The common reagents in direct cancer treatment involve monoclonal antibodies, tyrosine kinase inhibitors, and angiogenesis inhibitors. Monoclonal antibody production, which is one of the preferred approaches for the treatment of cancer, has a significant extent because monoclonal antibody treatment has fewer side effects than the previous agents used. One example for direct treatments is the use of the Rituximab, a monoclonal antibody against β-cell lymphomas. In indirect treatment, epigenetic regulators and hormone receptor inhibitors are used. Hormone treatment against cancer is one of the most abundant anti-cancer strategies, and the agents that have been used to inhibit hormone receptors, have been extensively tested in the cancerous cell lines. These drugs may either inhibit hormone receptors or block hormone production. As a result, the expression of various genes may decrease so that apoptosis is either inhibited or triggered.

In addition, there are many other cancer strategies developed parallel with the advancements in technology, molecular methods, and therapies. These advancements enabled novel ways to treat cancer, such as suppressing cancer stem cells [157].

1.5.2. Antiglycolytic Targets

Metabolic changes occurring in cancer cells are indicated as the most important characteristics of cancer among the cancer hallmarks. The regulation of metabolic pathways differs based on the cancer type. Upregulated aerobic glycolysis by lactic acid fermentation is the most important mechanism which is known as the Warburg effect [156]. Warburg effect is a beneficial advantage for most cancer cells. Even in the presence of adequate oxygen, proliferating cancer cells tend to produce lactate, yielding less energy by glycolysis than OXPHOS. This metabolic behavior seen in cancer cells offers them a vital advantage compared to normal cells for rapid proliferation. It makes them resistant under hypoxic conditions, contributes to the production of amino acids and nucleosides for their reproduction, and provides energy production by increasing glycolysis by the rapid route [159].

There are many active intermediates and enzymes involved in the redirection of glucose metabolism in cancer cells, such as specific membrane transporters; glucose transporters (GLUTs) and lactate transporters (MCTs). Many chemical agents targeting glycolytic pathways have been developed and used until now. Anti-cancer targets in different steps of the glycolytic pathways are glucose and lactate membrane transporters, hexokinases, phospho-fructokinases, enolases, pyruvate kinases, lactate dehydrogenases, monocarboxylate transporters [190].

Anti-metabolite drugs are not only against a single type of cancer. As in resistant cancers, the same mutations are common in these types of cancer-sensitive cancers, but for most cancers, the response to malignancy is difficult to predict genetically. In fact, faster response to anti-metabolite chemotherapies promoted a metabolic therapeutic approach, and this orientation provided a window beyond the response to DNA damage and proliferation rate. Although the ongoing changes as a result of antimetabolite therapies cannot be fully understood, understanding all the changes in the pathways and development of anti-metabolite drugs will enable to provide precise solutions against cancer, directly and effectively [191].

Glucose transporters are composed of a series of proteins which provide mobility across the bilayer membrane. There are 14 isoforms of the GLUT proteins possessing similar

characteristics, however, residing in different locations in the cell, and varying in kinetic properties, and their affinity to glucose and other hexoses. Expression level of GLUT was associated with metastatic potentials of the relevant cancer type [244]. With the discovery of the crystal structure of GLUT 1, the discovery of GLUT1 inhibitors as anti-cancer drugs have drawn significant interest [245]. After the discovery of GLUT inhibitors, various chemical agents have been developed. For example, WZB117, a kind of phenolic ester, was one of the first developed GLUT inhibitors. It has been reported to exhibit antiproliferative effect on H1299 lung cancer [245,247] by suppressing the uptake of glucose by a high rate of GLUT inhibition. The synergetic effect of this agent with oligomycin, which is a mitochondrial inhibitor, has been tested on the A549 lung cancer line and found to reduce proliferation rate of this cell line. As a result, senescence, cell cycle arrest and necrosis were shown in the cells.

In addition, one of the most frequently considered targets is hexokinase enzymes and specific inhibitors against hexokinases have been also developed. The first step in glycolysis is carried out by the hexokinase enzyme which transfers the phosphate group from the ATP to glucose. The HK2 isoform of this enzyme is known to play an important role in the reprogramming of glycolysis in tumor cells. First, the increase in the expression level of HK2 causes an increase in the glycolytic rate. Also, HK2 forms a complex with the voltage-dependent anion channel (VDAC) on the outer membrane of the mitochondria, and inhibits apoptosis by blocking the release of cytochrome C from mitochondria [243].

1.5.2.1. Phosphofructokinase (PFK)

Phosphofructokinase has 2 isoforms, PFK1 and PFK2. The conversion of fructose-6 phosphate to fructose 1-6 biphosphate is done by the addition of a phosphate group from ATP. This reaction is an irreversible reaction which is very sensitive to environmental changes, such as pH. When the activity of this enzyme increases, glycolysis is promoted. The activity of PK1 is determined by the concentration of 6-phosphofructo-2-kinase / fructose-2.6-biphosphatase (PFK-2 / FBPase). Because it serves as a kinase and phosphatase, PFKFB3 belonging to the PFK2 / FBPase family is overexpressed in hypoxic tumor microenvironment for the regulation of HIF-1α. The increased kinase activity of PFKFB3 enzyme in these tumors probably contributes to high glycolytic activity. Today,

PFK inhibitors are still being developed, even some of the inhibitors are being used in phase trials. Some inhibitors have proven to be successful, but they are only effective in toxic doses, therefore cannot be used as an effective agent.

1.5.2.2. Phosphoglycerate mutase (PGM)

Pyruvate kinase is involved in the transfer of a phosphate group from phosphoenolpyruvate to ADP in the glycolytic pathway. One isoform of this enzyme, PKM2, can exhibit differential levels of activity in its tetrameric and dimeric forms. Allosteric activators of this enzyme are fructose-1,6-biphosphate and serine amino acid, which are intermediates of glycolysis. The increase of less active dimeric PKM2 decreases the rate of glycolysis, but its increase has also been observed in different cancer types. In its dimeric form, PKM2 can cause accumulation of all glycolytic intermediates, thus ensuring an increment in the levels of metabolic intermediates required for the anabolic reactions. Because of these opposing properties, many PKM2 activators and inhibitors have been developed. Pyrazole-carboxamide, SGI-10067 and AG-348 are among the PKM2 activators that have been developed and employed in clinical trials [160-161-162].

1.5.2.3. Enolase (ENO)

Enolase is a glycolytic enzyme which is responsible for its conversion to 2-phosphoglycerate to 2-phosphoenolpyruvate. The expression level of the alpha-enolase isoform (ENO1) of this enzyme has been shown to increase in some cancer types. Muller et al. showed that enolase may be the target of anti-cancer treatment. The ENO2 isoform replaces ENO1 when the ENO1 gene is deleted in glioblastomas. In a similar example, the ENO1 gene knockout cells have proven to be very sensitive against substrate-enolase inhibitor analogue called phosphonoaceto-hydroxamate.

1.5.2.4. Pyruvate kinase (PK)

Pyruvate kinase is involved in the transfer of a phosphate group from phosphoenolpyruvate to ADP in the glycolytic pathway. One isoform of this enzyme, PKM2, can exhibit

differential levels of activity in its tetrameric and dimeric forms. Allosteric activators of this enzyme are fructose-1,6-biphosphate and serine amino acid, which are intermediates of glycolysis. The increase of less active dimeric PKM2 decreases the rate of glycolysis, but its increase has also been observed in different cancer types. In its dimeric form, PKM2 can cause accumulation of all glycolytic intermediates, thus ensuring an increment in the levels of metabolic intermediates required for the anabolic reactions. Because of these opposing properties, many PKM2 activators and inhibitors have been developed. Pyrazole-carboxamide, SGI-10067 and AG-348 are among the PKM2 activators that have been developed and employed in clinical trials [160-161-162].

1.5.2.5. Lactate dehydrogenase (LDH)

Lactate dehydrogenase is one of the substantial enzymes in the glycolytic pathway which transforms pyruvate to lactate as it promotes the conversion of its cofactor NADH to NAD by oxidation. The isoforms of LDH in muscle and liver tissues in humans are LDH-A and LDH5, respectively. In some studies, it is suggested that increased LDH-A levels in aggressive cancers play a role in cell proliferation, thus promote survival even in low oxygen conditions. For this reason, inhibition of this enzyme in the glycolytic pathway has been accepted as a crucial target in cancer research [163].

1.5.2.6. Monocarboxylate transporters (MCT)

The enzymes responsible for intracellular transport of monocarboxylate derivative compounds, such as lactate and ketones are monocarboxylate carriers. In humans, there are 14 MCT isoforms, MCT1 and MCT4 being the most well-knowns. Due to their overexpression in certain cancer types, MCT1 and MCT4 have been pointed out as anti-cancer agents [164].

1.5.2.7. Hexokinase (HK)

The enzyme in the first stage of glycolysis is hexokinase, which initiates the glycolysis reaction. It transfers a phosphate group from ATP to glucose to form glucose-6-phosphate.

The increase in the hexokinase enzyme increases the rate of glycolysis. It also interacts with the voltage-dependent anion channel (VDAC) present in the outer membrane of the mitochondrion, thereby inhibiting the release of cytochrome c from the outer membrane of the mitochondria, and preventing apoptosis. Because of these important properties, the role of isoform 2 of hexokinase in tumor cells has been linked to modified glycolytic mechanism in cancerous cells [165].

It has been a selective target for cancer treatment, and highly selective and active inhibitors are still being investigated by many pharmaceutical companies [165,166].

Akt (protein kinase B) promotes the association of VDAC with HK2 in the mitochondrial outer membrane by signaling, thus activates the enzyme, eventually resulting in inhibition of apoptosis [165-166]. The molecular mechanism of the anti-apoptotic activity of hexokinase is still not fully understood [169-170-171].

A glucose kinase enzyme which is a hexokinase type-IV was found to be present in the mitochondrial complex containing another BAD, which is particularly expressed in the liver and interacts with VDAC [172]. BAD is a pro-apoptotic molecule of the Bcl-2 family, inhibiting Bcl-XL and taking part in apoptosis. Hexokinase and the mitochondrial complexes in which it interacts, may play an important role in homeostatic processes, such as glucose and apoptosis. Thus, it is possible that this enzyme plays an important role in the survival of cancer cells and apoptosis, and may be one of the precursors of possible anti-cancer targets [173].

1.6. MITOCONDRIA AND CANCER

Mitochondria are not only a cell energy depot, but also a signaling organelle that can detect and manage stress signals, functioning in the adaptation to the environment. Mitochondria are known to have a role in cell death pathways, stress perception, and metabolic events. It will be useful to investigate mitochondrial pathways in detail in terms of development and feasibility of cancer therapies [237].

1.6.1. Mitochondrial Cell Death Mechanisms

Escaping from cell death mechanisms which is one of the cancer hallmarks, is closely related to the mitochondria. The pro-apoptotic Blc-2 family BAX and BAk settle into the outer membrane of the mitochondria, and oligomerized to permeabilize mitochondrial outer membrane. Membrane pores are formed, and cytochrome C (Cyt *c*) molecules are released, which in turn activates caspases. In healthy cells, anti-apoptotic regulators Bcl-XL and Bcl-2 bind to each other, and inhibit the BAX / BAK complex. However, tumor cells regulate these pro-apoptotic genes, they either downregulate Bcl-2 genes or upregulate anti-apoptotic Bcl-2 genes. This balance between pro- and anti-apoptotic genes or proteins affects the sensitivity of the cancer cell to apoptosis [235-236].

Cyt *c* release in cultured cells is one of the first markers of apoptosis. In this process, bioenergetic processes either slow or stop. The respiratory rate, the membrane potential, and the pH in the cytosol begins to decrease. The decrease in the membrane potential and the respiratory rate is consistent with each other since cyt *c* acts as an electron shuttle in the electron transport chain in the mitochondria. Release of cyt *c* cannot activate caspases if the muscle inhibitors are activated, and apoptosis is blocked. In this case, respiration rate and membrane potential are preserved despite the release of cyt *c* from the mitochondria [236]. The permeability of the plasma membrane is increased by using digitonin, and it can be restored with the addition of extra cyt *c*.

1.6.1.1. Apoptosis and Pancreatic Cancer

Bcl-xL plays an important role in the prevention of apoptosis mediated by Fas and TRAIL in pancreatic carcinoma cell lines. By binding to APAF-1, it inhibits the association of APAF-1 with procaspase-9, and prevent caspase-9 activation. Unlike Bcl-2, Bcl-xL is overexpressed in the pancreatic cell lines so that resistance against Fas-mediated apoptosis is established [241].

Another pro-apoptotic protein is BAK. In pancreatic cancers, BAK expression and apoptosis are upregulated at the sites of tumor inflammation. This has been shown to accelerate tumor progression and metastasis. Bad has been shown to bind to BAK via the BH3 domain, and also bind to both Bcl-2 and Bcl-X1, therefore mediate apoptosis [240].

1.7. GLYCOLYSIS AND CANCER

Dependence of cancer cells on glucose and increased their aerobic glycosylation capacity have been considered to be a feature that distinguishes them from normal cells. Their sensitivity to glucose is a useful feature for monitoring tumors. Also, the metabolic differences between healthy and cancerous cells are known as the most known cancer hallmark. Since the discovery of the metabolic hallmark of cancer, it became a widely investigated topic in oncogenic research [186].

In the 1920s, when the cancer cells were found to have a high rate of aerobic glycolysis by Otto Warburg, Warburg asserted that cancer cells gained this function through dysfunction of oxidative phosphorylation. In later years, it has been suggested that the OXPHOS system in the mitochondria may be suppressed in cancer cells. Sidney Weinhouse claimed that the tumor cells could not oxidize glucose and started a discussion with Warburg [187,188].

While high levels of glycolysis are provided in normal cells, and OXPHOS can be maintained normally, the same does not apply to cancer cells. Since cancer cells require high energy in anabolic processes, they have to increase the capacity of both glucose and OXPHOS metabolism to sustain vital activities [189]. Cells located near the center of the tumor along with the tumor progression are exposed to high hypoxic conditions, and the glycolysis rate increases as the OXPHOS rate decreases.

Glucose metabolism is involved not only in glycosylation but also many other pathways. One of them is the pentose phosphate pathway which is required for NADH and ribonucleotide synthesis. The hexamine pathway is necessary for biosynthesis of glucose and proteins as it allows the formation of glycogen stores and the biosynthesis of serine, respectively. In addition, carbon metabolism is required in the production of NADPH. It is also necessary for purine and glutathione synthesis, and methylation processes.

The first step in glycolysis is the reaction catalyzed by hexokinase which transfers phosphate to glucose to produce glucose-6 phosphate (G6P). This allows the transport of glucose via the glucose transporters. In this step, phosphorylation of glucose is common not only for glycolysis but also for the pentose phosphate pathway (PPP), glycogen, and hexamine processes. The pentose phosphate pathway is composed of two separate

branches which are oxidative and non-oxidative. Oxidative pathway can form NADPH and ribulose-5 phosphate in three irreversible reactions. Non-oxidative pathway can induce the synthesis of ribonucleotides by many reversible reactions. NADPH production through PPP is important because NADPH modulates redox balance, fatty acid synthesis in cells, and the synthesis of DNA and RNA by producing the pentose phosphates. Both oxidative and non-oxidative pathways of PPP are upregulated in in fast-growing cancer cells, but they can be modulated by the abundance of various metabolites and the redox status of the cells. Cancer cells upregulate the excretion of hexokinase2, thus glucose uptake, as opposed to normal cells. Thereby, the first step of glycolysis is upregulated. The second step of the glycolysis is performed by phosphofructokinase1 (PFK1), while the third step is catalyzed by pyruvate kinases. PFK1 converts F6P into fructose-1,6 bisphosphate, and pyruvate kinases convert phosphophenolpyruvate (PEP) into pyruvate. Downregulation of the last stage of glycolysis directs the intermediate metabolites to different pathways, including PPP, and serine biosynthesis pathway. This orientation promotes the upregulation of anabolic reactions required for the growth and proliferation of the cells. Since the last step of glycolysis in which the conversion of PEP into pyruvate is downregulated, the conversion of pyruvate to lactate is significantly increased. Although pyruvate formation is inhibited, it is ensured that NAD^+ is regenerated to be used in the other biochemical pathways.

1.7.1. Hexokinase and 3-Bromopyruvic Acid

3BP is a second-generation glycolytic inhibitor. Co-treatment of 3BP and cis-platinum have shown that the combination of the two drugs are more effective than the independent effect of each drug. 3BP treatment results in a reduction of ATP levels in the cell, thereby inactivating the resistance mechanism against cisplatin. Therefore, 3BP is a powerful chemical that reverses the phenotype in cancer cells having multiple drug resistance mechanisms. 3BP treatment has been used as an anti-glycolytic stand-alone agent or a co-treatment component, resulting in promising effects [193-195]. 3BP is a structural analog of pyruvic acid, and is a highly reactive chemical. 3BP functions in protein alkylation. The alkyl chain preferably binds to cysteine residues of certain proteins, altering their structure. In protein alkylation, this change in the active region of the protein is also called protein pyruvylation. As a result of this process, a bromide radical is released [196,197].

It is envisaged that 3BP enters to the cells via MCT which normally functions in lactate transport. This transport in cancer cells is thought to be highly effective due to excessive expression of MCTs [199]. In addition, lactic acid and 3BP differ only in a single atom. The increased glycolysis rate in the cancer cells provides a pH gradient across the membrane. This makes it easy to take up 3BP (Figure 1.5). When the appropriate 3BP concentration is given, normal cells and erythrocytes are not damaged because of the low expression level of MCT [191-201]. In the latest studies, VDAC in the mitochondrial membrane has been shown to inhibit 3BP and the mitochondria-associated hexokinase, which is a HK2 isoform. In addition, 3BP is also known to react with the sulfhydryl groups [199].

Another target of 3BP is the GAPDH enzyme. In most cancer cells, this enzyme is also highly expressed, and it is associated with tumor progression. In addition to being a glycolysis inhibitor, 3BP reduces the synthesis of mitochondrial ATP. Therefore, ATP reserves are rapidly decreased, thus the cells undergo apoptosis [202-205]. After 3BP treatment, apoptotic bodies have been reported to be formed [206]. The reason why each cell has a different sensitivity level to 3BP is that 3BP has different transport mechanisms in different types of cell, being mainly regulated by the differences in the pH gradient of the membranes. Another mechanism of action of 3BP is the production of ROS. One of the defense mechanisms used by the cells to get rid of the harmful effects of ROS is to reduce the production of glutathione (GSH). The sensitivity of the cells to 3BP is linked to its association with GSH [212].

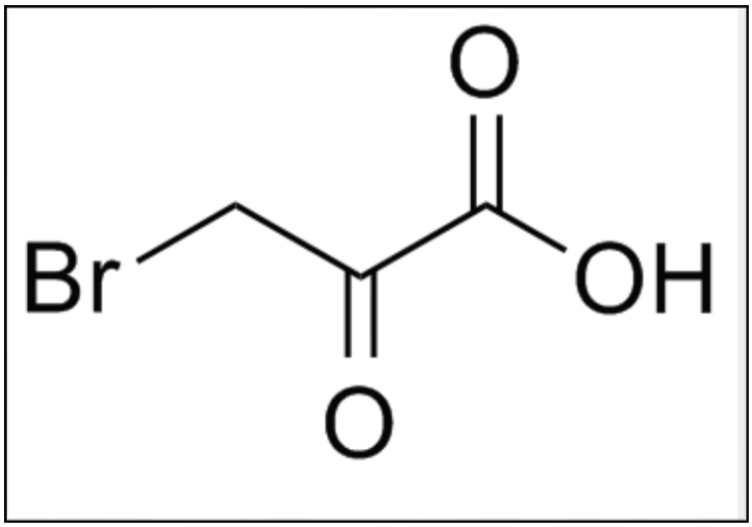

Figure 1.5. Chemical structure of 3-bromopyruvic acid [199]

1.8. SIRTUIN PROTEINS AND THEIR ROLES IN CANCER TREATMENT

The relationship between cancer metabolism and sirtuins is complex, and there are many targets of sirtuins that have not yet been identified. Downregulation of sirtuin activity is correlated with susceptibility to cancer. In contrast, sirtuins can aid in the development of resistance against chemotherapic drugs when their expression is upregulated. For example, knockout of SIRT1, SIRT2, SIRT3, SIRT4, or SIRT6 is found to increase the susceptibility to cancer in mice models. SIRT1 has been shown to inhibit tumor progression in the mouse model. SIRT3 in humans significantly decreases in breast and ovarian cancer. SIRT4 expression was decreased in gastric cancer, some types of leukemia, stomach, bladder and breast cancer. SIRT6 was observed to decrease in colon cancer and pancreatic cancer. For example, drug resistance was found in tumors with high SIRT1 activation. In other studies, SIRT1 levels were found to be increased in cancerous tissues compared to healthy tissues. The other nuclear sirtuin, SIRT7, was found to promote cancer. Mitochondrial sirtuin SIRT3, was reported to inhibit the apoptosis of cancer cells in oral squamous cell carcinoma. Thus, it is possible to say that sirtuins are important in both the progression and prevention of cancer. Research on sirtuins, which possess positive or negative regulatory functions in different cancer cell types, may illuminate cancer progression [213-216].

1.8.1. The Glycolytic Regulation by Sirtuins

In addition to the modulation of HIF, sirtuins can also modulate glycolysis. SIRT1 regulates the glycolytic pathway in which the MYC is a transcriptional activator. SIRT3 regulates PDH activity by deacetylating, enabling the enzyme to participate in the TCA cycle of the pyruvate from direct glycosylation by activating the catalytic E1a subunit. In the absence of SIRT3, the introduction of pyruvate into the TCA cycle is inhibited. As a result, it is thought that glycolytic intermediates are redirected to biosynthetic pathways and that lactate production is performed [217-218].

Most cancer cells, may be addicted to amino acids or fatty acids for energy production, except for glycolysis. The use of these alternative energy fuels is called anaplerosis, which means reintroduction of the TCA cycle. Anaplerotic pathways are inquire alternative intermediate fuel products to form the TCA intermediates and feed the loop. In cancer

cells, the PHD enzyme that directs the pyruvate to the TCA cycle is limited, so that oxaloacetate is also restricted. The TCA cycle can be promoted from alternate pathways including glutamine, and reverses the TCA cycle and fatty acid oxidation [219-220].

Sirtuins are thought to be related to the transcriptional control and oxidative metabolism of mitochondrial biogenesis in the light of cancer researches. This transcriptional control provides Peroxisome proliferator-activated receptor γ coactivator 1α (PGC-1α). This transcriptional activator promotes tumor metastasis and progression in mitochondrial biogenesis and respiratory acceleration. Direction of mitochondrial metabolism with PGC1- α. can be directed by SIRT1 and SIRT3. This relationship with stratigraphy is still unclear. In case of fasting, SIRT1 deacetylates and activates PGC-1 α. SIRT3 promotes PGC-1 α expression and promotes mitochondrial biogenesis. SIRT1 and SIRT3 promote energy metabolism in the case of fasting [221-224].

1.8.2. The Regulation of Reactive Oxygen Species by Sirtuins

Sirtuins can regulate the ROS level in the cells. Mitocondrial and nuclear sirtuins have different functions. p53, forkhead homeobox type O (FOXO) proteins, PGC-1a, heat shock factor protein 1 (HSF1) and nuclear erythroid factor 2-related factor 2 (NRF2) is one of the transcriptional regulators in the stress defense. SIRT1 activates these regulators by deacetylates. Even at increasing ROS levels, these targets are aimed at increasing the antioxidant production in terms of regulation of ROS level and apoptosis. For example, in the event of increased starvation condition and oxidative stress, SIRT1 depresses FOXO. The postponement of FOXO may trigger some of the stress resistance genes. Furthermore, SIRT2 also deacetylates cytosolic FOXO. When PGC-1 is deacetylated with SIRT1, ROS also increases mitochondrial biogenesis and oxidative capacity to limit production [225-226].

1.8.3. Mitochondrial Sirtuins

SIRT3 can reduce ROS production via the electron transport system. SIRT3 can activate complex 1 and and succinate dehydrogenase A (SDH-A) and Complex II. After complex 1 and 2 are activated, NADH and FADH2 can accelerate the flow of electrons. Finally,

activation of complex 5 accelerates ATP production. Additionally, when the cancer cells were grown in galactose medium, it was observed that SIRT3 mediated ETS capacity increased. SIRT3 deacetylates cyclophilin D and HK2 is released from the mitochondria, hk2 being in the mitochondria is directly proportional to the increase in glycosylated metabolism at the cellular level at the same time, the released HK2 also increases oxidative phosphorylation. Through these multiple mechanisms, SIRT3 boosts cellular oxidative capacity, decreases ETC stalling and promotes antioxidant. It also promotes SIRT3's ROS production as well as ROS removal [227-228] (Figure 1.6).

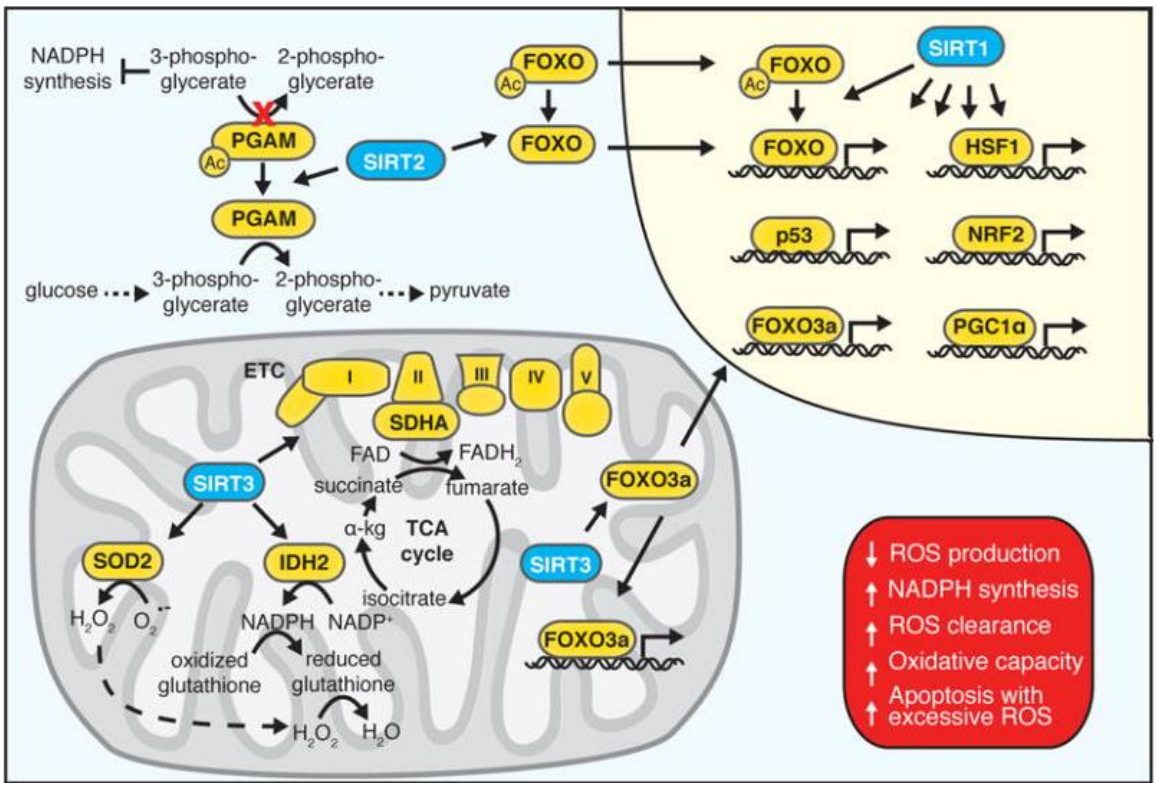

Figure 1.6. Metabolic reprogramming by sirtuins through different signaling pathways [251]

It has the task of deacetylating SOD2, which is an important enzyme in antioxidant defense. In order to remove ROS, H_2O_2 is converted to water which provides the glutathione molecule.SIRT3 can increase the level of direct glutathione [229-230].

By deacetylating and activating the TCA cycle, IDH2 (isocitrate dehydrogenase 2) provides the conversion of alpha ketoglutarate from isositrite, which produces SIRT3 NADPH. Finally, oxidative phosphorus increases the incidence of SIRT3 by interacting

with FOXO and by promoting antioxidant genes in the nucleus. With these versatile functions, SIRT3 enhances cellular oxidative activity, promotes ETC and activates antioxidant defense cascade [231].

It is a pro-apoptotic signal in which SIRT3 is capable of directing ROS cells to death by limiting the level of ROS in increasing the viability of cancer cells. Increasing or decreasing ROS production but also the role of Sirtuins as a tumor-inducing or stimulating role of Sirtuins is a research subject that should be revealed for further studies. Reduction of ROS production means restriction of tumor progression by SIRT3.

In healthy cells, ROS is reduced, inhibiting PDH enzyme activity and inhibition of HIF. Finally, SIRT3 suppresses the transition to Warburg effect and limits the pathway that provides neoplastic transformation. In the study, it was shown that increased SIRT3 expression of pancreatic cancer lines decreased ROS and suppressed proliferation by iron metabolism. Redox iron with reductions of ROS regulates the proteins associated with these proteins in which the responsive proteins are suppressed. In cases where there was no SIRT3, the level of iron increased and the pancreatic cell growth was increased [233-235].

SIRT1 is a deacetylase enzyme and can deacetylate or deactivate a large number of substrates, especially histones, and is thus associated with a doxinial pathway. Many studies have shown that SIRT1 has both tumor suppressor and tumor promoting role

For cancer cells, Sirtuin1 has been the subject of research for many years. In terms of cancer cells, the signals they target the various pathways in which they are involved vary depending on the type of tissue , the aggressiveness of the cancer cell and the cell type (Figure 1.7). However, p53, p73, and HIC1 are tumor suppressors, suppressing by deacetylating, suggesting that SIRT1 is tumor-promoting. SIRT1 can inhibit tumor growth by suppressing NF-Kβ that is a tumor suppressor and is involved in the initiation of immune response in cancer, any disorder in its regulation will trigger tumor progression. It is also involved in SIRT1 energy homoestasis, response to hypoxic conditions, and in the PI3K / AKT pathway, DNA repair mechanisms.

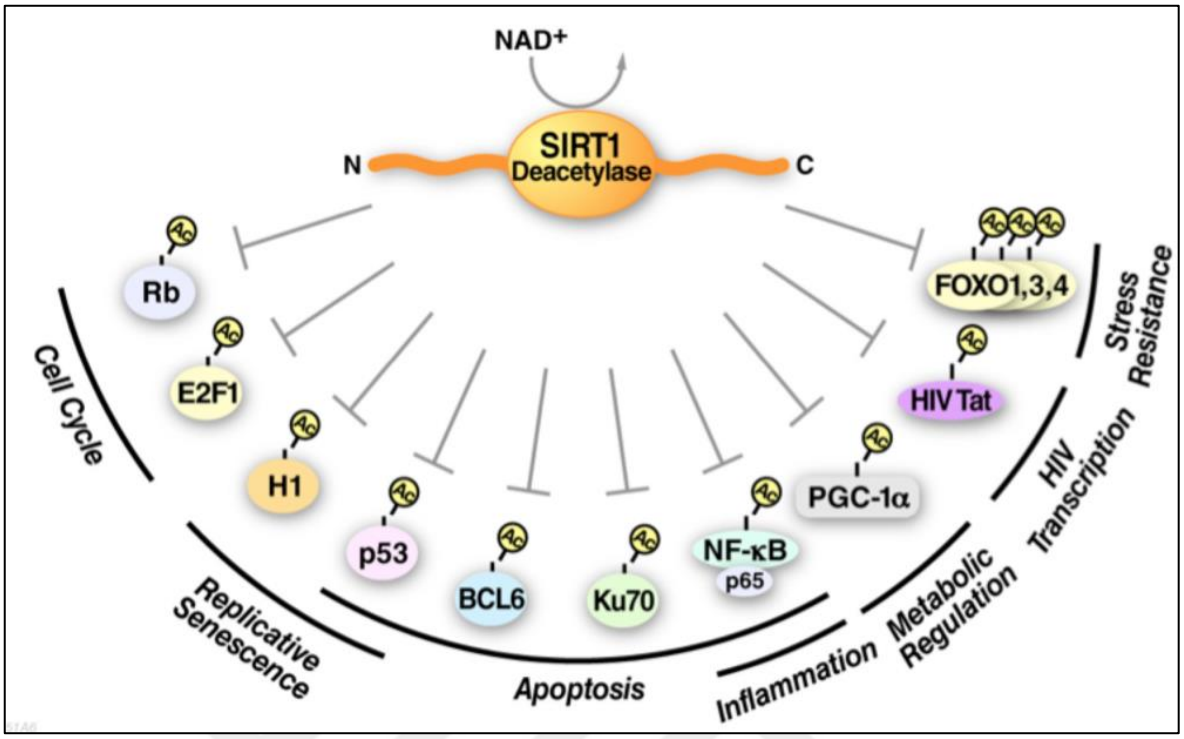

Figure 1.7. The targets of SIRT1

1.9. AIM OF THE STUDY

The aim of this study is to investigate pancreatic cancer treatment strategies, Miapaca-2 cells by using a combination of 3-bromopyruvic acid and EX527, sirtuin-1 inhibitor. This co-treatment strategy will be tried to explain whether they have synergetic effects on the cell death. Metabolic differences in Miapaca-2 cells will be elucidated and explained.

2. MATERIALS AND METHODS

2.1. CELL CULTURE

The cell line of pancreatic cancer, which is used in this study, was commercially obtained from ATCC (American Type Cell Collection).Miapaca-2 cell line was cultured with using Dulbecco's Modified Eagles's Medium- (DMEM)-High Glucose media. The media was prepared with 1 percent FBS (Fetal Bovine Serum) and 1 percent antibiotic as Streptomycin and Penicillin and 0.1 percent Amphotericin.

The Miapaca-2 cell line was taken from the frozen stock such as -86 ° C and ıt was performed after the T25 flask was suspended in complete media.

Prior to application of the EX527 chemical to the cells, the main stocks were prepared by dissolving 2 mg of EX527 in 5 ml DMSO reagent and stored at -20 ° C in aliquots. The final concentration of EX527 was added to the 5 x 10^6 concentration cells in the T75 flask with 5 µM.

Before the 3-Bromopyruvic acid was applied to the cells, the main stocks were calculated to be 1 M and the chemical material was weighed and dissolved in the cell culture incomplete media. Then, the main stock diluted to 100 µM and from this intermediate stock diluted to 50 µM 3-BP and stored at -20 ° C. The 50 µM stock was applied to cells. Cells were treated with 3-BP medium in 12 ml of media at a concentration of 12 ml in T75, and the material was freshly prepared in each experiment and applied to the cells at room temperature. After the preparation of EX527 5 µM and 50 µM 3-BP, the co-treatment concentration was determined from the same stocks, and the co-treatment agent was added to the cells in the T75 flask in 12 ml cell culture.

2.2. CELL SUBCULTURING

After the cells are attached to the flask, the old media flask containing the waste are removed and DPBS is placed to cover the surface of the cells and the cells are washed.

Depending on the flask volume, 1 to 3 milliliters of trypsin-EDTA enzyme is added to the cells.

After the addition of trypsin enzyme, the bond between the cells and the flask breaks off, and the cell-cell and cell-surface linkage disappear. Trypsin incubated with the cells in the incubator for 5 minutes that ıt is to allow the enzyme to activate and function and the cells are separated from the surface. After resuspend the cells separated from the surface to seeding the new flask ,fresh media is added to the 2 times as much as the added enzyme and then the cells taken from the falcon are centrifuged at 1500 rpm for 5 min in centrifuge.

2.3. DETERMINATION OF CONCENTRATION FOR PROTEIN SAMPLES FROM CELLS

Miapaca-2 cells were grown in T75 flasks and then resuspended with 900 microliters of RIPA solution and the resulting pellet was thawed. In the preparation of the lysis buffer content, the master mix was prepared twice as much as the pellet. Master mix called as RIPA lysis buffer that contains 1 percent protease inhibitor cocktail, 1 percent sodium orthavanadate and finally 1 percent deacetylase inhibitor cocktail in the lysis buffer called master mix. Cells resuspended with master mix were incubated on ice for 30 min and then 14000 g were centrifuged for 10 minutes. After centrifugation, the supernatant portion was removed and transferred to new Eppendorf tubes, which contained protein lysate. This process was carried out on ice as before. Protein samples obtained from control, EX-527 treatment, 50 μm 3-BP and co-treatment respectively. Samples were applied BCA test and total protein concentrations of the samples were determined. The protein lysates were sequentially diluted 1: 5 and 1:10 when performing this test. These diluted samples were placed into 96 well plates, respectively. The samples and the blank well were added to the BCA test reagent at 1:50.The plate was wrapped with aluminum foil on a 96-well plate for 30 minutes at 37 C°. After the waiting period plate 562 nm measurements were taken in the spectROScopic device and the results were analyzed in excel and total protein concentrations in each treatment and control cells were determined. All samples were aliquoted at -80 ° C and 1 percent PMSF reagent was added to the refrigerator.

2.4. IMMUNOBLOTTING

After the BCA assay, 30 micrograms of protein were loaded into wells of 10 percent Acrylamide gel in total for each sample according to determined concentrations. The wells have control, 3-BP, 5um EX527 and finally co-treatment respectively. The gel was run for 90 volts for 30 minutes and 120 for 2.5 hour. The gel was left in the hand-made Running Buffer after the running of the gel. The PVDF membrane was prepared proportionally to the size of the gel and left in methanol for 10 minutes. Methanol was kept in the transfer buffer after activation of the membrane during the incubation.

At the same time, 2 thin and 2 thick-sized filter papers were absorbed in the transfer buffer and all were paid attention to be wet. Then, following the membrane sandwich model of Thermo G2 transfer Blotter device manual, respectively; first, thick, fine filter papers the membrane taken from the transfer buffer, and finally activated and transfer buffer in the membrane that was put on and on it in the same way in 2 thin and thick filter papers were placed in the order. Both of the membranes were tightly applied over the sandwich model to prevent the formation of bubble, which was paid attention to be wet. Thermo G2 transfer device was placed in the cathode section after the cover was made sure that the closure of the membrane cassette was placed in the device properly and programmed. Transfer conditions 25 minutes 0.2 -0.5 A constant was performed. After the transfer time, the Coomasie Brilliant Blue dye was applied for 1-2 hours to ensure the accuracy of the transfer of the carefully taken gel from the device. In order to prevent the membrane from drying out, the membrane was treated with a pre-prepared blocking solution in a shaker for 1 hour. The properties of the blocking solution were changed according to the antibody used and 5 percent BSA and 5 percent milk powder were prepared in TBS-T and incubated with the membrane for 1 hour respectively. After the blocking period was over, the membrane was washed three times with TBS-T solution at 15 min intervals. After the washing steps was completed, Sirtuin3 antibody was prepared in 1: 1000 ratio in TBS-T and then poured onto the membrane and was subjected to overnight +4 degrees on the shaker. After the incubation period is over, the primary antibody is stored in a tube for storage and the secondary antibody is added at a ratio of 1: 2500 according to the antibody datasheet. After the incubation period is over, the primary antibody is stored in a tube for storage and the secondary antibody is added at a ratio of 1: 2500 according to the antibody

datasheet. The Sirtuin1 antibody was also prepared in the same manner at a ratio of 1: 1000, and the ratios and secondary antibody ratios were the same as stated above. In addition, Acetylation Antibody (Ac-K Mouse) applied in this study was prepared in 1: 2500 percent BSA in 2.5 percent BSA and 5 percent BSA was used as blocking for this antibody, and the last was Total Rodent OXPHOS Antibody Cocktail 1: It was prepared in 5000 TBS-T solution and prepared and applied as a blocking 5 percent milk powder. Finally, all of the aforementioned primary antibodies were prepared at a concentration of 1: 2500 in mouse and rabbit antibodies as secondary antibody according to the origin of each of them, as indicated in the datasheet, after each overnight in appropriate concentration and solutions. These antigens were incubated for 1 hour at room temperature on shaker and after 3 hours, TBS-T was washed 3 times with an interval of 15 minutes.

In the determination of total acetylation and OXPHOS results, wet transfer method was preferred for the transfer process. The samples were prepared for both acetylation and OXOHOS antibody, 30 µg were prepared in 10 percent Acrylamide gel followed by Wet transfer buffer (Towbin buffer contains 20 percent Methanol).

Bio-Rad Mini Trans Blot Cell System is made by a different method than the other Thermo G2 device. In the cassettes in the system, the plastic latch is inserted into one another and the other one is white and the other one is black. called sponges. Gel and fiber pad, membrane and filter paper in the Towbin buffer for 15 min and then the sandwich model was prepared. The sandwich model varies according to the white and black sides of the system the sandwich pattern made in the cassette, which faces the white surface, is as follows; first of all, after the filter pads, thin-thick filter papers, membrane, filter papers and finally wetted pads. After the latches of the gel holder cassettes are closed, the black and white surfaces must be placed in the cassette tank with the same direction. The system is embedded in ice before it is started to transfer and transfer buffer was used as cool. The running condition of the system is obtained as 1.5 h 135 mA, voltage constant. After the transfer was completed, appropriate blocking solutions were prepared for the antibodies mentioned above. Three times after blocking, TBS-T was washed .Secondary antibody treatment was performed as described above. After administration of the secondary antibody, the membrane was washed 3 times with TBS solution at 15 min intervals.

The membrane was then treated in the dark with 1ml of ECL solution (1: 1 ratio), making sure that the pipette and ECL were spread evenly over each lane in the membrane, and the

protein bands of each sample in the membrane with the ChemiDoc + XRS System after 1 minute in the dark. Chemiluminescence signals were determined. For the analysis of incoming signals, Image Lab Software 6.2 compatible with ChemiDoc + XRS System was used.

After determining the protein band profile of each sample, the membrane was washed with TBS-T 3 times for 15 min intervals. The B-actin control antibody, which had been prepared for the administration of the control antibody, was applied at a temperature of +4 degrees for 16 hours. After the incubation period, the membrane was washed 3 times with TBS-T solution for 15 minutes and the secondary anti-mouse antibody was treated on the membrane at 1: 5000 for 1 hour at room temperature. The membrane was washed 3 times in 15 minutes with TBS solution after the period was over. Then, to view the tape profile of the samples. Then, to view the tape profile of the samples. The membrane was incubated in 1: 1 ratio with 1ml of ECL solution and was used to determine the bands of samples with Chemidoc + XRS System.

2.5. QUANTIFICATION OF IMMUNOBLOTTING RESULTS

In order to analyze the Chemiluminescence signals of the protein bands in Western Blotting, Image Lab 6.0.2 Software program on the Bio-Rad website was installed on the computer and then the signals from the bands were analyzed. section "Lane and Band". After the lane numbers were determined, the lanes were placed into the resulting frame and were aligned to cover all the bands along the lane. From the lane profile tab, the boundary lines around each band and the band line on the band to be in the middle are centered in each band. For the quantification analysis of band profiles taken within the frame of each sample and for limiting background signals, the "Lane profile", which was embedded in the Image Lab program tab, was selected and the signaling of the background signal content and band profile limits specific to each band were set in peaks. This was applied to each band profile, respectively, for the beta-actin used as the control antibody and other the Western Blotting data which in this study, respectively, sirtuin1 and 3, OXPHOS and acetylation blotting. During this process, the background signals are confined to a minimum so that the difference from the background in the band profiles is minimized, and then the band boundaries are properly confirmed. After the background signal adjustments

were made for each band, lane statistics tab was clicked in Image Lab and the data was recorded in Microsoft Excel format. The next step was used as control antibody and the blotting bands were determined according to the beta-actin band profiles in excel.

However, control, 3-BP, EX-527 treated and co-treatment samples in the experimental set up were normalized to the signals from the control. In the continuation of normalization; the values of each sample taken in the triple replicates of each experiment were divided by the values obtained from the beta actin mean, respectively, and then multiplied by 100. The standard deviations and averages calculated from the values of normalization and the error bars of each sample were added on that graph.

2.6. CONFOCAL IMAGING

Miapaca-2 cells were seeded into six-well plates at a concentration of 1 $x10^6$ and left to growth conditions for 1 day to attach to the flask. The following day, after the cells were observed under a microscope, the first confocal dye was added to each plate in the DAPI incomplete cell culture media at a concentration of 5 µg / ml, the cells were incubated for 1 hour. At the end of the period, 3 times concisely and surfically washings with DPBS were performed. After washing, cells were incubated with Mitoracker-Green FM-200 nM and 5 µg / ml Rhodamine 123 dyes, respectively, for 30 minutes at 37 ° C in the dark. The plates were then washed 3 times with DPBS for 2 minutes. After the washing steps was completed, the cells on the cover slides were placed on the coverslip and quickly imaged using immersion oil in the 100X objective by Zeiss Axio M2 Imager Laser Scanning Microscope After the wash was completed, the cells on the cover slides were placed on the coverslip and quickly imaged using immersion oil in the 100X objective by Zeiss Axio M2 Imager Laser Scanning Microscopy. Pinhole size is set to 1 Airy units, Laser power is set to percent 2 and digital gain set is set between 0.7-1.0 and master gain set is set at 523-1021. On all triple repeat images, these settings were kept constant.

The main stocks of the DAPI dye were prepared to be 20 µg / ml, 10 mg of dye was weighed and dissolved with 0.5 ml of distilled-water and stored in the refrigerator at -20 C. The dye was diluted 1: 100 to be fresh and the final concentration was calculated as 200 µg / ml. 25 µl of DAPI dye was added to this wells in 1 ml incomplete media.

The stocks of Rhodamine 123 dye were also dissolved in 25 ml of distilled water to a weight of 1 mg / ml. The concentration was added to the wells in 1 ml of incomplete media at 5μg / ml.

Mitotracker-Green FM was dissolved in 74 μL of DMSO chemical to a final concentration of 1mM. Subsequently, this was reduced to a 1uM concentration from the main stock by 1: 100 dilution in the complete media.

2.7. QUANTIFICATION OF CONFOCAL IMAGING RESULTS

The images are taken from the ZEISS ZEN Lite Black 2.3 SP1 software program. After opening in the format, Mitotracker Green FM and Rhodamine dyes in the cells were determined especially by the rounded areas of all mushroom mitochondria. These drawings were done by a round selection from the toolbox drawing tab in the program. Circles drawn on mitochondria were also drawn around both cytoplasmic and nucleus for background computation. Then click on the statistics section in the program, the data was copied into Microsoft Excel. From each mitochondrial signal, the nucleus and cytoplasm were subtracted from the sum of background signals and the averages of each circle were calculated in the same excel file. Circles drawn on mitochondria were also drawn around both cytoplasmic and nucleus for background computation .Then click on the statistics section in the program, the data was copied into Microsoft Excel.

From each mitochondrial signal, the nucleus and cytoplasm were subtracted from the sum of background signals, and the averages of values for each circle were calculated in the same excel file. The calculations were calculated respectively for control, 3-BP, EX-527 and Co-treatment samples, respectively and normalized. Finally, the normalized values were multiplied by 100 and the standard deviations were calculated after the averages of each of the triple repeats were taken. For comparative graphics, Rhodamine values were divided by Mito-Tracker signals and the values were shown on the graph and error bars were placed on the graph.

2.8. DETERMINATION OF ROS LEVEL

After the Miapaca-2 cells were seeded at 6 well plates with concentrations of 1 x 10^6, the cells to be treated after the next day growth were checked under light microscopy, 3-BP, EX-527 and Co-treatment agents were prepared freshly and given in the cell culture media.

Since the total volume within each flow tube will be 100 µl. First determine how many tubes are to be used in the 10X buffer contained in the kit and then dilute to 1X.Then 1X Supplemented buffer was prepared. For each sample in supplemented buffer, 10 ul of FBS (Fetal Bovine Serum) was mixed with 90 10l of 1X kit buffer. Finally; DCFDA (2',7' – dichlorofluorescin diacetate) and TBHP solution were prepared respectively.

The DCFDA in the kit was diluted to 20 µM with 1X buffer from 20mM and stored in the dark at -20 ° C in aliquots. This dilution was prepared by mixing 1 µl DCFDA with 1ml 1X buffer for each sample during the experiment and giving 100 µl volumes to the samples.

For the cells prepared as positive control, THBP solution was taken 1 µl for each sample and mixed with 100 µl supplemented buffer to give to the cells. The final concentration of THBP (Tert-Buty Hydrogen Peroxide) each flow tube is 50 µM. After the treatment time of cells was over 24 h, Positive control cells were first treated with 50 µM of THBP solution 4 hours before and in the Eppendorf tubes, the cells were mixed into the foil and placed in a 37 degree incubator. At the end of 4 hours, the cells were spun at 1500 g after centrifugation and the supernatant part was discarded. The cells in the control and treatment and positive control tubes, except for the negative control, were mixed with 500 µM THBP solution and the final concentration was allowed to incubate at 37 degrees for 30 minutes. The tubes were placed in the incubator wrapped with aluminum foil.

In cells with negative control, PBS was transferred to flow tubes. Without any washing, direct cells were given to the flow device to read. The laser settings for flow were read at the Excitation 485 nm laser / Emission 535 nm constant at the FL1 and the gated values were calculated.

2.9. QUANTIFICATION OF ROS LEVEL BY FLOW CYTOMETRY

In the BDFACsCalibur Flow Cytometry device, the readings of the samples were studied in the instrument at the Excitation / Emission nm values mentioned above, negative control, positive control, non-treated control cells, 3-BP, EX-527 treated, Co-treated cells respectively.

After the necessary measurements have been made by the responsible technical personnel, the cells that are gated are identified in the Microsoft World file. The graph includes examples of which are calculated in different colors.

The gated values were written into the Microsoft Excel file manually. After the averages of each of the three replicates were calculated, the mean of the control cell sample was divided into the mean of the control cells after the sum of the cells were taken, and all values were normalized by multiplying by 100.

The standard deviations of the values taken as a result of the normalization and the mean values are calculated from the average of the independent repeats are calculated with the average value of the graph in the error bars are processed.

2.10. DETERMINATION OF MITOCHONDRIAL MEMBRANE POTENTIAL WITH FLOW CYTOMETRY

Miapaca-2 cells were cultured in six well plates at a concentration of 1 x 10^6. After the cells were checked under light microscopy, treatment agents applied for 24 h were given 3-BP, EX-527 and Co-treatment, respectively. The reagents in the kit are prepared in advance after the treatment time has elapsed. The FCCP (a mitochondrial membrane distruptor) used for positive control was calculated to have a final concentration of 200 nM from the main stock concentration of 50 µM in each flow tube. TMRE (Tetramethylrhodamine ethyl ester perchlorate) for determination of membrane potential of cells while the main stock was 1000 µM, the final volume was diluted to 2 µM per tube.

First, the positive control cells given FCCP were transferred to Eppendorf tubes with a volume of 1 million and then centrifuged at 1500 g for 5 minutes, then 100 µl of FCCP were treated at a concentration of 50 µM and incubated at 37 ° C for 15 minutes in a cell

incubator. After time elimination, the same cells were centrifuged again under the same conditions and after the supernatant was discarded, treated with 200nM TMRE dye at 37 ° C for 20 minutes. TMRE staining was given to non-treated control cells and treated cells (3-BP, EX-527-Co-treatede) after positive control cells. After the time has elapsed, all tubes were centrifuged at 1500 rpm for 5 minutes and washed once with PBS solution. Samples for measurement in the BIOFACs Flow Cytometry instrument for analysis were taken in flow tubes wrapped in aluminum foil in PBS. Measurement settings for the flow device Excitation: 550 / Emission: set to 580 nm. The readings of the FL1 laser were performed and the gated values were taken.

TMRE dye was dissolved in 55 µl of DMSO solution and the final concentration obtained as 1000 µM and was stored at -20 ° C in aliquots at without seeing light.

2.11. QUANTIFICATION OF MITOCHONDRIAL MEMBRANE POTENTIAL WITH FLOW CYTOMETRY

In the BDFACs Calibur Flow Cytometry device, the readings of the samples were studied in the instrument at the Excitation / Emission nm values mentioned above, negative control, positive control, non-treated control cells, 3-BP, EX-527 treated, Co-treated cells respectively.

After the necessary measurements have been made by the responsible technical personnel, the cells that are gated are identified in the Microsoft World file. The graph includes examples of which are calculated in different colors.

The gated values were written into the Microsoft Excel file manually. After the averages of each of the three replicates were calculated, the mean of the control cell sample was divided into the mean of the control cells after the sum of the cells were taken, and all values were normalized by multiplying by 100.

The standard deviations of the values taken as a result of the normalization and the mean values are calculated from the average of the independent repeats are calculated with the average value of the graph in the error bars are processed.

2.12. CELL DEATH ANALYSIS WITH ANNEXIN-PI STAINING

After the Miapaca-2 cells were planted in 1 x 10^6 six wells, the cells to be treated were treated for 24 hours and 3-BP, EX-527 and Co-treated (3-BP: EX-527) were applied respectively. The field Annexin FITC-V buffer was calculated from the sample number and delimited from 10X to 1X. After adding buffer to cells with a concentration of 1 ml, the cells were resuspended. In next step , 1 µl of Annexin V-FITCH conjugate with Propodium Iodide (PI) was added to each Eppendorf tube. All control and treated and positive control are given to PI except negative control. Negative and positive control tubes in the experiment procedure, treated and non-treated control tubes were wrapped in aluminum foil and read on BIOFACs Flow Cytometry device. The recorded data of the Microsoft World file by the device technical personnel is processed and entering the gated values into the Microsoft Excel file.

The gated values were written into the Microsoft Excel file manually. After the averages of each of the three replicates were calculated, the mean of the control cell sample was divided into the mean of the control cells after the sum of the cells were taken, and all values were normalized by multiplying by 100.

The standard deviations of the values taken as a result of the normalization and the mean values are calculated from the average of the independent repeats are calculated with the average value of the graph in the error bars are processed.

2.13. THE ISOBOLOGRAM ANALYSIS FOR THE SYNERGETIC EFFECT OF 3BP AND EX527

When two or more drugs are given in the treatment of cancer, it may show superadditive synergistic effect as a result of the combination effect. This effect means the effect of the individual effect of each drug. In contrast to the synergistic effect, some drug combinations may show simple additivity or subadditivity. Additivity effect; does not mean the simple addition of the effect size of drugs on each other. It comes from the concept of dose equality and quantitative modeling based on synergism and antagonism. The most basic quantitative assessment method for estimating the interaction between drugs or the direction in which this effect is conducted is the isobol graphs. This process, which was

produced by graphical drawing, was first developed by Loewe, and these graphical processes were developed to determine dose combination sets showing the effect of each drug at a specific dose expected. The effect level of the drug applied in order to determination of the maximum effect of the drug with a maximum 50 percent effect is the most used effect level in this analysis. Therefore, doses of the drug at different concentrations of the drug, which show this separately for the full antagonistic effect of each drug, are IC50 doses. In the simplest form of this procedure, IC50 doses are preferred. In the literature, different IC values are used in the graphs included in this thesis due to the compatibility of different combinations which are used in different and wide range in addition to ED50 doses. In addition to the effect of ED50 dose, respectively; The IC30,IC70, IC90 values were chosen to determine a full effect dose of different doses of both EX527 and 3BP drugs and to confirm the compliance of this effect dose with the expected 50 μM 3BP and 5 μM EX527 chemicals. Because these percentages belonging to IC values increase as 30,50,70 percent and 90 percent, the comparison of maximum death values is facilitated and the reliability of compliance between drug doses increases. This selected IC (Effective dose) percentage values give us the most effective drug doses with maximum death. For this experiment, we tried different doses from the chemicals of both 3BP and EX527, respectively, and the cells were cultured in 96 well plates at 7500 cell / well concentrations and MTT Assay test was applied. The values obtained from the absorbances were obtained from the generated Microsoft Excel chart table and the data corresponding to the dose of IC50, IC50 percent maximum cell death, were obtained from the generated Microsoft Excel chart table and these values were calculated from the slope in the graphical formula. However, the data obtained from the MTS test for the use of different doses of 3BP and EX527 were processed to determine the values of 30,50,70 percent and 90 percent IC (ED) values for each treatment. The resulting data were plotted in a single graph and ED values in a single graph were plotted separately in a single graph, with different ED percentage values, each belonging to 3BP and EX527 at different concentrations. Subsequently, the combination concentrations of individual drugs are placed in this Microsoft Excel graph, where x and y axes represent different drugs in a Cartesian coordinate system. IC (ED) percentages of the graphs and slope formulas after the creation of the formula for the Isobologram analysis for each ED 30 percent -90 percent determined 3BP, EX527 and combinations of different concentrations for both treatments were processed in the excel file. Isobol graph values were calculated for each IC

value. The number of 50 μM used in this thesis for 3BP was divided by 30 percent IC of this concentration, and the result was divided by the number of EX527 concentration in the same combination divided by IC30.The data in the most recent process represents the combination index. If the combination index is greater than 1, antogonism is determined as synergism in small and as additive effect if it is equal to 1.

After creating slope curves drawn between each IC percent values, the resulting combination values for those values were placed on the slop. Details of this calculation have been published by Tallarida and are listed in the 190th section in the references part.

2.14. STATISTICAL ANALYSIS

The average of the data obtained from all experiments was calculated by calculating the standard deviations of the means. Each of the data obtained from all experiments was performed in triplicate repeats.

In the analysis of all experiments, unpaired Student-t test was performed using Unequal variance and selected from the "Data Analysis" tab in the additional packaged in the Microsoft Excel tool. P-values were compared with 0.05 for each experiment and the values of samples with a value less than 0.05 were determined as significant and evaluable

3. RESULTS

3.1. THE OPTIMIZATION OF MIAPACA-2 CELL TREATMENT

For the determination of the appropriate concentration of 3-bromopyruvic acid on Miapaca-2 cells, the cells were cultured at the determined time intervals about 7000 cell/well in 96 well plate with time intervals of 6, 14, 24, 48, 72 hours. Then the images of the cells were taken in 10x, 20x and 40x objectives of light microscopy. Cells were administered 10, 20, 50, and 100 μM 3BP respectively. At the end of the 24th housr, Miapaca-2 cells were directed to the colony form in which they moved away from each other and at the same time they observed their attachment properties in the plates. At the end of 48th hours, they lost their attachment to the plate. We concluded that that the 24th hours was suitable for 3BP treatment. Another treatment applied to Miapaca-2 cells was EX527, an inhibitor of SIRT1. Doses of EX527 was prepared to be 1, 2, 5, and 10 μM, respectively, and cultured in the same way. It was estimated that the chemical activity of the EX527 was observed at the end of 24 hours.

Pre-doses of 3BP and EX527 treatment agents were co-treated at the same concentrations respectively at the same time intervals. Morphologically, they tend to display their proper appearance more quickly. Cell shape of the Miapaca-2 was long and thin but after the co-treatment of cells began they appeared to be round (Figure 3.1-2-3)

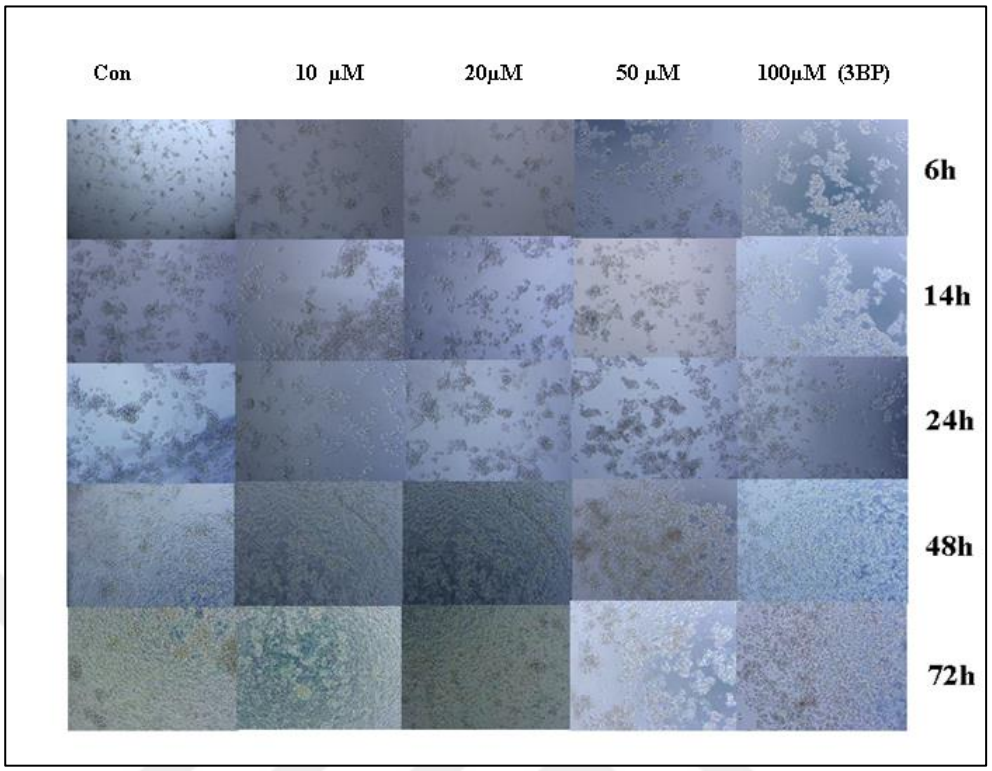

Figure 3.1. The images of cells treated with 3BP under the light microscope

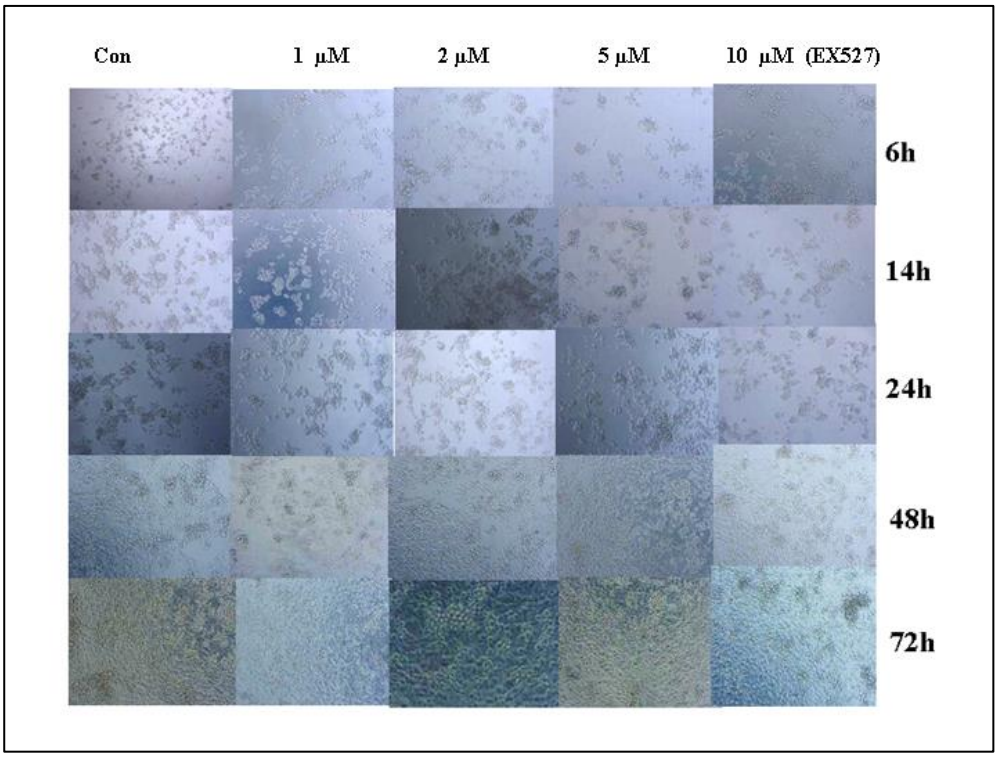

Figure 3.2. The images of cells treated with EX527 under the light microscope

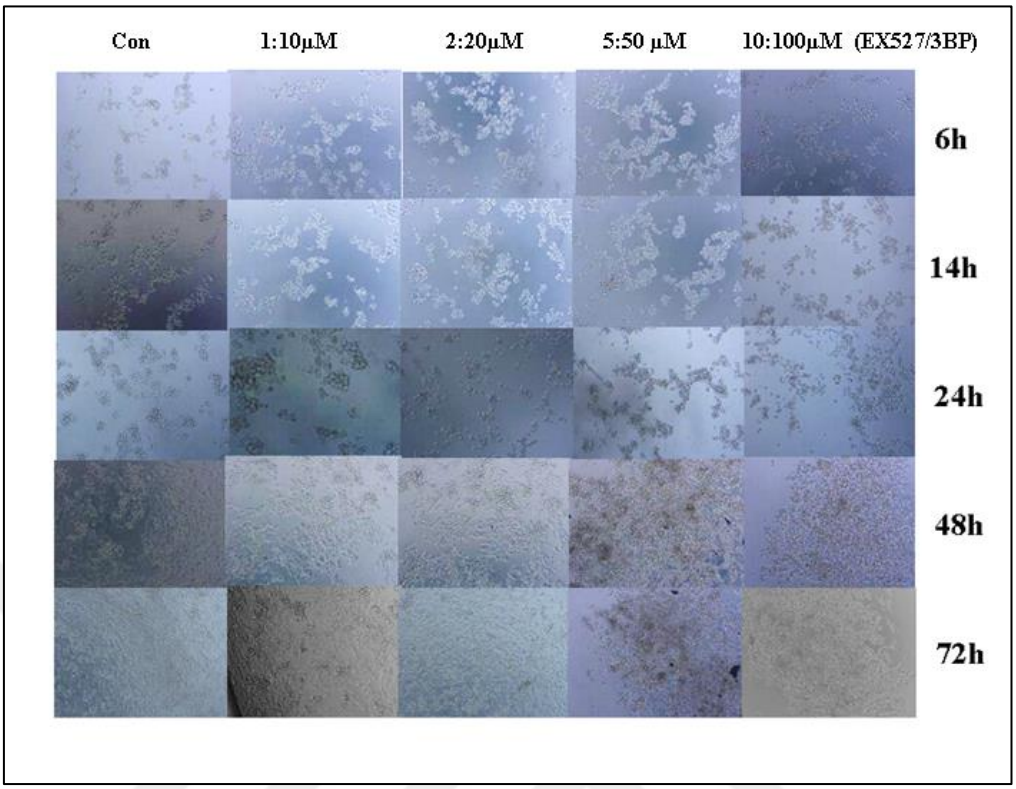

Figure 3.3. The images of cells co treated with EX527/3BP under the light microscope

3.2. THE CELL VIABILITY ASSAY WITH MIAPACA-2 CELLS

Cell viability was determined by using MTS assay kit (Abcam). The mortality rates of 3BP-treated cells with varying concentrations as 10, 20, 50, and 100 µM were determined as 80, 82, 83, and 77 percent, respectively. However, significant differences were observed for only 20 and 50 µM of 3-BP.

Cell viability of 1, 2 , 5, and 10 µM of EX527-treated cells were found as 70, 83, 77, and 68 percent, respectively (Figure 3.4-5-6). The only significant results were with 2 and 5 µM of EX527.

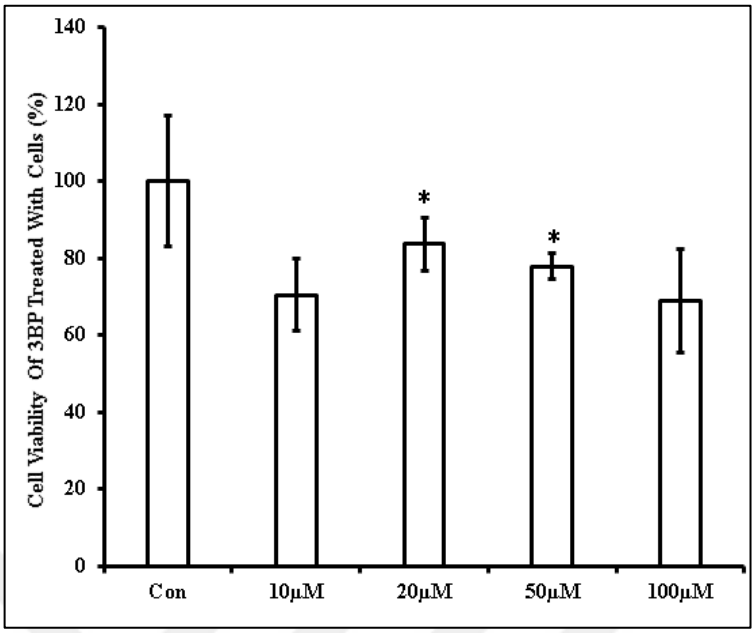

Figure 3.4. Cell proliferation assay with Miapaca-2 cell lines treated with 3BP. Signals were quantified relative to control (Con) after normalized by using corresponding treated samples. t-test was applied and $p < 0.05$ (*) was taken as significant.

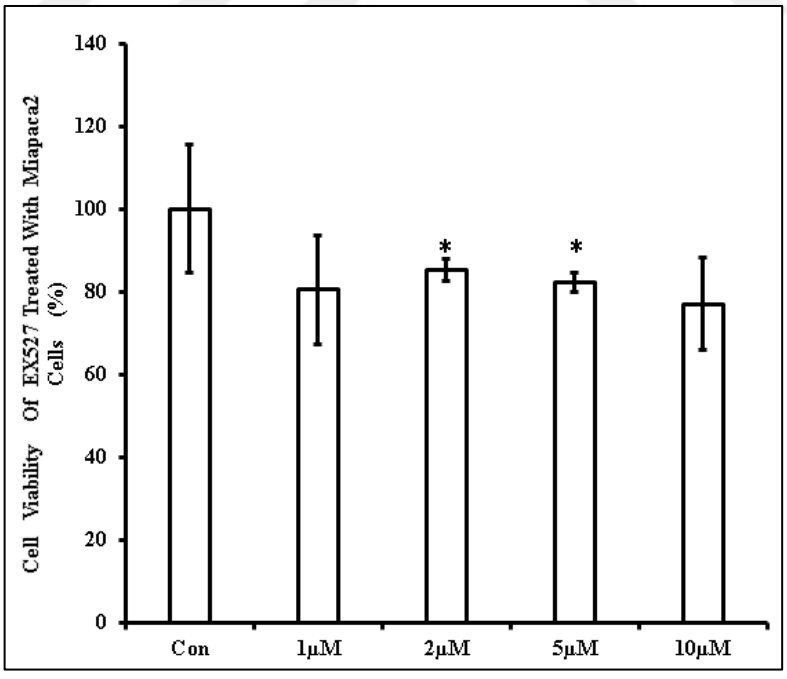

Figure 3.5. The cell viability of Miapaca-2 cells treated with EX527. Signals were quantified relative to control (Con) after normalized by using corresponding treated samples. t-test was applied and $p < 0.05$ (*) was taken as significant

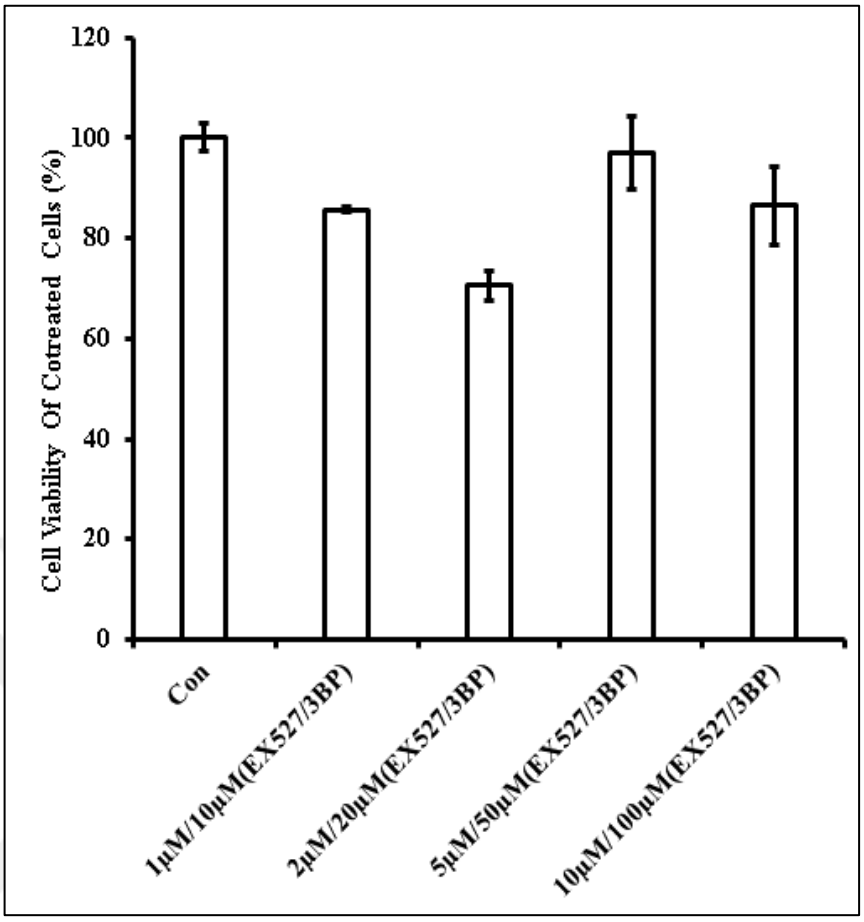

Figure 3.6. The cell viability of Miapaca-2 cells cotreated with EX5527 and 3BP

3.3. ANALYSIS OF DEATH MECHANISM BY USING ANNEXIN-PI

Annexin V-FITC early apoptotic test was used to investigate the mechanisms of death with respect to differing treatments. Annexin V-FITC is a conjugated protein that binds to phosphatidylserines present on the cell surface, which is the early apoptosis marker. It refers to necrosis in cells stained with propodium iodide (PI) that is a non-membrane permeable DNA dye. The cell viability ratio of co-treated cells compared to control was reduced by 60 percent. It was observed that necrotic tendency increased in Miapaca-2 cells treated with 3BP and EX527. The necrotic percentage in 50 μM 3BP-treated cells increased by 413 percent compared to the control and increased by 686 percent in the EX527 treated cells. The rate of late apoptosis in Miapaca-2 cells treated with 3BP and EX527 were increased by about 4,000 and 3,000 percent compared to control, which were the highest level of changes upon treatment.

The most important outcome is that when control cells and co-treatment cells are compared, the apoptosis increased approximately by 14,000 percent. In addition, samples with the highest rate of apoptosis were observed in co-treated cells with an increase of 174 percent. One of the most crucial information is that cells are directed to late apoptosis due to synergetic effect by co-treatment. The ratio of late apoptosis in cells treated with EX527 and 3BP separately is less than 3 times when compared to the co-treated cells. This is an evidence that an effective treatment strategy is applied on Mipaca-2 cells (Figure 3.7).

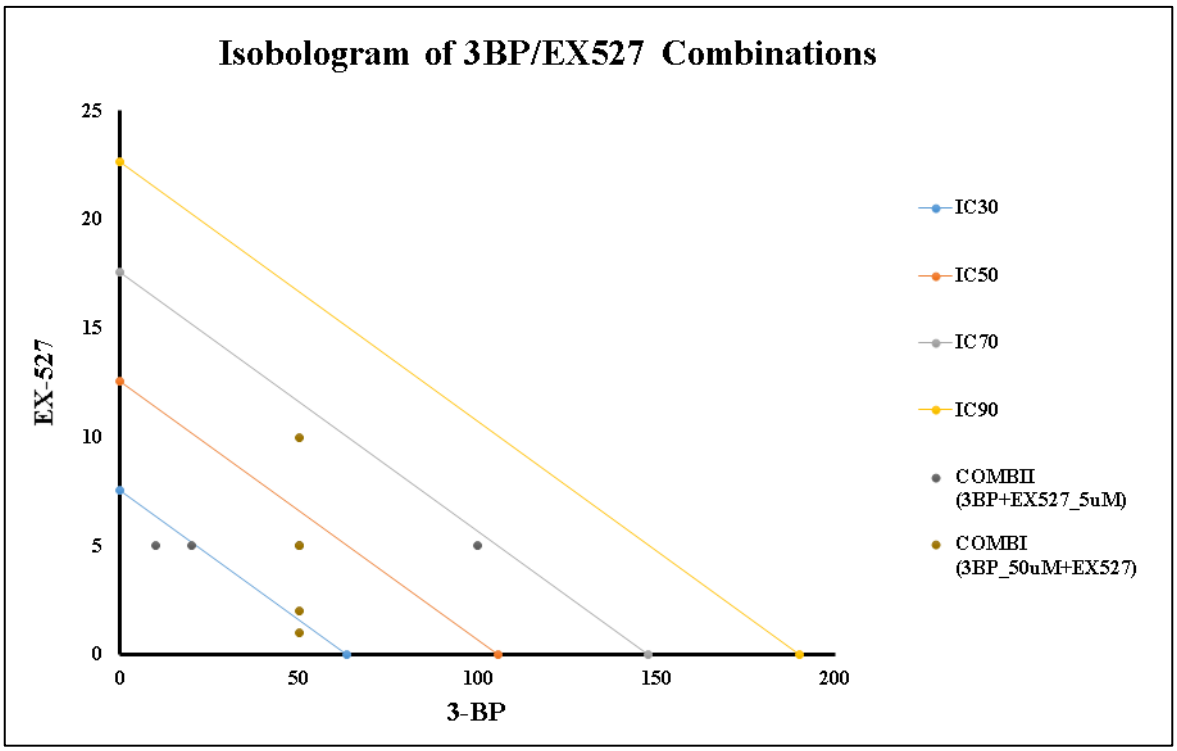

Figure 3.7. Isobologram analysis in the Miapaca-2 cell lines. Miapaca-2 cells were treated with 3-bromopyruvic acid (50 µM 3BP), 6-Chloro-2,3,4,9-tetrahydro-1H-Carbazole-1-carboxamide (5 µM EX527), and both (CoT).

3.4. ANALYSIS OF SYNERGETIC EFFECT IN MIAPACA-2 CELLS TREATED 3BP,EX527 AND CO-TREATMENT

The synergetic effect of the cells on the Miapaca-2 cells were determined after IC30, 50, 70, and 90 values of the 3BP and EX527 treated cells were calculated. The 50 μM of 3BP treated cells were then co-treated with 1 , 2, 5, and 10 μM of EX527, respectively. In the next step, 5 μM EX527 treated cells were co-treated with 10, 20, 50, and 100 μM 3BP subsequently. These combinations were shown in Figure 3.7 as COMBI and COMBII, respectively. Each (maximal inhibitory combination) value was shown in the graph. The points above and below the lines belong to the combination index. Since the cell death rate increased as the IC values increased, the consistency between each combination index was found and the combination index (CI) were indicated by dots under the lines (Figure 3.7). In COMBII (3BP + EX527_5uM), the combination index for IC30 was calculated as 2.241, for IC50 as 0.872 IC, as for 0.249 for 70, and as 0.273 for IC90. It shows the combination indices of Miapaca-2 cells corresponding to IC30, 50, 70, and 90 respectively. Combination indexes were calculated as 2.114 for IC30, 0.871 for IC50, 0.452 for IC70, and 0.307 for IC90. Combination index values were significant only for IC50, IC70 and IC90. The combination indices for co-treatments corresponding to IC50, IC70, and IC90 values are synergistic because they were smaller than 1.

3.5. SIRTUIN-1 EXPRESSION PROFILE IN MIAPACA-2 CELLS TREATED WITH 3BP, EX527, AND BOTH

The Miapaca-2 cells were treated with 50 μM of 3BP, 5 μM of EX527 separately and together with the same concentrations of co-treatment cells in a 24 hour period. SIRT1 protein expression profile changes in cells were determined by immunoblotting assay. In normalized data, as shown in Figure 3.8 SIRT1 reduction in cells treated with 3-BP compared to control was not significant. However, there was a 26 percent decrease in SIRT1 protein level in cells treated with EX527 in addition to the significant reduction in co-treated cells (21.4 percent, $p < 0.05$) (Figure 3.8).

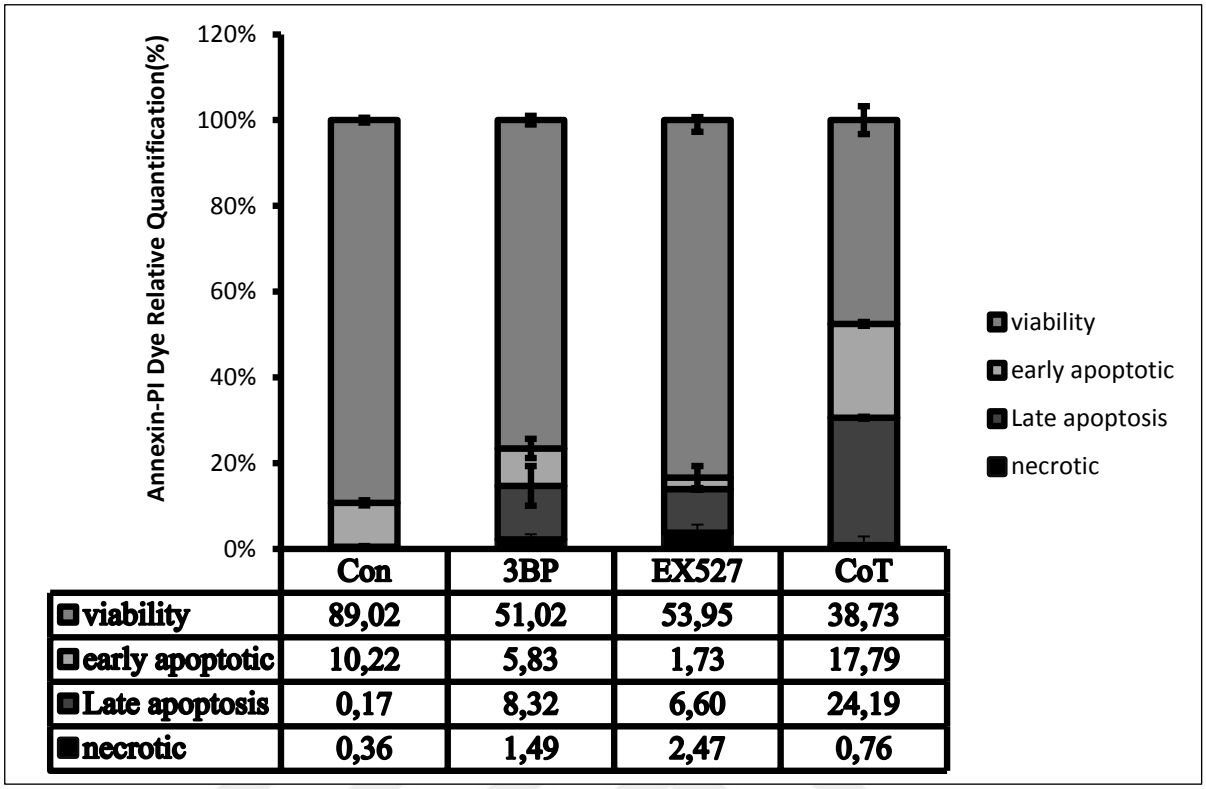

	Con	3BP	EX527	CoT
viability	89,02	51,02	53,95	38,73
early apoptotic	10,22	5,83	1,73	17,79
Late apoptosis	0,17	8,32	6,60	24,19
necrotic	0,36	1,49	2,47	0,76

Figure 3.8. Cell death mechanism analysis in the Miapaca-2 cell lines. Respectively, the miapaca-2 cells were treated with 5 μM of 3-bromopyruvic acid, 5 μM M EX-527 (sirtuin-1 inhibitor), and both with the same concentrations of co-treatment cells in a 24 hours.

3.6. SIRTUIN-3 EXPRESSION PROFILE IN MIAPACA-2 CELLS TREATED WITH 3-BP, EX-527, AND BOTH

SIRT3 protein expression changes in Miapaca-2 cells treated with 50 μM of 3BP and 5 μM of EX527 separately or together were also determined by immunoblotting. A significant reduction in all treated cells was observed for SIRT3 reduction, 10, 24, and 18.1 percent respectively. This noticeable difference is not surprising in the treated samples, especially for the EX527. The normalization values were obtained by dividing the mean of the triple repeats by the control values and multiplying by percent (Figures 3.9, 3.10).

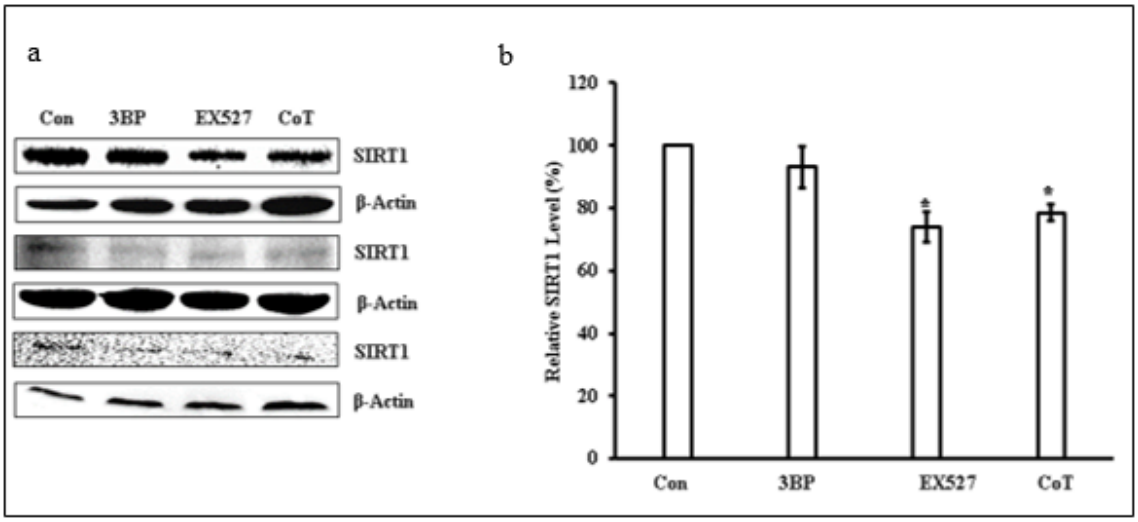

Figure 3.9. Immunoblotting analysis of Sirtuin-1 expression profile. Miapaca-2 cells were treated with 3-BP (50 μM), EX527 (5 μM), and both (CoT). (a) Immunoblotting assays were performed against sirtuin 1 (SIRT1) and beta-actin (β-Actin) antibodies. (b) Signals were quantified relative to control (Con) after normalized by using corresponding β-Actin results. t-test was applied and $p < 0.05$ (*) was taken as significant.

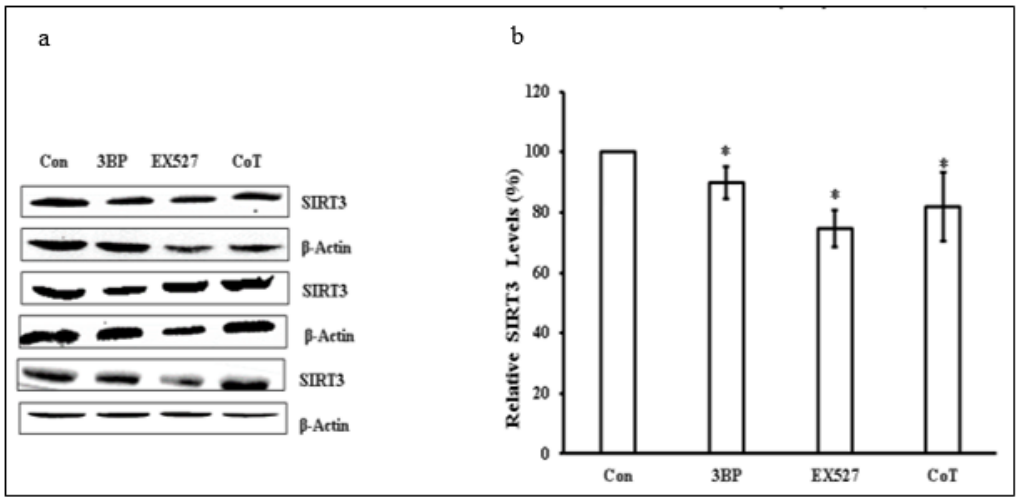

Figure 3.10. Immunoblotting analysis of Sirtuin-3 expression profile. Miapaca-2 cells were treated with 3-BP (50 μM), EX527 (5 μM), and both (CoT). (a) Immunoblotting assays were performed against sirtuin 3 (SIRT3) and beta-actin (β-Actin) antibodies. (b) Signals were quantified relative to control (Con) after normalized by using corresponding β-Actin results. t-test was applied and $p < 0.05$ (*) was taken as significant.

3.7. ANALYSIS OF CELLULAR ACETYLOME IN MIAPACA-2 CELLS

The total acetylation pattern changes in each treated protein sample were examined respectively. The different profile belongs to acetylation in the 3BP and co-treated samples were not significant. The p values are 0.35 and 0.45, respectively. The increase in the acetylation profile was found to be only 25 percent in EX527 treated cells compared to control samples ($p < 0.05$). The differences of acetylation which were obtained from the treated and non-treated samples were normalized by beta actin expression levels as control (Figures 3.11, 3.12).

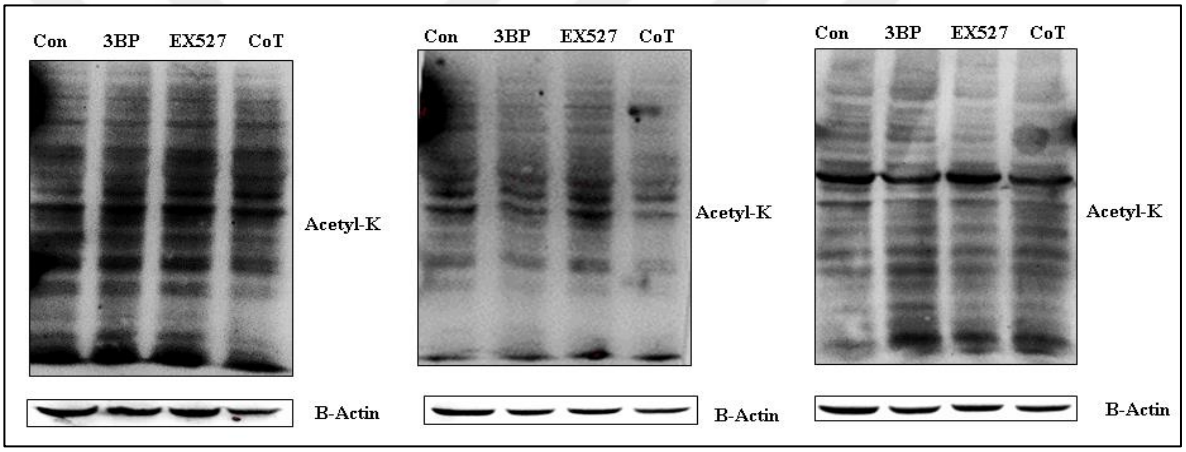

Figure 3.11. Acetylation pattern changes among non-treated and treated Miapaca-2 cells

3.8. DETERMINATION DIFFERENCES BETWEEN REACTIVE OXYGEN SPECIES IN TREATED AND NON-TREATED CELL SAMPLES

Co-treatment samples of the Miapaca-2 cells, respectively 50 μM of 3BP, 5 μM of EX527, and both of the same concentrations were applied as described in the DCFDA ROS detection assay kit protocol. The cells were seeded into the well plates, and after the procedure was performed as indicated in the kit, the cells were measured in the flow cytometry device at the appropriate excitation and emission setting. Triple samples were normalized and the differences between control and treatment samples were determined. When compared to control samples, the difference was only 33.69 and 21.2 percent in EX527 and cotreatment samples, respectively. In both cases, the number of cellular

reactive oxygen species was confirmed to decrease in all data. The p values were calculated as 0.0039 and 0.0024, respectively (Figure 3.13).

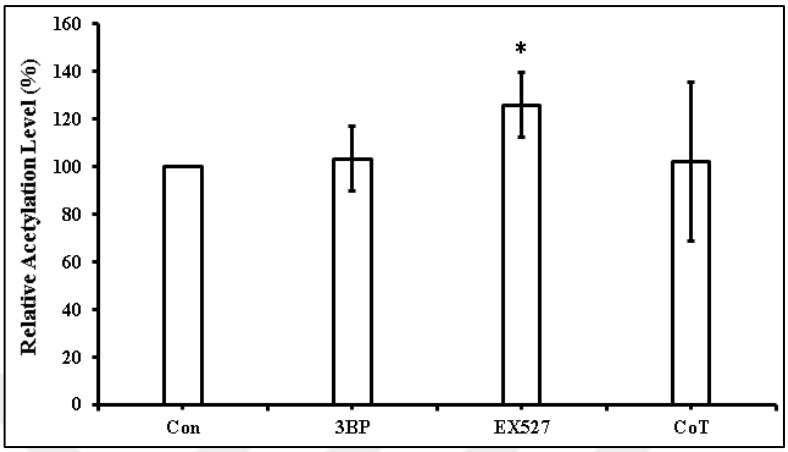

Figure 3.12. Acetylation pattern changes among non-treated and treated Miapaca-2 cells. The acetylation profile was found to be only 25 percent in EX-527 treated cells compared to control samples. ($p < 0.05$*).

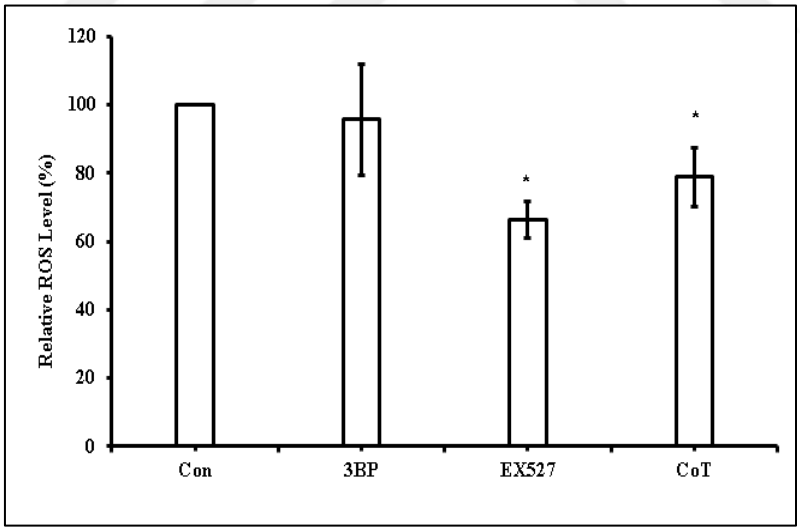

Figure 3.13. Differences in reactive oxygen species among control and treated Miapaca-2 cells. The graphic obtained from the normalized values were using the control data of the triple repeats and the treated and non-treated samples is shown above. Reactive oxygen species in EX-527 and Co-treated cells show a significant decrease in total cell. ($p < 0.005$).

3.9. DETERMINATION OF DIFFERENCES OXPHOS COMPLEXES BETWEEN TREATED AND NON-TREATED SAMPLES

The differences in mitochondrial OXPHOS complexes were examined for 50 μM of 3BP, 5 μM of EX527 and co-treated samples of Miapaca-2 cells. There was no significant change in their expression when normalized to the control, beta actin. As a result, the evaluation of the OXPHOS complexes belonging to each treatment was performed. Each triple data of treated and non-treated samples normalized by HSP60, mitochondrial control antibody (Figure 3.14). We have not found any significant difference in OXPHOS complexes (Figure 3.15).

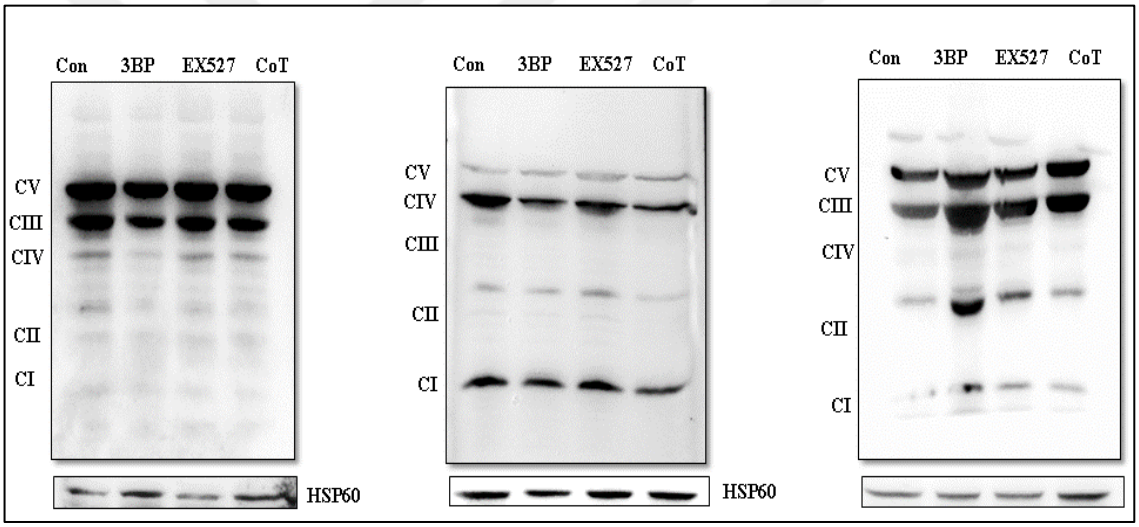

Figure 3.14. Immunoblotting analysis of respiratory chain complexes among Miapaca-2 cells

3.10. ANALYSIS MITOCHONDRIAL INNER MEMBRANE POTENTIAL AND MASS

The Miapaca-2 cells treated with EX527, 3BP and both were stained with Rhodamine123 and Mitotracker-Green FM dye. Rhodamine-123 indicates the polarized mitochondrial inner membrane, while Mitotracker dye gives information about mitochondrial mass in the corresponding cells.

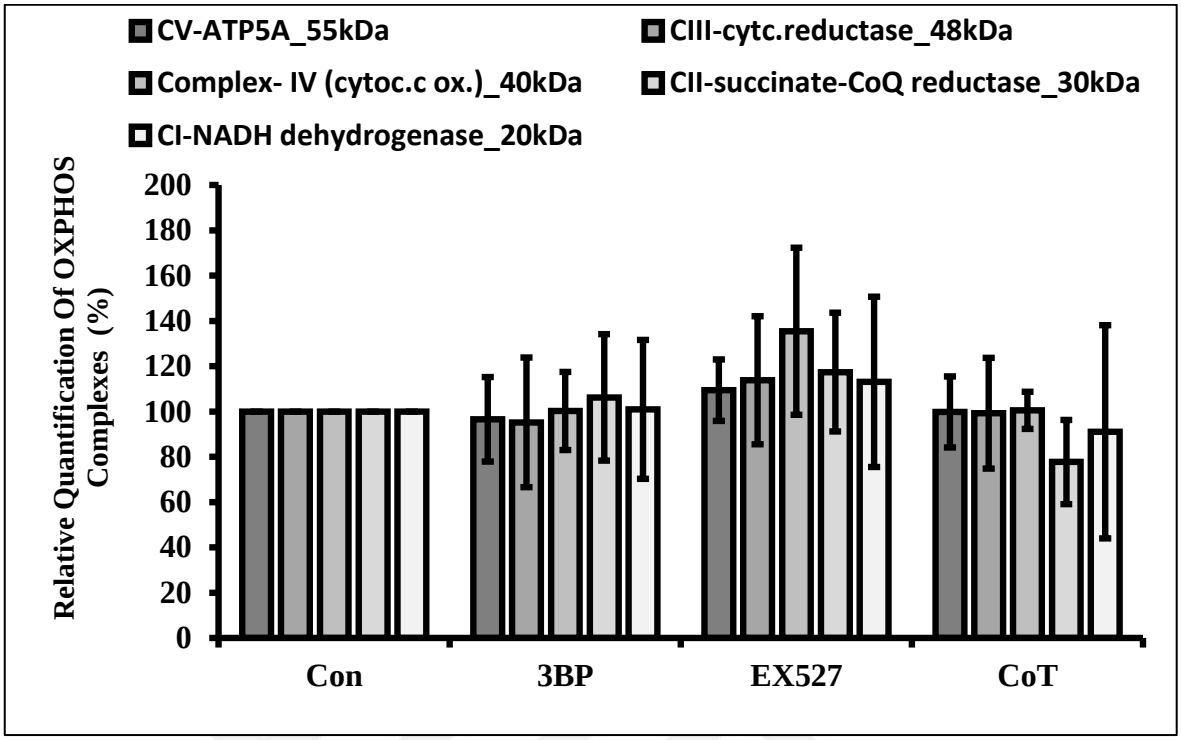

Figure 3.15. Relative quantification of changes in OXPHOS complexes in Miapaca-2 cells

Images were quantified using Zen software as triplicates. However, as a result of mitochondrial membrane potential measurement of all samples, p-value values were not lower than 0.005 and no significant changes could be obtained and co-treated samples were stained with Rhodamine 123 and Mitotracker-Green FM dye, respectively.(Figures 3.16, 3.17, 3.18, 3.19)

Mitotracker-Green FM dye binds to proteins in mitochondria and mitochondrial membrane proteomes. Rhodamine-123 is a cationic dye for measuring the mitochondrial membrane potential. Thus these two dyes were used for the indication of the total membrane potential changes on Miapaca-2 cells.

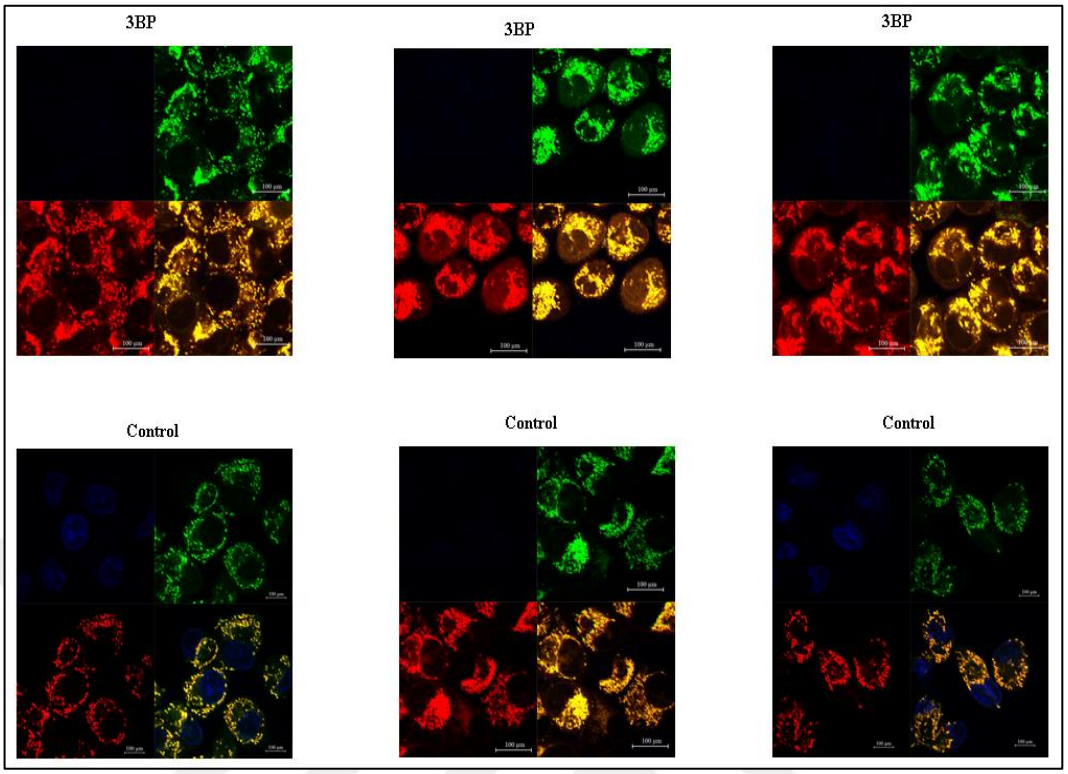

Figure 3.16. The images represent mitochondrial membrane potential differences between 3-BP treated cells and non-treated cells

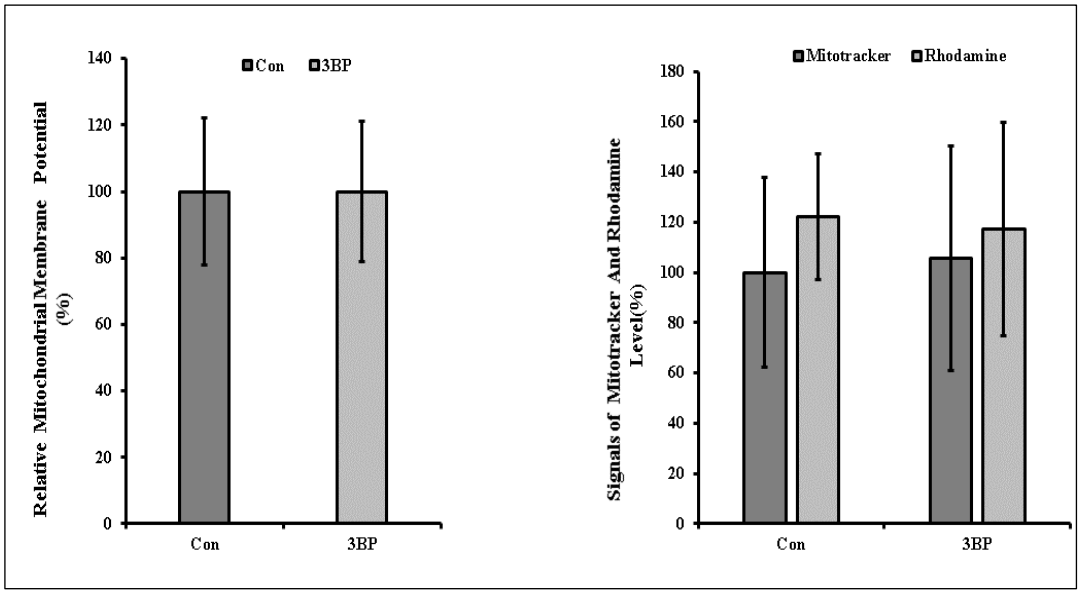

Figure 3.17. Analysis of mitochondrial membrane potential differences between 3-BP treated cells and control cells

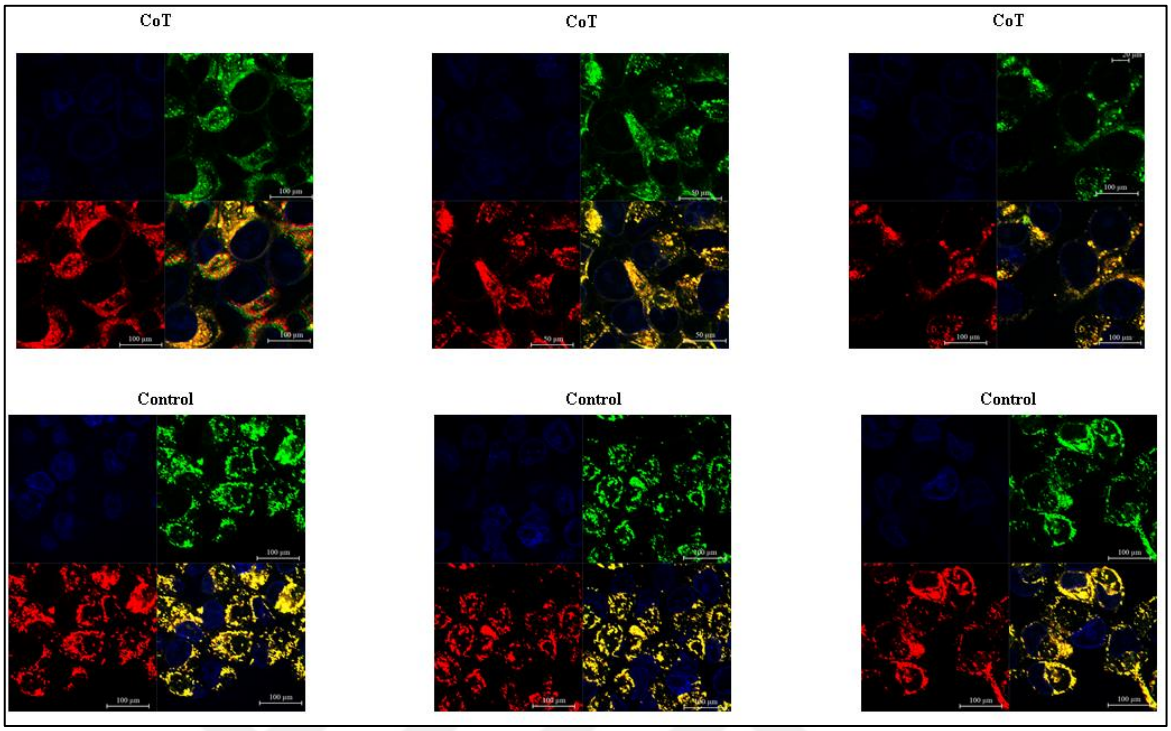

Figure 3.18. The images represent mitochondrial membrane potential changes compared to cotreated cells

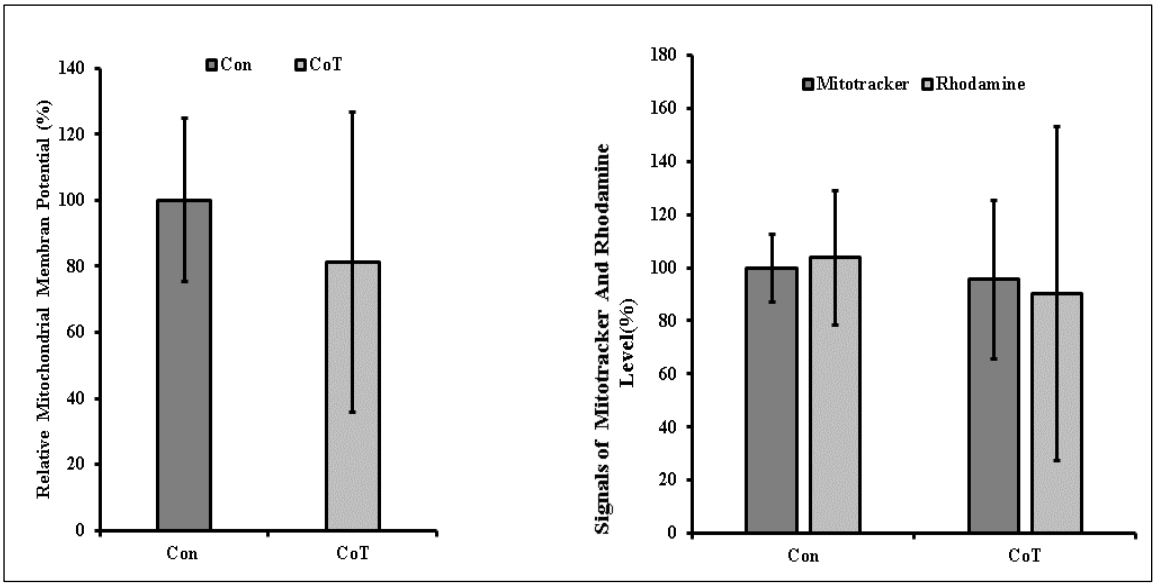

Figure 3.19. Analysis of mitochondrial membrane potential differences compared to cotreated cells

3.11. QUANTIFICATION OF MITOCHONDRIAL INNER MEMBRANE POTENTIAL BY USING FLOW CYTOMETRY

Since no change was observed in the confocal results of 50 μM 3-Bromopyruvic acid , 5 μM EX527 and co-treated (50 μM 3BP: 5 μM EX527) samples, flow cytometry was measured with another kit that could measure membrane potential in the cells. TMRE (tetramethylrhodamine ethyl ester percholarate), a cationic dye, was used for the measurement of membrane potential in living cells. As a negative control, CCCP (carbonyl cyanide 3-chlorophenylhydrazone) mitochondrial membrane disrupting agent was used.

TMRE is a cationic and cell permeable fluorescent dye, which is permeable to intact and non-dysfunctional mitochondria. Mitochondrial membrane potential is measured by TMRE entrance to the intact mitochondria. Because the TMRE cannot enter in either the depolarizing or in the inactive mitochondria, the accumulation of TMRE will either be none or less. As a result, a decrease in mitochondrial membrane potential will be observed.

The TMRE cell is a permeable cationic dye with high membrane potential and gives a response to the negative charge in the membrane. When in the absence of the membrane potential or in the presence of an impair in mitochondrial activity, TMRE fluorescent dye will not accumulate in the cells.

Orange fluorescence that emerges as a result of the emission generated by TMRE indicates both the potential of the mitochondrial membrane and also the determination of whether the cells are healthy or apoptotic.

A significant change was observed in only 50 μM 3BP treated cells in terms of membrane potential changes in treated and untreated samples, and an increase of 38 percent in mitochondrial membrane potential was observed compared to control cells. There was no significant difference in the treated cells with 5μM EX527 and co-treatment(Figure 3.20).

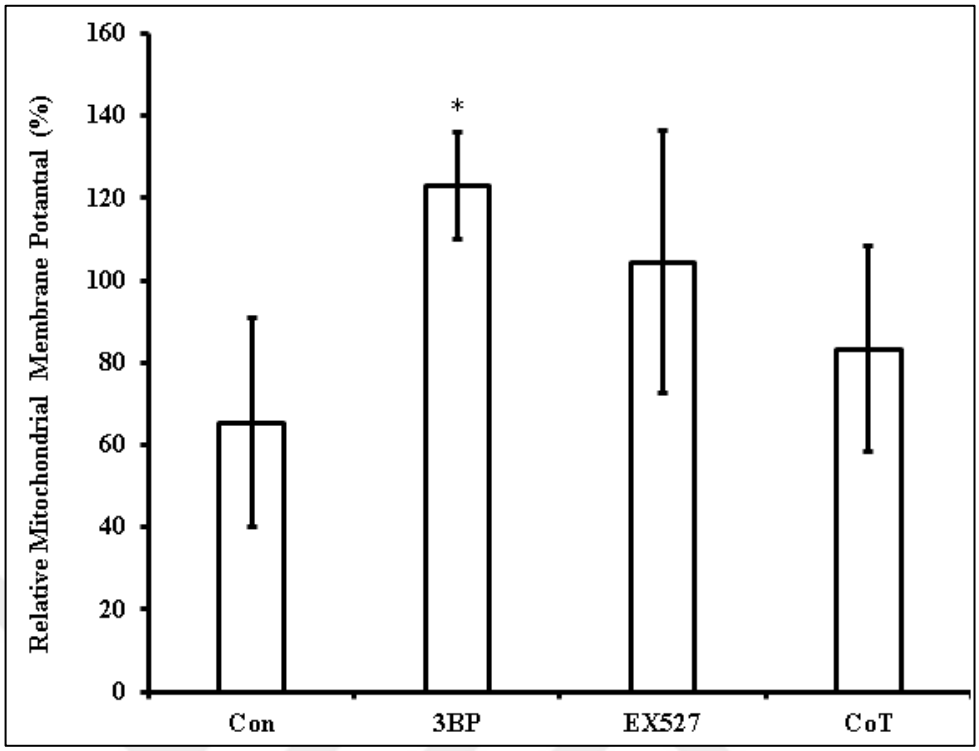

Figure 3.20. Differences of mitochondrial membrane potential from flow cytometry analysis. The graphic obtained from the normalized values were using the control data of the triple repeats and the treated and non-treated samples is shown above Mitochondrial membrane potential in 3BP treated cells show a significant decrease in total cell. ($p < 0.005$).

4. DISCUSSION

One of the most promising anti-cancer drugs that have been used in the treatment of cancer is 3-bromopyruvate (3BP). 3BP has been shown to cause fatal effects by triggering many pathways, even when applied in low doses in different cancers [236]. As an important anti-metabolic agent for cancer biology it is connected with various pathways. This property is related with its chemical structure that resembles acetate (the precursor of lipogenesis), pyruvate (pioneer of Krebs cycle), and lactate (associated with Warburg effect) [237]. Cancer cells are known to have different metabolic and biological properties compared to normal cells. The cancer cells possess high glycolytic rate, hexokinase-II activity, more transporters of monocarboxylate and glucose, accompanied by low antioxidant activity. Hence, more effective therapy would be achieved by targeting these together. Furthermore, the antiangiogenic effect of 3BP and the inhibition of ATP-binding cassettes cooperate for the termination of chemoresistance [238]. The 3BP is capable of inducing cell death pathways through multiple mechanisms by limiting ATP availability by the inhibition of energy-associated pathways of both glycolysis and mitochondria. By the way, 3BP is highly reactive but it has not been associated with any harmful side effect in animal studies [236,237].

It is known that sirtuin1 is involved in many cancers, including pancreatic cancer. SIRT1 is particularly implicated in drug resistance and tumor formation via p53 deacetylation, PTEN, BAX / Bcl-2, and E2F1 transcription factor. Because of these, we incorporated EX527, specific SIRT1 inhibitor, in our studies with human pancreatic cancer cell line Miapaca-2, where the expression of SIRT1 is high [239].

Morphological changes caused by 3BP application to Miapaca-2 cells were recorded with a light microscopy. Reduced cellular surface attachment and round shape morphology were observed in Miapaca-2 cells with 3BP (50 μM and 100 μM) (Figure 3.1, 3.2, 3.3). These morphologic changes were also found with 5 μM and 10 μM of EX527-treated Miapaca-2 cells. In a previous study, HUVECs cells were also demonstrated prominent shrinkage and less surface attachment [239]. In addition, there were significant morphological changes in MCF-7 cells when EX527 was applied to these cells at a concentration of 50 μmol/ml [240].

In recent years, combination chemotherapy has been widely used in cancer treatments. The conventional combination of cancer drugs creates a pharmacokinetic diversity, sometimes which ends as non-useful application. Various drug combinations showing synergistic, additive and potential effects are included in the literature [241]. On the other hand, a variety of problems may be encountered related to the efficacy of the drug while providing chemotherapy with adjunctive therapy; such as drug release problems or drug resistance. In addition, traditional cancer drugs may cause resistance or toxic side effects to healthy cells in patients. Combination therapy is becoming an increasingly crucial to prevent long-term diagnosis and the occurrence of undesirable side effects. Thus, the effects of the drugs can be synergistic and this could maximize their efficacy. Moreover, this method could be a way for overcoming drug resistance. The development and the emergence of new drug combinations is a promising improvement, specific mechanisms triggered by these combinations could help us understand further the mechanisms in which each agent triggered separately [242]. In this study, a combination of 3BP and EX527 was administered to Miapaca-2 cells, which presumably allows different signal pathways to be modulated in different ways at the same time [243]. 3BP (50 μM) and EX527 (5 μM) were selected to be used in combination therapy due to the observed effects of these concentrations on cell death both via light microscope and MTS cell viability assay results. These doses lead cell death within 24 hours and they lost their cell attachment properties and showed a tendency to overlap. Therefore, based on the consistent results from microscope images and 3-(4,5-dimethylthiazol-2-yl)-2,5-diphenyltetrazolium bromide) tetrazolium (MTS) assays, isobologram analysis was modeled over this combination, 3BP (50 μM) and EX527 (5 μM) (Figures 3.1, 3.2, 3.3)

Estimation of the effect of drug combination is based on the dose equivalence concept. If the effect of the drug combination is additive, the combination therapy will show a cumulative contribution of the effects of the two drugs which are used in a dose equivalent manner. If the chemical used for the treatment causes a decrease in the effectiveness of the other chemical, it is called the antagonism effect, but this is called synergism if the two chemicals used to be more efficient than the other. The determination of the isobole of the substance is a necessary method to demonstrate the synergistic and antagonistic relationship. The aim of these isobologram calculations is to distinguish between additive effects and synergetic effects [244]. The reason why we prefer isobologram analysis in this

study is that it can offer a simple and rapid result and also the ability to easily calculate synergetic effect by a single cell viability assay (MTS) and related IC50 values.

In order to establish isobologram curve for 3BP and EX527 applied in this study, IC50 values were calculated from the absorbance values and each combination-specific indexes were shown on the isobologram (Figure 3.4, 3.5, 3.6). The IC50 value means the measurement of the maximum inhibition concentration of the substrates that is used to inhibit a specific biological or biochemical function. The result with a combination index less than 1 is considered to have synergetic effect, and in this study the combination index of 3BP (50 μM) and EX527 (5 μM) was less than 1 (Figure 3.7). Thus, the combination of 50 μM of 3BP and 5 μM of EX527 was concluded to have synergetic effect.

The anti-glycolytic agent, 3BP and sirtuin1 inhibitor, EX527 were applied together on Miapaca-2 cells of pancreatic cancer. When 3BP and EX527 were administered both separately and together on Miapaca-2 cells, Annexin-V assay was applied to understand the affected cell death mechanism. As a result, the rate of apoptosis in co-treated cells increased several times higher than in the individual administration of these agents, particularly early apoptosis rate. The purpose of this experiment was to understand how these chemotherapeutic drugs, administered in combination and separately, lead death of Miapaca-2 cells. Individual 3BP treatment was associated with the depletion of ATP in cells, which causes necrosis. In the light of this information, the very rapid increase of this apoptosis in co-treated cells, was related to the effect of 3BP in addition to the connection of EX527 with Ku70. 3BP inhibits hexokinase-II and so ATP production is reduced. In addition, BAD (BCL2 associated agonist of cell death) is dephosphorylated. Bcl-2 and Bcl-Xl, members of anti-apoptotic protein family, interact with Bad or BAX to prevent apoptosis under normal conditions. However, Bad is dephosphorylated and causes BAX2 to migrate mitochondria through the inhibition of glycolysis. Thus, VDAC, located in the mitochondrial membrane and normally interacting with hexokinase, cannot interact with hexokinase any longer after its inhibition with 3BP and BAX is located in the mitochondrial membrane where Hexokinase-2 is bound. As a result of this pro-apoptotic stimulus, programmed cell death is triggered and caspases are activated by the release of cytochrome *c* from the mitochondrial outer membrane. BAX stays inactive in the cytoplasm under normal conditions and in this case the DNA repair factor Ku70 is tightly associated with BAX [245-246]. It is known that SIRT1 physically interacts with Ku70

which is a DNA repair protein and protects cells from DNA damage. In this study as well, SIRT1 provides this by deacetylating Ku70. Due to EX527 inhibitor that was applied in co-treated cells, the Ku70 protein could not be deacetylated and the DNA repair mechanism was not activated, so more cells were found to be dead [247]. The apoptosis of the Miapaca-2 cells was more rapid and efficient when they were treated with sirtuin-1 inhibitor, EX527. High mortality rate was observed in early apoptosis against control; however, it was not high as in the co-treated Miapaca-2 cell lines.

SIRT1 can restrain tumor development by suppressing NF-κB, a transcription factor that is involved in the regulation of immune response and carcinogenesis. Additional substrates of SIRT1 are involved in the pathways of the hypoxia response, the PI3K / AKT pathway, the transforming growth factor-β (TGF-β) signaling pathway, the Wnt signaling pathway, and DNA repair pathways. These targets demonstrated us that SIRT1 was directly related to the metabolic processes of cancer cells [248]. Another important member of sirtuin family is SIRT3, which resides in mitochondria and functions in cell survival, apoptotic pathways, and metabolism. It has been associated with cancer-related activities including; apoptosis, survival, immune responses, genomic instability, unlimited replication, metastasis, angiogenesis, and metabolic dysfunction. Hence, SIRT1 and SIRT3 have been thought to play dual roles in common pathways due to their roles in cancer biology and may also be efficient targets in the treatment of cancer cells [249]. In our study, changes in their protein expression levels have been studied. A significant decrease in SIRT1 in cells treated with only EX527 and co-treated with 3BP and EX527 was revealed (Figure 3.9). As a result of presumable decrease in the SIRT1 activity, p53 deacetylation would not occur leading cells to apoptosis. At the same time, these cells cannot activate DNA repair mechanisms to protect themselves from DNA damage since Ku70 protein would not be deacetylated by SIRT1. Another SIRT1 target is PGC-1alpha, which induces mitochondrial biogenesis through ERR promoter region in the nucleus and also promotes SIRT3, which might explain the reduction in SIRT3 upon treatment with EX527 [250-251].

It was shown that AMPK controls the expression of genes involved in the energetic metabolism of skeletal muscle mainly through NAD^+-dependent deacetylase, SIRT1. AMPK increases cellular NAD^+ levels enhancing SIRT1 activity, which results in modulation of downstream activity of SIRT1 targets including PGC-1alpha, FOXO1 and FOXO3A. This also leads to the deacetylation of these SIRT1 targets [248-249]. There are

AMPK, OXPHOS, and ROS regulation circumstances between SIRT1 and SIRT3. Yet, there is no mechanism to illustrate the effect of 3BP on the PGC-1alpha and OXPHOS complexes mechanism to illustrate the effect of 3BP on the PGC-1alpha and OXPHOS complexes [250]. Upon deacetylation by SIRT1 in the cytosol, PGC-1alpha migrates to relevant transcription region in the nucleus and induces the expression of OXPHOS complexes and SIRT3. In our results, EX527 treatment inhibits PGC-1alpha migration through SIRT1 decrease, and thus the expression of SIRT3 and OXPHOS complexes cannot be promoted (Figure 3.10).

SIRT3 promotes mitochondrial function by deacetylation of enzymes mostly involved in the TCA cycle and fatty acid oxidation. SIRT3 limits the glycolytic metabolism from multilateral direction to reduce ROS production and reduce HIF1-alpha activity. SIRT3 suppresses ROS by promoting HIF-1alpha degradation and PHD activity. Loss of SIRT3 significantly elevates ROS level in the cell [265]. Without the information about the total sirtuin activity assay or SIRT1 and SIRT3 specific activities, it would still be unclear the relation of those corresponding enzymes with co-treatment of Miapaca-2 cells.

Acetylation of protein through lysine residues is an important covalent post-translational modification for the regulation of the functions of proteins. Lysine acetylation has effects on glycolysis, glycogenesis, TCA cycle, urea, and fatty acid cycle [252]. In this study, the total lysine acetylation antibody was used to show the changes in the protein acetylation caused by the affected sirtuins. We have found that total acetylome level was elevated particularly in EX527-treated cells, where SIRT1 was downregulated (Figure 3.11). A detailed investigation of the proteins that are regulated by reversible acetylation could be revealed by mass spectrometry-based proteomics. These results will unravel the pathways related with the pancreatic cancer [252,253]. The acetylated proteins we have found in our results can be the targets for both SIRT1 and SIRT3 (Figure 3.11); for instance, Ku70 protein (70 kDa) and the subunits of respiratory chain complexes, NADH dehydrogenase (18 kDa), succinate dehydrogenase (29 kDa), cytochrome *c*-oxidoreductase (48 kDa), cytochrome *c*-oxidase (22 kDa), ATP synthase (54 kDa). PGC1-alpha is about 100 kDa and p53 is about 50 kDa. In order to confirm these targets, immunoprecipitation assays need to be performed to demonstrate the direct interaction between them.

One of the cellular intermediates produced in aerobic respiration is ROS. It is kept at baseline in normal conditions in the cell, which is important for antioxidant defense

mechanism. The accumulation of excess ROS in the cell occurs in many metabolic dysfunctions including cancer. ROS has a complex role in the development of cancer and affects many mechanisms including metabolic signaling pathways [254]. In the case of prolonged stress, ROS production can continue for a long time in the cell and damages cell structure and function, also induces somatic mutations and neoplastic transformation. There are both free ROS radicals and non-free ROS radicals in the cell, their production is carried out by the electron transport chain in the mitochondria and in the case of cancer the electrons can easily escape from the chain. These electrons can react with oxygen to form harmful radicals [255]. ROS production in pancreatic cancers has been shown to be high, particularly in PanIN lesions. The production of K-Ras induced ROS in pancreatic cancers is mediated by NADPH oxidases (NOX) and mitochondrial respiratory chain complexes [256]. ROS production by Kras-NOX has been identified in some PDAC patients and the expression of NOX is increased compared to non-transformed pancreatic tissues The production of mitochondrial ROS produced in response to oncogenic K-Ras leads to the formation of pre-cancerous lesions in the pancreas. The signaling in the pathway of mitochondrial ROS is NF-1B, a protein kinase D1 (PKD1) which is a sensor of oxidative stress and has previously been found to be involved in the formation of K-Ras mediated PanIN [256]. It has been shown that SIRT1 cooperates with K-Ras in the lung tumorigenesis, therefore, it is an important therapeutic target [257]. It has also been shown that SIRT1 can deacetylate K-Ras from its lysine 104 residues resulting in activation. Therefore, the decrease in ROS in Miapaca-2 cells treated with EX527 leading to SIRT1 inhibition can be related with K-Ras [258]. In addition, EX527 treated cells, have decreased ROS levels, so it is supposed that EX527 does not inhibit SIRT1 entirely, but the rate of its expression is reduced. Thus, decreased ROS level can be associated with ROS-independent apoptosis which were higher than the untreated cells. Therefore, all of the proteins in SIRT1 targets may not be in the acetylated state and it may have favorably supported SIRT1-mediated survival in cells.

Cancer cells have the potential for hyperpolarized mitochondrial membrane, while the potential in normal cells is -140 mV, which is approximately -220 mV in cancer cells. The cause of this difference is not fully explained. Membrane potential changes may also be the research subject of the anti-cancer drugs [259]. In this study, the mitochondrial membrane potential of EX527-, 3BP-, and co-treated Miapaca-2 cells was determined by TMRE flow

cytometric analysis. In the results, 3BP treatment demonstrated a direct effect on mitochondrial membrane potential, which is 38 percent increased.

5. CONCLUSIONS AND FUTURE PERSPECTIVE

In this study, our results provided the metabolic changes in Miapaca-2 cells co-treated with 3BP and EX527. For the further investigation of the apoptosis-associated pathways in co-treated cells, and the expression of caspases might elucidate the specific cell death mechanism. This would conclude whether the mechanism of death in co-treated cells is nucleus- and mitochondrial-mediated or both.

Additionally, the mouse models of Ku70 could be employed to study the affected mechanism of DNA repair upon co-treatment. This may also be accompanied with the knockdown of Sirtuin1 and/or Sirtuin3, which play roles death-related metabolic pathways. The histological samples from these mouse models could also be examined using dyes such as Hemotoxylin-Eosin to demonstrate the differences in PanIN lesions showing the progression of pancreatic cancer. Next, the changes in protein expression levels in pancreatic healthy cells compared to cancer cells upon co-treatment might be quantified by using mass spectrometry-based proteomics, which will illuminate the affected metabolic pathways in a global scale. Furthermore, all acetylome changes in proteins in treated and untreated cells could be determined using specific labeling techniques such as stable isotope labeling with amino acids in cell culture (SILAC).

Overall, these studies will provide a more comprehensive view for the synergetic effect of 3BP and EX527 in pancreatic cancer cells. The outcome of these findings will enlighten how we would proceed with this co-treatment strategy to target aggressive type of cancers.

REFERENCES

1. OpenStax. Anatomy and Physiology. 2013[Cited 2013, 10 March]. Available from https://opentextbc.ca/anatomyandphysiology.pdf

2. Ellis H. Anatomy of the pancreas. *Surgery.* 2005;25(2):72-73.

3. Longnecker DS, Gorelick F, Thompson ED. *The Pancreas: an integrated the textbook of scicence, medicine and surgery.* New Jersey:Wiley and Sons Press;2018.

4. Wittingen J, Frey CF. Islet concentration in the head, body, tail and uncinate process of the pancreas. *Annals of Surgery*.1974;179(4):412-414.

5. Bockman DE. Morphology of the exocrine pancreas related to pancreatitis. *Microscopy Research and Technique*.1997;37(56):509-519.

6. Bolender RP. Stereological analysis of the guinea pig pancreas: analytical model and quantitative description of nonstimulated pancreatic exocrine cells. *The Journal of Cell Biology*. 1974;61(2):269-87

7. Iwatsuki N. Electrical coupling and uncoupling of exocrine acinar cells. *The Journal of Cell Biology*.1978;79(2):533-545.

8. Petersen OH. *Human physiology.* Oxford:Blackwell;2007.

9. Park MK, Lomax RB, Tepikin AV, Petersen OH. Local uncaging of caged Ca2 reveals distribution of Ca2 -activated Cl- channels in pancreatic acinar cells. *National Academy of Sciences*. 2001;98(19):10948-10953.

10. Lee MG, Ohana E, Park HW, Yang D, Muallem S. Molecular mechanism of pancreatic and salivary gland fluid and hco3− secretion. *Physiological Reviews*. 2012;92(1):39-74.

11. Banks PA, Freeman ML. Practice guidelines in acute pancreatitis. *The American Journal of Gastroenterology*.2006;101(10).2379-2400.

12. Open Stax, LL. Anatomy and Physiology II. 2019 [Cited 21 April 2019] Available from https://courses.lumenlearning.com/suny-ap2/chapter/the-endocrine-pancreas/

13. Alsamarrai A, Das SL, Windsor JA, Petrov MS. Factors that affect risk for pancreatic disease in the general population: a systematic review and meta-analysis of prospective cohort studies. *Clinical Gastroenterology and Hepatology*. 2014; 12(10)

14. Tong G, Geng Q, Chai J, Cheng J, Chen P, Liang H, Wang D. Association between pancreatitis and subsequent risk of pancreatic cancer: a systematic review of epidemiological studies. *Asian Pacific Journal of Cancer Prevention.* 2014;15(12):5029-5034.

15. Testoni PA. Acute recurrent pancreatitis: etiopathogenesis, diagnosis and treatment. *World Journal of Gastroenterology*. 2014;20(45):16891.

16. Shiokawa M, Kodama Y, Yoshimura K, Kawanami C, Mimura J, Yamashita Y, Chiba T. Risk of cancer in patients with autoimmune pancreatitis. *The American Journal of Gastroenterology*. 2013;108(4):610-617.

17. Lowenfels AB, Maisonneuve P, Dimagno EP, Elitsur Y, Gates LK, Perrault J, Whitcomb DC. Hereditary pancreatitis and the risk of pancreatic cancer. *Journal of the National Cancer Institute*. 1997;89(6):442-446.

18. Talamini G, Falconi M, Bassi C, Mastromauro M, Salvia R, Pederzoli P. Chronic pancreatitis: relationship to acute pancreatitis and pancreatic cancer. *Journal of Pancreas.* 2000;1(3):69–76.

19. Rahib L, Smith BD, Aizenberg R, Rosenzweig AB, Fleshman JM, Matrisian LM. Projecting cancer incidence and deaths to 2030: the unexpected burden of thyroid, liver, and pancreas cancers in the united states. *Cancer Research*. 2014;74(11):2913-2921.

20. Siegel RL, Miller KD, Jemal A. Cancer statistics. *A Cancer Journal for Clinician.* 2016;66(1):7-30.

21. Witsch E, Sela M, Yarden Y. Roles for growth factors in cancer progression. *Physiology*. 2010;25(2):85-101.

22. Paul MK, Mukhopadhyay AK. Tyrosine kinase – role and significance in cancer. *International Journal of Medical Science*s. 2004;1(2):101-115.

23. Revisiting the hallmarks of cancer. 2019 [Cited 2019 21 April] Available from https://www.readbyqxmd. com/read/28560055/revisiting-the-hallmarks-of-cancer

24. Jiang BH, Liu LZ. PI3K/PTEN signaling in angiogenesis and tumorigenesis. *Advance Cancer Research*. 2009;102(1):19–65

25. Ratner N, Miller SJ. A RASopathy gene commonly mutated in cancer: the neurofibromatosis type 1 tumour suppressor. *Nature Review Cance*r. 2015;15(5):290-301.

26. Csermely P, Korcsmaros T, Nussinov R. Intracellular and intercellular signaling networks in cancer initiation, development and precision anti-cancer therapy: RAS acts as contextual signaling hub. *Semin Cell Development Biology*. 2016;58:55-59.

27. Hanahan D, Weinberg R. Hallmarks of cancer: the next generation. *Cell.* 2011;144(5): 646-674.

28. Hung C, Garcia-Haro L, Sparks CA, Guertin DA. mtor-dependent cell survival mechanisms. *Cold Spring Harbor Perspectives in Biology*. 2013;4(12):1-72.

29. Faivre S, Kroemer G, Raymond E. Current development of mtor inhibitors as anticancer agents. *Nature Reviews Drug Discovery*. 2006;5(8):671-88.

30. Rozengurt E, Soares HP, Sinnet-Smith, J. Suppression of feedback loops mediated by pi3k/mtor induces multiple overactivation of compensatory pathways: an unintended consequence leading to drug resistance. *Molecular Cancer Therapeutics.* 2014;13(11):2477-2488.

31. Driscoll DR, Karim SA, Sano M, Gay DM, Jacob W, Yu J, Morton JP. Mtorc2 signaling drives the development and progression of pancreatic cancer. *Cancer Research.* 2016; 76(23): 6911-6923.

32. Chandarlapaty S. Negative feedback and adaptive resistance to the targeted therapy of cancer. *Cancer Discovery*. 2012;2(4):311-319.

33. Hassan Z, Schneeweis C, Wirth M., Veltkamp C, Dantes Z, Feuerecker B, Schneider G. Mtor inhibitor-based combination therapies for pancreatic cancer. *British Journal of Cancer. 2018;*118(3):366-377.

34. Malumbres M, Barbacid M. Cell cycle, cdks and cancer: a changing paradigm. *Nature Reviews Cancer*. 2009;9(3):153-166.

35. Vermeulen K, Bockstaele DR, and Berneman ZN. The cell cycle: a review of regulation, deregulation and therapeutic targets in cancer. *Cell Proliferatio*n.2003;36(3):131-149.

36. Classon M, Harlow E. The retinoblastoma tumour suppressor in development and cancer. *Nature Reviews Cancer*. 2002;2(12):910-917.

37. Simabuco FM, Morale MG, Pavan IC, Morelli AP, Silva FR, Tamura RE. P53 and metabolism: from mechanism to therapeutics. *Oncotarget*. 2018;9(34):23780–23823.

38. Pelosi E, Castelli G, Testa U. Pancreatic cancer: molecular characterization, clonal evolution and cancer stem cells. *Biomedicines.* 2017;5(4):1-65.

39. Yachida S, Jones S, Bozic I, Antal T, Leary R, Fu B, Iacobuzio-Donahue CA. Distant metastasis occurs late during the genetic evolution of pancreatic cancer. *Nature*. 2010;467(7319):1114-1117.

40. Petrilli AM, Fernández-Valle C. Role of Merlin/NF2 inactivation in tumor biology. *Oncogene*. 2015;35(5):537-548.

41. Morrison H. The NF2 tumor suppressor gene product, merlin, mediates contact inhibition of growth through interactions with CD44. *Genes and Development.* 2001;15(8):968-980.

42. Shaw RJ, Mcclatchey AI, Jacks T. Regulation of the neurofibromatosis type 2 tumor suppressor protein, merlin, by adhesion and growth arrest stimuli. J*ournal of Biological Chemistr*y. 1998;273(13):7757-7764.

43. Shaw RJ. Tumor suppression by lkb1: sik-ness prevents metastasis. *Science Signaling*. 2009;2(86):1-55.

44. Partanen JI, Nieminen AI, Klefstrom J. 3D view to tumor suppression: Lkb1, polarity and the arrest of oncogenic c-myc. *Cell Cycle.* 2009;8(5):716-724.

45. Tian M, Neil JR, Schiemann WP. Transforming growth factor-β and the hallmarks of cancer. *Cellular Signalling*. 2011;23(6):951-962.

46. Fernald K, Kurokawa, M. Evading apoptosis in cancer. *Trends in Cell Biology.* 2011;23(12):620-633.

47. Edlich F. BCL-2 proteins and apoptosis: Recent insights and unknowns. biochemical and biophysical .*Research Communications*. 2018;500(1):26-34. 90

48. Deng J. How to unleash mitochondrial apoptotic blockades to kill cancers? *Acta Pharmaceutica Sinica B.* 2017;7(1):18-26.

49. Luciano F, Jacquel A, Colosetti P, Herrant M, Cagnol S, Pages G, Auberger P. Phosphorylation of Bim-EL by Erk1/2 on serine 69 promotes its degradation via the proteasome pathway and regulates its proapoptotic function. *Oncogene*. 2017;22(43):6785-6793.

50. Essafi A, Mattos SF, Hassen YA, Soeiro I, Mufti GJ, Thomas NS, Lam EW. Direct transcriptional regulation of Bim by FoxO3a mediates STI571-induced apoptosis in Bcr-Abl-expressing cells. *Oncogene.* 2005;24(14):2317-2329.

51. Moller C. Stem cell factor promotes mast cell survival via inactivation of foxo3a-mediated transcriptional induction and mek-regulated phosphorylation of the proapoptotic protein bim. *Blood*. 2005;106(4):1330-1336.

52. Peso LD. Interleukin-3-induced phosphorylation of bad through the protein kinase akt. *Science.* 1997;278(5338):687-689.

53. Yamaguchi H, Wang H. The protein kinase pkb/akt regulates cell survival and apoptosis by inhibiting BAX conformational change. *Oncogene. 2*001;20(53):7779-7786.

54. Sax JK, Fei P, Murphy ME, Bernhard E, Korsmeyer SJ, El-Deiry WS. BID regulation by p53 contributes to chemosensitivity. *Nature Cell Biology*. 2002;4(11):842-849.

55. Huang F, Wang B, Wang Y. Role of autophagy in tumorigenesis, metastasis, targeted therapy and drug resistance of hepatocellular carcinoma. *World Journal of Gastroenterology*. 2018;24(41):4643-4651.

56. Glick D, Barth S, Macleod KF. Autophagy: Cellular and molecular mechanisms. *The Journal of Pathology*. 2010;221(1):3-12.

57. Bellot G, Garcia-Medina R, Gounon P, Chiche J, Roux D, Pouyssegur J, Mazure NM. Hypoxia-induced autophagy is mediated through hypoxia-inducible factor induction of bnip3 and bnip3l via their bh3 domains. *Molecular and Cellular Biology.* 2009;29(10):2570-2581.

58. Zhang X, Chen L. The recent progress of the mechanism and regulation of tumor necrosis in colorectal cancer. J*ournal of Cancer Research and Clinical Oncology*. 2015;142(2):453-463.

59. Wang T, Jin Y, Yang W, Zhang L, Jin X, Liu X, Li X. Necroptosis in cancer: An angel or a demon. *Tumor Biology*. 2017;39(6):101042831771153.

60. Seifert L, Werba G, Tiwari S, Giao LN, Alqunaibit D, Alothman S, Miller G. The necrosome promotes pancreatic oncogenesis via cxcl1 and mincle-induced immune suppression. *Cancer Research.* 2016;532(7598):245-976.

61. Yang S, Wang X, Contino G, Liesa M, Sahin E, Ying H, Bause A, Li Y, Stommel JM, Dell'antonio G, Mautner J, Tonon G, Haigis M, Shirihai OS, Doglioni C, Bardeesy N, Kimmelman AC. Pancreatic cancers require autophagy for tumor growth. *Genes Development.* 2011;25(7):717-29.

62. Maycotte P, Aryal S, Cummings CT, Thorburn J, Morgan MJ, Thorburn A. Chloroquine sensitizes breast cancer cells to chemotherapy independent of autophagy. *Autophagy.* 2012;8(2):200–212

63. Werba G, Seifert L, Miller, G. Necroptotic cell death -an unexpected driver of pancreatic oncogenesis. *Cell Cycle*. 2016;15(16):2095-2096.

64. Blagosklonny MV. Cell immortality and hallmarks of cancer. *Cell Cycle.* 2003;2(4): 295-298.

65. Maqsood MI, Matin MM, Bahrami AR, Ghasroldasht M. Immortality of cell lines: challenges and advantages of establishment. *Cell Biology International.* 2013;37(10): 1038-1045.

66. Vitis MD, Berardinelli F, Sgura A. Telomere length maintenance in cancer: at the crossroad between telomerase and alternative lengthening of telomeres (alt). *International Journal of Molecular Sciences.* 2018;19(2):606.

67. Olovnikov AM. A theory of marginotomy. The theory of marginotomy: the incomplete copying of template margin in enzymic synthesis of polynucleotides and biological significance of the phenomenon. *Journal of Theoretical Biology*.1973; 41(1):181–190.

68. Greider CW, Blackburn EH. Identification of a specific telomere terminal transferase activity in tetrahymena extracts. *Cell.* 1985;43(2):405-413.

69. Hapangama D, Kamal A, Saretzki G. Implications of telomeres and telomerase in endometrial pathology. *Human Reproduction Update.* 2016;23(2):166-187.

70. Opresko PL and Shay JW. Telomere-associated aging disorders. *Ageing Research Reviews*. 2017;33:52-66.

71. Akincilar SC, Unal B, Tergaonkar V. Reactivation of telomerase in cancer. *Cellular and Molecular Life Sciences.* 2016;73(8):1659-1670.

72. Stewart SA, Hahn WC, O'Connor BF, Banner EN, Lundberg AS, Modha P, Mizuno H, Brooks MW, Fleming M, Zimonjic DB. Telomerase contributes to tumorigenesis by a telomere length-independent mechanism. *Proceedings of the National Academy of Sciences.* 2002;99(20):12606–12611

73. Kim N, Piatyszek M, Prowse K, Harley C, West M., Ho P, Shay J. Specific association of human telomerase activity with immortal cells and cancer. *Science.* 1994;266(5193):2011-2015.

74. Gaspar TB, Sá A, Lopes JM, Sobrinho-Simões M, Soares P, Vinagre J. Telomere maintenance mechanisms in cancer. *Genes*. 2018;9(5):241.

75. Barthel FP, Wei W, Tang M, Martinez-Ledesma E, Hu X, Amin S. B, Verhaak RG. Systematic analysis of telomere length and somatic alterations in 31 cancer types. *Nature Genetics.* 2017;49(3):349-357.

76. Skinner HG, Gangnon RE, Litzelman K, Johnson RA, Chari ST, Petersen GM, Boardman L. A. Telomere length and pancreatic cancer: a case-control study. *Cancer Epidemiology Biomarkers and Prevention*. 2012;21(11):2095-2100.

77. Weis SM, Cheresh DA. Tumor angiogenesis: molecular pathways and therapeutic targets. *Nature Medicine*. 2011;17(11):1359-1370.

78. Folkman J. Role of angiogenesis in tumor growth and metastasis. *Seminars in Oncology*. 2002;29(6):15-18.

79. Weis SM, Cheresh DA. Tumor angiogenesis: molecular pathways and therapeutic targets. *Nature Medicine.* 2011;17(11):1359-1370.

80. Folkman J. Hanahan D. Switch to the angiogenic phenotype during tumorigenesis. *Princess Takamatsu Symposium*. 1991;22(77):339–347.

81. Weis SM, Cheresh DA. Pathophysiological consequences of vegf-induced vascular permeability. *Nature*. 2005;22;437(7058):497-504.

82. Franco OE, Shaw AK, Strand DW, Hayward SW. Cancer associated fibroblasts in cancer pathogenesis. *Semier Cell Developmental Biology*. 2010; 21(1):33–39

83. Xing F, Saidou J, Watabe K. Cancer associated fibroblasts (CAFs) in tumor microenvironment. *Frontier Bioscence.* 2010;1(15):166–179.

84. Sund M. Function of endogenous inhibitors of angiogenesis as endothelium specific tumor suppressors. *Proceedings of the National Academy of Sciences.* 2005;102(8):2934–2939.

85. Longo V, Brunetti O, Gnoni A, Cascinu S, Gasparini G, Lorusso V, Silvestris N. Angiogenesis in pancreatic ductal adenocarcinoma: A controversial issue. *Oncotarget.* 2016;8(56):95773–95779.

86. Erkan M, Reiser-Erkan C, Michalski CW, Deucker S, Sauliunaite D, Streit S, Esposito I, Friess H, Kleeff J. Cancer-stellate cell interactions perpetuate the hypoxia-fibrosis cycle in pancreatic ductal adenocarcinoma. *Neoplasia*. 2009;11(5):497–508

87. Masamune A, Kikuta K, Watanabe T, Satoh K, Hirota M, Shimosegawa J . Hypoxia stimulates pancreatic stellate cells to induce fibrosis and angiogenesis in pancreatic cancer. *American Journal of Physiology: Gastrointestinal and Liver Physiology.* 2008; 295(4):G709-17

88. Jiang WG, Sanders AJ, Katoh MH, Ungefroren F, Gieseler M. Prince, SK. Thompson M. Zollo D, Spano P, Dhawan D, Sliva PR, Subbarayan M, Sarkar K, Honoki H, Fujii AG, Georgakilas A, Amedei E, Niccolai A, Amin SS, Ashraf L, Ye WG, Helferich X, Yang CS, Boosani G, Guha MR, Ciriolo K, Aquilano S, Chen A, Azmi WN, Keith A, Bilsland D, Bhakta D, Halicka S, Nowsheen F, Pantano D, Santini. Tissue invasion and metastasis: Molecular, biological and clinical perspectives. *Seminars in Cancer Biology*. 2015;35(2):1183-32.

89. Cavallaro U, Christofori G. Cell adhesion and signalling by cadherins and Ig-CAMs in cancer. *Nature Reviews Cance*r. 2004;4(2):118-32

90. Bogenrieder T, Herlyn M. Axis of evil: molecular mechanisms of cancer metastasis. *Oncogene.*2003;22(42):6524-36.

91. Bogenrieder T, Herlyn M. Axis of evil: molecular mechanisms of cancer metastasis. *Oncogene.* 2003;22(42):6524-6536.

92. Martínezestrada M, Cullerés A, Soriano F, Peinado H, Bolós V, Martínez V.O, et al. The transcription factors slug and snail act as repressors of claudin-1 expression in epithelial cells. *Biochem Journal.* 2006;14:394-50.

93. Balkovetz DF, Gerrard E, Li S, Johnson D, Lee J, Tobias W, et al. Gene expression alterations during HGF-induced dedifferentiation of a renal tubular epithelial cell line (MDCK) using a novel canine DNA microarray. *American journal of physiology renal physiology.* 2003; 286(4):702–710.

94. Huber MA, Kraut N, Beug H. Molecular requirements for epithelial–mesenchymal transition during tumor progression. *Cell Biology* .2005;17(5):548-558.

95. Dimagno EP, Reber HA, Tempero MA. A technical review on the epidemiology, diagnosis, and treatment of pancreatic ductal adenocarcinoma. *Gastroenterology*. 1999;117(6):1464-1484.

96. Keleg S, Büchler P, Ludwig R, Büchler MW, Friess H. Invasion and metastasis in pancreatic cancer. *Molecular cance*r. 2003; 22(2):14.

97. Neoptolemos J, Dunn J, Stocken, D, Almond J, Link, K., Beger H, Büchler, M. Adjuvant chemoradiotherapy and chemotherapy in resectable pancreatic cancer: A randomised controlled trial. *The Lancet*. 2001;358(9293), 1576-1585.

98. Kim J, Yu W, Kovalski K, Ossowski L. Requirement for specific proteases in cancer cell intravasation as revealed by a novel semiquantitative pcr-based assay. *Cell*. 1998;94(3):353-362.

99. Negrini S, Gorgoulis VG, Halazonetis TD. Genomic instability an evolving hallmark of cancer. *Nature Reviews Molecular Cell Biology*. 2010;11(3):220-228.

100. Fishel R, Lescoe MK, Rao M, Copeland NG, Jenkins NA, Garber J, Kolodner R. The human mutator gene homolog MSH2 and its association with hereditary nonpolyposis colon cancer. *Cell.* 1993;75(5):1027-1038.

101. Leach FS, Nicolaides NC, Papadopoulos N, Liu B, Jen J, Parsons R, Vogelstein B.Mutations of a mutS homolog in hereditary nonpolyposis colorectal cancer. *Cell.* 1993;75(6):1215-1225.

102. Nowell PC. Discussion of the presence of genomic instability in tumours and its role in cancer progression: The clonal evolution of tumor cell populations. *Science.* 1976;194(1):23–28.

103. Loeb LA. Mutator phenotype may be required for multistage carcinogenesis. *Cancer Res*. 1991;51(12):3075–3079.

104. Kinzler KW, Vogelstein B. Cancer-susceptibility genes. gatekeepers and caretakers. *Nature.* 1997; 24;386(6627):761, 763

105. Iankin AV, Waddell N, Kassahn KS. Pancreatic cancer genomes reveal aberrations in axon guidance pathway genes. *Nature.* 2012;491(7424):399–4

106. Witkiewicz AK, McMillan EA, Balaji U. Whole-exome sequencing of pancreatic cancer defines genetic diversity and therapeutic targets. *Nature Communications.* 2015;(9)6:6744-7744.

107. Sahin IH, Lowery MA, Stadler ZK, Salo-Mullen E, Iacobuzio-Donahue CA, Kelsen DP, O'Reilly EM. Genomic instability in pancreatic adenocarcinoma: a new step

towards precision medicine and novel therapeutic approaches. *Expert Review of Gastroenterology and Hepatology.* 2016; 10(8):893-905.

108. Campbell PJ, Yachida S, Mudie LJ, et al. The patterns and dynamics of genomic instability in metastatic pancreatic cancer. *Nature.* 2010;467(7319):1109–1113.

109. Ward P, Thompso C. Metabolic Reprogramming: A cancer hallmark even warburg did not anticipate. *Cancer Cell.* 2012;21(3), 297-308.

110. Szablewski L. Expression of glucose transporters in cancers. *Biochimica Et Biophysica Acta (BBA) - Reviews on Cancer*. 2013;1835(2):164-169.

111. Pavlova N, Thompson C. The Emerging Hallmarks of Cancer Metabolism. *Cell Metabolis*m.2016;23(1):27-47.

112. Hay N. Reprogramming glucose metabolism in cancer: can it be exploited for cancer therapy? *Nature Reviews Cancer.* 2016;16(10):635-649.

113. Cairns RA, Harris IS, Mak TW. Regulation of cancer cell metabolism. *Nature Reviews Cancer.* 2011;11(2):85-95.

114. Hay N. Reprogramming glucose metabolism in cancer: can it be exploited for cancer therapy? *Nature Reviews Cancer.* 2016;16(10):635-649.

115. Vyas S, Zaganjor E, Haigis MC. Mitochondria and cancer. *Cell.* 2016;166(3):555-566.

116. Deberardinis RJ, Chandel NS. Fundamentals of cancer metabolism. *Science Advances*. 2016;2(5)18-1.

117. Sabharwal SS, Schumacker PT. Mitochondrial ROS in cancer: initiators, amplifiers or an achilles heel? .*Nature Reviews Cancer*.2014;14(11):709-721.

118. Grivennikov SI, Greten FR, Karin M. Immunity, inflammation, and cancer. *Cell.* 2010;140(6):883-899.

119. Lin W, Karin, MA cytokine-mediated link between innate immunity, inflammation, and cancer. *Journal of Clinical Investigation*.2007;117(5), 1175-1183.

120. Visser KE, Eichten A, Coussens LM. Paradoxical roles of the immune system during cancer development. *Nature Reviews Cancer*. 2006;6(1): 24-37.

121. Dunn GP, Old LJ, Schreiber RD. The immunobiology of cancer immunosurveillance and immunoediting. *Immunity*. 2004;21(2):137-148.

122. Mantovani A, Allavena, P, Sica, A, Balkwill, F. Cancer-related inflammation. *Nature*. 2008;454(7203):436-444.

123. Bartsch DK, Gress TM, Langer P. Familial pancreatic cancer—current knowledge. *Nature Reviews Gastroenterology and Hepatology*. 2012;9(8):445-453.

124. Zambirinis CP, Pushalkar S, Saxena D, Miller G. Pancreatic cancer, inflammation, and microbiome. *The Cancer Journal*. 2014;20(3):195-202.

125. Yadav D, Lowenfels AB. The Epidemiology of pancreatitis and pancreatic cancer. *Gastroenterology*. 2013;144(6):1252-61.

126. Löhr M, Klöppel G, Maisonneuve P, Lowenfels AB, Lüttges J. Frequency of k-ras mutations in pancreatic intraductal neoplasias associated with pancreatic ductal adenocarcinoma and chronic pancreatitis: a meta-analysis. *Neoplasia*. 2005;7(1):17-23.

127. Gupta R, Amanam I, Chung V. Current and future therapies for advanced pancreatic cancer. *Journal of Surgical Oncology*. 2017;116(1):25-34.

128. Kamisawa T, Wood LD, Itoi T, Takaori K. Pancreatic cancer. T*he Lancet*. 2016;388(10039):73-85.

129. Siegel R, Ma J, Zou Z, Jemal A. Cancer statistics. *A Cancer Journal for Clinicians*. 2004;64(1):9-29.

130. Hruban RH, Canto MI, Goggins M. Update on familial pancreatic cancer. *Advance Surgery*. 2010;44:293-311.

131. Iodice S, Gandini S, Maisonneuve P. Tobacco and the risk of pancreatic cancer: a review and meta-analysis. *Langenbecks Archievs of Surgery*. 2008; 393(4):535-*45*

132. Raimondi S, Lowenfels AB, Morselli-Labate AM, et al. Pancreatic cancer in chronic pancreatitis; etiology, incidence, and early detection. *Best practice and research clinical gastroenterology abbreviation.*2010; 24(3):349-58.

133. Bosetti C, Rosato V, Li D, et al. Diabetes, antidiabetic medications, and pancreatic cancer risk: an analysis from the international pancreatic cancer case-control consortium. *Ann Oncology.* 2014;25(10):2065–72.

134. Sah RP, Nagpal SJS, Mukhopadhyay D. New insights intonpancreatic cancer-induced paraneoplastic diabetes. *Nat Rev Gastroenterol Hepato*logy. 2013;10(7):423–33.

135. Hruban RH, Boffetta P, Hiraoka N, Iacobuzio-Donahue C .Ductal adenocarcinoma of the pancreas. WHO classification of tumors of the digestive system. In:Bosman FTJ, Lakhani SR, Ohgaki H. WHO classification of tumors. *International Agency for Research on Cancer.* 2010;4(4)281–91.

136. Vincent A, Herman J, Schulick R, Hruban RH, Goggins M. Pancreatic cancer. *The Lancet*. 2011;378(9791):607-620.

137. Fukushima N, Hruban RH, Kato Y, et al. Ductal adenocarcinoma variants and mixed neoplasms of the pancreas: WHO classification of tumours. *International Agency for Research on Cancer*. 2010:20(4)292–95.

138. Tomlinson JS, Jain S, Bentrem DJ, et al. Accuracy of staging node-negative pancreas cancer: a potential quality measure. *Arch Surg*. 2007;142(8):767-723.

139. Adsay NV, Fukushima N, Furukawa T, et al. Intraductal neoplasms of the pancreas. In: Adsay NV, Furukawa T, Hruban RH, et al. WHO classifi cation of tumours of the digestive system. *International Agency for Research on Cancer*. 2010;14(3):185–194.

140. Vogelstein B, Papadopoulos N, Velculescu VE, Zhou S, Diaz LA, Kinzler K. W. Cancer Genome Landscapes. *Science.* 2013;339(6127):1546-1558.

141. Jones S, Zhang X, Parsons DW, et al. Core signaling pathways in human pancreatic cancers revealed by global genomic analyses. *Science*. 2008;26;321(5897):1801-6

142. Rozenblum E, Schutte M, Goggins M, et al. Tumor-suppressive pathways in pancreatic carcinoma. *Cancer Reserarch.* 1997;9(1)57:1731–34.

143. Van Heek NT, Meeker AK, Kern SE, et al. Telomere shortening is nearly universal in pancreatic intraepithelial neoplasia. *The American Journal of Pathology*.2002;161(5):1541–47.

144. Kanda M, Matthaei H , Wu J, et al. Presence of somatic mutations in most early-stage pancreatic intraepithelial neoplasia .*Gastroenterology*. 2012;142(4):730-733.

145. Wood LD, Hruban RH. Pathology and molecular genetics of pancreatic neoplasms. *Cancer J*.2012;18(6):492-501.

146. Murphy SJ, Hart SN, Lima JN, et al. Genetic alterations associated with progression from pancreatic intraepithelial neoplasia to invasive pancreatic tumor. *Gastroenterology*. 2013;145(5):1098-1109.

147. Wu J, Jiao Y, Dal Molin M, et al. Whole-exome sequencing of neoplastic cysts of the pancreas reveals recurrent mutations in components of ubiquitin-dependent pathways. *Proceedings of the National Academy of Sciences U*SA. 2011;108(52):21188-21193.

148. Yabar CS, Winter JM. Pancreatic Cancer. *Gastroenterology Clinics of North America*. 2016;45(3):429-445.

149. Canto MI, Hruban RH, Fishman EK, et al: Frequent detection of pancreatic lesions in asymptomatic high-risk individuals. *Gastroenterology*. 2012;142(4):796-804

150. Winter JM, Cameron JL, Campbell KA. 1423 pancreaticoduodenectomies for pancreatic cancer: A single-institution experience. *Journal of Gastrointest Surgery* .2006;10(9):1199-1210.

151. Siegel RL, Miller KD, Jemal A. Cancer statistics. *CA Cancer Journal Clinical*. 2016;66(1):7-30.

152. Berger AC, Garcia M, Hoffman JP, et al: Postresection CA 19-9 predicts overall survival in patients with pancreatic cancer treated with adjuvant chemoradiation: a prospective validation by RTOG . *Journal of Clinical Oncology* .2008; 20(36): 5918-592.

153. Huguet F, Girard N, Guerche CS. Chemoradiotherapy in the management of locally advanced pancreatic carcinoma: a qualitative systematic review. *Journal of Clinical Oncology*. 2009; 27(13):2269-2277.

154. Stoff JA. Selected office based anticancer treatment strategies. *Journal of Oncology*. 2019;1-14.

155. Warburg O. On the origin of cancer cells. *Science*.1956; 24;123(3191):309-14.

156. Seyfried TN, Flores RE, Poff AM, D'Agostino DPD. Cancer as a metabolic disease: implications for novel therapeutics. *Carcinogenesis*. 2014;35(3):515-27**.**

157. Popovici-Muller J, Saunders JO, Zahler R, Cianchetta G. An update on therapeutic opportunities offered by cancer glycolytic metabolism.2014;24(21):4915-4925.

158. Close Y, Xu Li X, , Saunders M, Pearce S,Foulks JM, Parnell KM, Clifford A, Nix RN, Bullough J, Hendrickson TF, Wright K, McCullar MV, Kanner S, Ho M. *Bioorganic & Medicinal Chemistry Letters*.2014;(2)24:515.

159. Guo C, Linton A, Jalaie M, Kephart S, Ornelas M, Pairish M, Greasley S, Richardson P, Maegley K , Hickey M, Li J, Wu X, Ji X, Xie Z. *Bioorganic and Medicinal Chemistry Letters.*2013; 23:3358

160. Kanno T, Sudo K, Maekawa M, Nishimura M, Ukita M, Fukutake M. *Clinical Chimica Acta. 1992*:89(2):158-162.

161. Granchi C, Fancelli D, Minutolo F. An update on therapeutic opportunities offered by cancer glycolytic metabolism. *Bioorganic and Medicinal Chemistry Letters*. 2014;24(21):4915-4925.

162. Mathupala SP, Ko YH, Pedersen PL. Hexokinase-2 bound to mitochondria: cancer's stygian link to the "warburg effect" and a pivotal target for effective therapy. *Seminer Cancer Biology*. 2009;19(1):17-24

163. Gottlob K, Majewski N, Kennedy S, Kandel E, Robey RB, Hay N. Inhibition of early apoptotic events by Akt/PKB is dependent on the first committed step of glycolysis and mitochondrial hexokinase .*Genes Development*. 2001;15(11):1406–1418.

164. Bryson J. M, Coy PE, Gottlob K, Hay N, Robey RB. Increased hexokinase activity, of either ectopic or endogenous origin, protects renal epithelial cells against acute oxidant-induced cell death. *Journal of Biological Chemistry. 2002*;11392–11400.

165. Pastorino JG, Shulga N, Hoek JB. Mitochondrial binding of hexokinase II inhibits BAX-induced cytochrome c release and apoptosis. *Journal of Biological Chemistry.2002*; 277(9): 7610–7618.

166. Rathmell JC, Fox CJ, Plas DR, Hammerman PS, Cinalli RM, Thompson CB. Akt-directed glucose metabolism can prevent bax conformation change and promote growth factor-independent survival. *Molecular Cell Biolog.*. 2003;23(20):7315–7328.

167. Majewski N, Nogueira V, Robey RB, Hay N. Akt inhibits apoptosis downstream of BID cleavage via a glucose-dependent mechanism involving mitochondrial hexokinases. *Molecular Cell Biologolgy.*2004;24(2):730–740.

168. Danial NN, Gramm CF, Scorrano L, Zhang CY, Krauss S, Ranger AM. BAD and glucokinase reside in a mitochondrial complex that integrates glycolysis and apoptosis. *Nature*. 2003;424(6951):952–956.

169. Pelicano H, Martin DS, Xu R, Huang P. Glycolysis inhibition for anticancer treatment. *Oncogene.* 2006;25(34):4633-4646.

170. Guerra F, Arbini AA, Moro L. Mitochondria and cancer chemoresistance. *Biochimica Et Biophysica Acta (BBA) - Bioenergetics*. 2017;1858(8):686-699.

171. Vyas S, Zaganjor E, Haigis MC. Mitochondria and Cancer. *Cell.* 2016;166(3):555-566.

172. Sciacovelli M, Gaude E, Hilvo M, Frezza C. The metabolic alterations of cancer cells. *Methods Enzymoogyl.*2014;542:1-23.

173. Vega NR, Loureiro KA, Mesquita I, Barbosa LC, Tavares AF, Branco JR, Erickson J, Holy EL, Perkins RA, Carvalho P, Oliveira J. Mitochondrial metabolism directs stemness and differentiation in P19 embryonal carcinoma stem cells. *Cell Death Differentiaon.*2014;21(3):1560-1574.

174. Wanet A, Arnould T, Najimi M, Renard P. Connecting mitochondria, metabolism, and stem cell fate . *Stem Cells Development*. 2015;24(17):1957-1971.

175. Cook CC, Higuchi M. The awakening of an advanced malignant cancer: an insult to the mitochondrial genome. *Biochim Biophyics Acta*. 2012;1820(5):652-662.

176. Wanrooij S, Goffart S, Pohjoismaki JL, Yasukawa Y, Spelbrink JN. Expression of catalytic mutants of the mtDNA helicase twinkle and polymerase POLG causes distinct replication stalling phenotypes. *Nucleic Acids Research*.2007;35(10):3238-3251.

177. Lee W, Johnson J, Gough DJ, Donoghue J, Cagnone GL, Vaghjiani V, Brown KA, Johns TG, St John GL. Mitochondrial DNA copy number is regulated by DNA methylation and demethylation of POLGA in stem and cancer cells and their differentiated progeny. *Cell Death Disorders*. 2015; 26(6):1664.

178. Fulda S, Galluzzi L, Kroemer G. Targeting mitochondria for cancer therapy. *Nature Reviews Drug Discovery*. 2010; 9:447-464.

179. Cairns RA , Harris IS, Ma TW. Regulation of cancer cell metabolism. *Nature Reviews . Cancer*. 2011;11(2):85-95.

180. Guaragnella N, Giannattasio S, Moro L. Mitochondrial dysfunction in cancer chemoresistance. *Biochem Pharmacology.* 2014; 92(1);62-72.

181. Hsu CC, Tseng LM, Lee HC. Role of mitochondrial dysfunction in cancer progression. *Experimental Biology and Medicine (Maywood)* .2016; 241(12):1281-1295.

182. Hay N. Reprogramming glucose metabolism in cancer: can it be exploited for cancer therapy? *Nature Reviews Cancer.* 2016;16(10):635-649.

183. Warburg O, Wind F, Negelein E. The metabolism of tumors in the body. *The Journal of General Physiology* 1927;8(6)519–530.

184. Crabtree HG. The carbohydrate metabolism of certain pathological overgrowths. *Biochemical Journal.* 1928;22:1289–1298.

185. Luengo A, Gui DY, Heiden MG. Targeting metabolism for cancer therapy. *Cell Chemical Biology*. 2017;24(9):1161-1180.

186. Granchi C, Fancelli D, Minutolo F. An update on therapeutic opportunities offered by cancer glycolytic metabolism. *Bioorganic and Medicinal Chemistry Letters.* 2014;24(21):4915-4925.

187. Tallarida RJ. Quantitative methods for assessing drug synergism. *Genes and Cancer*. 2011;2(11):1003-1008.

188. Ko YH, Smith BL, Wang Y, Pomper MG, Rini DA, Torbenson MS, Hullihen J, Pedersen PL . Advanced cancers: eradication in all cases using 3-bromopyruvic acid therapy to deplete ATP. *Biochem Biophysics Research Communication.* 2004;324(1):269-75.

189. Ihrlund LS, Hernlund E, Khan O, Shoshan MC. 3-bromopyruvic acid as inhibitor of tumour cell energy metabolism and chemopotentiator of platinum drugs. *Moecular Oncology*. 2008 Jun; 2(1):94-101.

190. Wu L, Xu J, Yuan W, Wu B, Wang H, Liu G, Wang X, Du J, Cai S .The reversal effects of 3-bromopyruvic acid on multidrug resistance in vitro and in vivo derived from human breast mcf-7/adr cells. *PLoS One*. 2014; 9(11):112132.

191. Ko YH, McFadden BA. Alkylation of isocitrate lyase from Escherichia coli by 3-bromopyruvic acid . *Archives of Biochemistry and Biophysics.*1990 May 1; 278(2):373-80.

192. Krátký M, Vinšová J. Advances in mycobacterial isocitrate lyase targeting and inhibitors. *Current Medicine Chemical.* 2012;19(36):6126-37.

193. Pinheiro C, Longatto-Filho A, Azevedo-Silva J, Casal M, Schmitt FC, Baltazar FJ. Role of monocarboxylate transporters in human cancers: state of the art. Journal of *Bioenergetics and Biomembranes.* 2012; 44(1):127-39.

194. Kaplan RS, Pratt RD, Pedersen PL. Purification and characterization of the reconstitutively active phosphate transporter from rat liver mitochondria.. *Journal of Biology and Chemical*. 1986;261(27):12767-73.

195. Pinheiro C, Longatto-Filho A, Azevedo-Silva J, Casal M, Schmitt FC, Baltazar F J. Role of monocarboxylate transporters in human cancers: state of the art. *Journal of Bioenergetics and Biomembranes.* 2012 Feb;44(1):127-39.

196. Sadowska-Bartosz I, Soszyński M., Ułaszewski S, Ko YH, Bartosz G. Transport of 3-bromopyruvic acid across the human erythrocyte membrane. *Cell Molecular Biology Letter.* 2014;19:201–214.

197. Ko YH, Smith BL, Wang Y, Pomper MG, Rini DA, Torbenson MS, Hullihen J, Pedersen PL. Advanced cancers: eradication in all cases using 3-bromopyruvic acid therapy to deplete ATP *Biochemical and Biophysical Research Communications.*2004; 324(1):269-75.

198. Dyląg M, Lis P, Niedźwiecka K, Ko YH, Pedersen PL, Goffeau A, Ułaszewski S. 3-Bromopyruvate: a novel antifungal agent against the human pathogen Cryptococcus neoformans. *Biochemical and Biophysical Research Communications* 2013;434(2):322-7.

199. Lis P, Jurkiewicz P, Cal-Bąkowska M, Ko YH, Pedersen PL, Goffeau A, Ułaszewski S. Screening the yeast genome for energetic metabolism pathways involved in a phenotypic response to the anti-cancer agent 3-bromopyruvic acid. *Oncotarget.* 2016 ; 7(9):10153-73.

200. Sun Y, Liu Z, Zou X, Lan Y, Sun X, Wang X, Zhao S, Jiang C, Liu H J . Mechanisms underlying 3-bromopyruvic acid-induced cell death in colon cancer. *Journal of Bioenergetics and Biomembranes.* 2015; 47(4):319-29.

201. Niedźwiecka K, Dyląg M, Augustyniak D, Majkowska-Skrobek G, Cal-Bąkowska M, Ko YH, Pedersen PL, Goffeau A, Ułaszewski S. Glutathione may have implications in the design of 3-bromopyruvic acid treatment protocols for both fungal and algal infections as well as multiple myeloma. *Oncotarget*. 2016 ;7(40):65614-65626.

202. Dyląg M, Lis P, Niedźwiecka K, Ko YH, Pedersen PL, Goffeau A, Ułaszewski S. Bromopyruvic acid: a novel antifungal agent against the human pathogen Cryptococcus neoformans. .*Biochemical and Biophysical Research Communications* 2013; 434(2):322-7.

203. Lis P, Jurkiewicz P, Cal-Bąkowska M, Ko YH, Pedersen PL, Goffeau A, Ułaszewski S. Screening the yeast genome for energetic metabolism pathways involved in a phenotypic response to the anti-cancer agent 3-bromopyruvic acid. *Oncotarget*. 2016;7(9):10153-73.

204. Kim JS, Ahn KJ, Kim JA, Kim HM, Lee JD, Lee JM, Kim SJ, Park JH . Role of reactive oxygen species-mediated mitochondrial dysregulation in 3-bromopyruvic acid induced cell death in hepatoma cells : ROS-mediated cell death by 3-brpa. Journal of *Bioenergetics and Biomembranes*. 2008;40(6):607-18.

205. Zhang Q, Zhang Y, Zhang P, Chao Z, Xia F, Jiang C, Zhang X, Jiang Z, Liu H. Hexokinase 2 inhibitor, 3-brpa induced autophagy by stimulating ros formation in human breast cancer cells. *Genes Cancer*. 2014;5(3-4):100-12.

206. Lis P, Dyląg M, Niedźwiecka K, Ko Y, Pedersen P, Goffeau A, Ułaszewski S. The HK2 Dependent "Warburg Effect" and Mitochondrial Oxidative Phosphorylation in Cancer: Targets for Effective Therapy with 3-bromopyruvic acid. *Molecules*. 2016;21(12):1730.

207. Chu F, Chou PM, Zheng X, Mirkin BL, Rebbaa A . Control of multidrug resistance gene mdr1 and cancer resistance to chemotherapy by the longevity gene SIRT1. *Cancer Research.* 2005 ;65(22):10183-7.

208. Jang KY, Noh SJ, Lehwald N, Tao GZ, Bellovin DI, Park HS, Moon WS, Felsher DW, Sylvester KG. SIRT1 and c-Myc promote liver tumor cell survival and predict poor survival of human hepatocellular carcinoma. *Plos One*. 2012;7(9):45119.

209. Barber MF, Michishita-Kioi E, Xi Y, Tasselli L, Kioi M, Moqtaderi Z, Tennen RI, Paredes S, Young NL, Chen K, Struhl K, Garcia BA, Gozani O, Li W, Chua KF . SIRT7 links H3K18 deacetylation to maintenance of oncogenic transformation. *Nature*. 2012 ;487(7405):114-8.

210. Alhazzazi TY, Kamarajan P, Joo N, Huang JY, Verdin E, D'Silva NJ, Kapila YL Sirtuin-3 (SIRT3), a novel potential therapeutic target for oral cancer. *Cancer*. 2011; 117(8):1670-8.

211. Roth M, Chen WY . Sorting out functions of sirtuins in cancer. *Oncogene*. 2014; 33(13):1609-20.

212. Jing E, O'Neill BT, Rardin MJ, Kleinridders A, Ilkeyeva OR, Ussar S, Bain JR, Lee KY, Verdin EM, Newgard CB, Gibson BW, Kahn CR. SIRT3 regulates metabolic flexibility of skeletal muscle through reversible enzymatic deacetylation. *Diabetes*. 2013;62(10):3404-17.

213. Sozden O, Park SH, Wagner BA, Song HY, Zhu Y, Vassilopoulos A, Jung B, Buettner GR, Gius D. SIRT3 deacetylates and increases pyruvate dehydrogenase activity in cancer cells. *Free Radical Biology Medicine*. 2014;76:163-172.

214. Lunt SY, Vander Heiden MG. Aerobic glycolysis: meeting the metabolic requirements of cell proliferation . *Annual Reviews Cell Developmental Biology*. 2011;27:441-64.

215. Patel MS, Roche TE . Molecular biology and biochemistry of pyruvate dehydrogenase complexes. *FASEB J*. 1990;4(14):3224-33.

216. Sullivan LB, Chandel NS. Mitochondrial reactive oxygen species and cancer. *Cancer Metabolisms.* 2014;2:17.

217. Rodgers JT, Lerin C, Haas W, Gygi SP, Spiegelman BM, Puigserver P. Nutrient control of glucose homeostasis through a complex of pgc-1alpha and SIRT1. *Nature*. 2005;434(7029):113-8.

218. Brenmoehl J, Hoeflich A. Dual control of mitochondrial biogenesis by sirtuin 1 and sirtuin 3. *Mitochondrion.* 2013;13(6):755-61.

219. LeBleu VS, O'Connell JT, Gonzalez Herrera KN, Wikman H, Pantel K, Haigis MC, de Carvalho FM, Damascena A, Domingos Chinen LT, Rocha RM, Asara JM, Kalluri R. PGC-1α mediates mitochondrial biogenesis and oxidative phosphorylation in cancer cells to promote metastasis .*Nature Cell Biology*. 2014;16(10):992-1003.

220. Brunet A, Sweeney LB, Sturgill JF, Chua KF, Greer PL, Lin Y, Tran H, Ross SE, Mostoslavsky R, Cohen HY, Hu LS, Cheng HL, Jedrychowski MP, Gygi SP, Sinclair DA, Alt FW, Greenberg ME. Stress-dependent regulation of FOXO transcription factors by the SIRT1 deacetylase. *Science*. 2004;303(5666):2011-5.

221. Wang F, Nguyen M, Qin FX, Tong Q. SIRT2 deacetylates FOXO3a in response to oxidative stress and caloric restriction. *Cell*. 2007;6(4):505-14.

222. Qiu X, Brown K, Hirschey MD, Verdin E, Chen D. Calorie restriction reduces oxidative stress by SIRT3-mediated SOD2 activation. *Cell Metab*olism. 2010;12(6):662-7.

223. Van Remmen H, Ikeno Y, Hamilton M, Pahlavani M, Wolf N, Thorpe SR, Alderson NL, Baynes JW, Epstein CJ, Huang TT, Nelson J, Strong R, Richardson A . Life-long reduction in MnSOD activity results in increased DNA damage and higher incidence of cancer but does not accelerate aging. *Physiology of Genomics*. 2003;16(1):29-37.

224. Sundaresan NR, Gupta M, Kim G, Rajamohan SB, Isbatan A, Gupta MP J. SIRT3 blocks the cardiac hypertrophic response by augmenting Foxo3a-dependent antioxidant defense mechanisms in mice .*Clinical Invesigations. 2009*;119(9):2758-71.

225. Yu W, Dittenhafer-Reed KE, Denu JM. SIRT3 protein deacetylates isocitrate dehydrogenase 2 (IDH2) and regulates mitochondrial redox status. *Journal of Biology and Chemical*. 2012;287(17):14078-86.

226. German N, Haigis M. Sirtuins and the metabolic hurdles in cancer. *Current Biology*. 2015;25(13).569-583.

227. Jeong SM, Lee J, Finley LW, Schmidt PJ, Fleming MD, Haigis MC. SIRT3 regulates cellular iron metabolism and cancer growth by repressing iron regulatory protein 1. *Oncogene*. 2015;34(16):2115-24.

228. Kim HS, Patel K, Muldoon-Jacobs K, Bisht KS, Aykin-Burns N, Pennington JD, van der Meer R, Nguyen P, Savage J, Owens KM, Vassilopoulos A, Ozden O, Park SH, Singh KK, Abdulkadir SA, Spitz DR, Deng CX, Gius D. SIRT3 is a mitochondria-localized tumor suppressor required for maintenance of mitochondrial integrity and metabolism during stress. *Cancer Cell*. 2010;17(1):41-52.

229. Bell EL, Emerling BM, Ricoult SJ, Guarente L. SIRT3 suppresses hypoxia inducible factor 1α and tumor growth by inhibiting mitochondrial ROS production. *Oncogene*. 2011;30(26):2986-96.

230. Lopez J, Tait SW. Mitochondrial apoptosis: Killing cancer using the enemy within. *British Journal of Cancer.* 2015;*112*(6):957-962.

231. Sarosiek K, Chi X, Bachman J, Sims J, Montero J, Patel L, Letai A. BID preferentially activates BAk while bim preferentially activates BAX, affecting chemotherapy response. *Molecular Cell.* 2015;51(6):751-765.

232. Vyas S, Zaganjor E, Haigis MC. Mitochondria and Cancer. *Cell.* 2016;166(3):555-566.

233. Forrest MD. Why cancer cells have a more hyperpolarised mitochondrial membrane potential and emergent prospects for therapy. *Biorxiv*.2015;21:159.

234. Cardaci S, Desideri E, Ciriolo MR. Targeting aerobic glycolysis: 3-bromopyruvate as a promising anticancer drug. *Journal of Bioenergetics and Biomembranes.* 2012;44(1):17-29.

235. Sayed SM. Enhancing anticancer effects, decreasing risks and solving practical problems facing 3-bromopyruvate in clinical oncology: 10 years of research experience. *International Journal of Nanomedicine.* 2018;13:4699-4709.

236. Oon CE, Strell C, Yeong KY, Östman A, Prakash, J. SIRT1 inhibition in pancreatic cancer models: Contrasting effects in vitro and in vivo. *European Journal of Pharmacology*. 2015;15(757):59-67.

237. Li Y, Wang K, Feng Y, Fan C, Wang F, Yan J, Qu Y. Novel role of silent information regulator 1 in acute endothelial cell oxidative stress injury. *Biochimica Et Biophysica Acta (BBA) - Molecular Basis of Disease.* 2014;1842(11):2246-2256.

238. Adachi M, Imai K. Bcl-XL interacts with Apaf-1 and inhibits Apaf-1-dependent caspase-9 activation. *Cell Death Differention.* 2002; 9(11):1240-7.

239. Hu Q, Sun W, Wang C, Gu Z. Recent advances of cocktail chemotherapy by combination drug delivery systems. *Advanced Drug Delivery Reviews.*2016;98(1):19-34.

240. Carrick S, Parker S, Thornton CE, Ghersi D, Simes J, Wilcken N. Single agent versus combination chemotherapy for metastatic breast cancer. *Cochrane Database System Review*. 2009; 15(2):3372.

241. Tallarida RJ. An Overview of Drug Combination Analysis with Isobolograms. *Journal of Pharmacology and Experimental Therapeutics*. 2006;319(1):1-7.

242. Amsel AD, Rathaus M, Kronman N, Cohen HY. Regulation of the proapoptotic factor BAX by Ku70-dependent deubiquitylation. *Proceedings of the National Academy of Sciences*. 2008;105(13):5117-5122.

243. Jeong J, Juhn K, Lee H, Kim S, Min B, Lee K. SIRT1 promotes dna repair activity and deacetylation of ku70. *Experimental and Molecular Medicine*. 2007;39(1):8-13.

244. Zimmer A, Tendler A, Katzir I, Mayo A, and Alon, U. Prediction of drug cocktail effects when the number of measurements is limited. *Plos Biology*. 2017;15(10):2002-2518.

245. Wang Z, Chen W. Emerging Roles of SIRT1 in Cancer Drug Resistance. *Genes and Cancer*.2013;4(3-4):82-90.

246. Chen G, Zhang B, Xu H, Sun Y, Shi Y, Luo Y, Wang F. Suppression of SIRT1 sensitizes lung cancer cells to WEE1 inhibitor MK-1775-induced DNA damage and apoptosis. *Oncogene*. 2017.36(50):6863-6872.

247. Lim C. SIRT1: Tumor promoter or tumor suppressor? Medical Hypotheses. 2016;67(2):341-344.

248. Martile MD, Bufalo DD, Trisciuoglio D. The multifaceted role of lysine acetylation in cancer: Prognostic biomarker and therapeutic target. *Oncotarget.* 2016;7(34): 55789–55810.

249. Prasad S, Gupta SC, and Tyagi AK. Reactive oxygen species (ROS) and cancer: Role of antioxidative nutraceuticals. *Cancer Letters*. 2017;387(28):95-105.

250. Nogueira V, Hay N. Molecular Pathways: Reactive Oxygen Species Homeostasis in Cancer Cells and Implications for Cancer Therapy. *Clinical Cancer Research.* 2013;19(16): 4309-4314.

251. Durand N, Storz P. Targeting reactive oxygen species in development and progression of pancreatic cancer. *Expert Review of Anticancer Therapy.* 2016;17(1):19-31.

252. Costa- Machado LF, Martín- Hernández R, Sanchez- Luengo MÁ, Hess K, Vales-Villamarin C, Barradas M, Fernandez- Marcos PJ. SIRT1 protects from K- Ras-driven lung carcinogenesis. *Embo Reports.* 2018;19(9):1-16.

253. Cheng D, Zhao L, Xu Y, Ou R, Li G, Yang H, Li W . K-Ras promotes the non-small lung cancer cells survival by cooperating with sirtuin 1 and p27 under ROS stimulation. *Tumor Biology. 2015*;36(9):7221 – 7232.

254. Prasad S, Gupta SC, and Tyagi AK. Reactive oxygen species (ROS) and cancer: Role of antioxidative nutraceuticals. *Cancer Letters.* 2017;387(28):95-105.